

MOLECULAR DETERMINANTS OF DIFFERENT GATING MECHANISMS  
IN INWARDLY-RECTIFYING POTASSIUM CHANNELS

by

XINYANG HUANG

B.Sc., The University of British Columbia, 2010

A THESIS SUBMITTED IN PARTIAL FULFILLMENT OF  
THE REQUIREMENTS FOR THE DEGREE OF

MASTER OF SCIENCE

in

THE FACULTY OF GRADUATE STUDIES

(Pharmacology)

THE UNIVERSITY OF BRITISH COLUMBIA

(Vancouver)

June 2012

© Xinyang Huang, 2012

## ABSTRACT

Inwardly-rectifying potassium (Kir) channels comprise a transmembrane domain (TMD) that makes up the conducting pore and a large cytoplasmic domain (CTD) that controls channel gating via ligand-binding. Tissue-specific expression and diverse gating mechanisms endow each Kir family with distinct physiological roles. To better understand channel function and improve treatments for Kir channel-associated diseases, we set out to determine the molecular mechanisms underlying channel gating and block.

Inward rectification via voltage-dependent polyamine block is important for maintaining a negative resting membrane potential and permitting the generation of action potentials in excitable cells. Polyamine block was studied in Kir2.1, a prototypical strong rectifier. Using inside-out patch clamp electrophysiology and sterically expanded polyamine blockers, our findings suggest that steep voltage-dependence and external  $K^+$ -dependence of high-affinity block do not require extensive polyamine interactions with the selectivity filter. Furthermore, by introducing MTS moieties into the inner cavity, as well as utilizing a hydrogen bond-deficient blocker and the disease mutant D172N, we determined that hydrogen bonding is crucial to high-affinity binding between spermine and the rectification controller (D172 in Kir2.1). It is important to note that spermine is structurally unique and binds very deep in the inner cavity. This is likely not the case for diamine blockers, which warrants caution when drawing conclusions from them about spermine.

A second gating mechanism in Kir channels is regulation by ligand-binding in the CTD. Ligand transduction to the channel gate is key to many physiological roles of Kir channels and can be demonstrated in  $K_{ATP}$  channels, which are responsible for transducing cellular metabolism to insulin secretion. Using inside-out patch clamp electrophysiology, we screened Kir6.2 slide helix mutants for ATP-sensitivity and voltage-dependent gating kinetics with a “forced gating” background mutation F168E that functionally rescues non-expressing mutants. We found that a highly conserved aspartate in the Kir slide helix is essential for ligand transduction. Further screening of nearby CTD residues revealed several potential interacting partners for this slide helix “aspartate anchor”. However, specific interactions between the aspartate anchor and the CTD remain unclear.

## TABLE OF CONTENTS

Abstract .....	ii
Table of contents .....	iii
List of tables .....	vi
List of figures .....	vii
List of illustrations.....	viii
List of symbols, abbreviations or other .....	ix
Acknowledgements .....	xi
Introduction .....	1
Kir channel structure and function .....	1
The transmembrane domain.....	2
The cytoplasmic domain.....	5
Kir channel regulation, physiology, and pharmacology .....	7
Kir2 – prototypical strong inward rectifiers .....	12
Channel localization .....	13
Physiological roles in major organs.....	14
Diseases .....	15
Kir6 – ATP-sensitive inward rectifiers.....	17
Physiological roles in major organs.....	19
Diseases .....	20
Illustrations .....	23
Chapter I: Blockade of the inward rectifier Kir2.1 by a series of sterically expanded polyamine analogs .....	24
Materials and methods.....	25
Kir2.1 channel constructs.....	25
Cell culture.....	26
Electrophysiology .....	26

Modeling of polyamine block in Kir2.1 .....	26
Results .....	27
Role of the selectivity filter in steeply voltage-dependent high-affinity block.....	27
Effects of internal and external K <sup>+</sup> on polyamine block .....	28
Kinetics of polyamine block in Kir2.1.....	29
Simulation and modeling of polyamine block in Kir2.1.....	30
Discussion.....	32
Does the selectivity filter play a role in mediating polyamine block?.....	32
Localization of polyamine blockers in the Kir channel inner cavity .....	33
Modeling polyamine block with a 3-state 2-step model.....	34
Conclusion.....	35
Tables and figures.....	35
Chapter II: Chemical basis for high-affinity polyamine block in the inner cavity of Kir2.1 .....	41
Materials and methods.....	42
Kir2.1 channel constructs.....	42
Cell culture.....	42
Electrophysiology .....	43
Analysis .....	43
Molecular modeling.....	44
Results .....	44
Effect on spermine affinity from I176C modification by MTS amines.....	44
Energy-minimized models of dimeric MTS modified channels.....	46
A hydrogen bond-deficient methylated spermine analog .....	46
Effect of MTS modification on polyamine analogs.....	47
Discussion.....	48
D172N and a hydrogen bond-deficient blocker provide insight into molecular mechanism...50	
Chemical interaction of MTS modifiers and polyamine analogs .....	50

Conclusion.....	51
Tables and figures.....	52
Chapter III: Transduction of ligand-binding to channel gating in the ATP-sensitive inward	
rectifier Kir6.2.....	57
Materials and methods.....	58
K <sub>ATP</sub> channel constructs .....	58
Cell culture and electrophysiology .....	58
Non-radioactive Rb efflux assay.....	59
Western blot detection of K <sub>ATP</sub> channel surface expression .....	59
Results .....	59
Functional scan of the Kir6.2 slide helix .....	59
Functional rescue of slide helix mutants by a “forced gating” mechanism .....	60
Kinetic features of Kir6.2[F168E] channels and impact of slide helix mutations .....	62
A keystone role for the slide helix “aspartate anchor” .....	62
Contacts between residue D58 and the CTD .....	64
Discussion.....	65
Conclusion.....	67
Tables and figures.....	68
Conclusion.....	76
Polyamine block underlying inward rectification of Kir channels .....	76
Regulation of Kir channels by nucleotides .....	79
Strengths, limitations, and future directions .....	80
Bibliography .....	84

## LIST OF TABLES

Table 1. Voltage-dependence ( $z\delta$ ) of polyamine block in Kir2.1 .....	35
Table 2. Parameters for a 3-state 2-step model of polyamine block of the inward rectifier Kir2.1 .....	36
Table 3. Ratio of experimental to simulation parameters.....	36

## LIST OF FIGURES

Figure 1. Determination of the position of polyamine binding site in the Kir2.1 inner cavity .....	37
Figure 2. Conductance-voltage relationship for polyamine block in Kir2.1 .....	38
Figure 3. Effects of varying internal and external $K^+$ concentrations on polyamine affinity and unbinding kinetics .....	38
Figure 4. Polyamine blocking kinetics in Kir2.1 .....	39
Figure 5. Polyamine unbinding kinetics in Kir2.1 .....	39
Figure 6. A 3-state 2-step model of polyamine block .....	40
Figure 7. Effects of MTS modification on spermine block in Kir2.1 .....	52
Figure 8. Spermine unbinding kinetics after MTS modification .....	53
Figure 9. MTS interactions with D172 in the inner cavity of Kir2.1 .....	53
Figure 10. High-affinity polyamine block in the D172N mutant .....	54
Figure 11. Effects of MTS modification on polyamine block in Kir2.1 .....	55
Figure 12. Polyamine unbinding kinetics after MTS modification .....	56
Figure 13. Unique characteristics of spermine binding in the inner cavity .....	56
Figure 14. Structural organization of Kir channels .....	68
Figure 15. Systematic scan of channel activity and expression of Kir6.2 slide helix mutants .....	69
Figure 16. ATP-sensitivity of Kir6.2 slide helix mutant channels .....	70
Figure 17. Effects of slide helix mutations on the unique kinetic features of Kir6.2[F168E] channels .....	71
Figure 18. Stringent aspartate requirement at position D58 .....	72
Figure 19. Schematic model illustrating ATP-binding and gating kinetics of Kir6.2[F168E] channels with slide helix mutations .....	73
Figure 20. Functional assessment of potential D58 interacting partners .....	74
Figure 21. Kinetic effects of mutations of candidate D58 interacting partners .....	75

**LIST OF ILLUSTRATIONS**

Illustration 1. Structural representation of a Kir channel .....23

## LIST OF SYMBOLS, ABBREVIATIONS OR OTHER

Kir	inwardly-rectifying potassium (channel)
Kv	voltage-gated potassium (channel)
GIRK	G protein-activated inwardly-rectifying potassium (channel)
ATP	adenosine-5'-triphosphate
K <sub>ATP</sub>	ATP-sensitive potassium (channel)
SUR	sulfonylurea receptor
TM	transmembrane
TMD	transmembrane domain
CTD	cytoplasmic domain
PIP <sub>2</sub>	phosphatidylinositol 4,5-bisphosphate
LOF	loss of function
E <sub>K</sub>	reversal potential for potassium ions
[K <sup>+</sup> ] <sub>i</sub>	intracellular potassium concentration
[K <sup>+</sup> ] <sub>o</sub>	extracellular potassium concentration
GHK	Goldman-Hodgkin-Katz
ADP	adenosine diphosphate
GPCR	G protein-coupled receptor
ACh	acetylcholine
PKC	protein kinase C
PKA	protein kinase A
ER	endoplasmic reticulum
RMP	resting membrane potential
LQT	long QT syndrome
SQT	short QT syndrome
GOF	gain of function
NDP	nucleotide diphosphate

ABC	ATP-binding cassette
NBD	nucleotide-binding domain
PHHI	persistent hyperinsulinemic hypoglycaemia of infancy
KCO	potassium channel opener
G-V	conductance-voltage
MTS	methanethiosulfonate
WT	wild-type

## **ACKNOWLEDGEMENTS**

Research work could not have been done without the guidance provided by my supervisor Harley Kurata, technical help with molecular biology from lab mate Runying Yang, technical help with electrophysiology from lab mate Yury Vilin, and cooperation with fellow students Jenny Li, Robin Kim, Roger Zhang, and Jordan Wright. All Rb flux assays and Western blots in Chapter III were done by Runying Yang and Jenny Li. Half of the electrophysiology work in Chapter III was done by Jenny Li. Insights and advices provided by my committee members Dr. Chris Ahern (University of British Columbia) and Dr. Steve Kehl (University of British Columbia) allowed my projects to progress smoothly. Special thanks to Dr. Stephan Pless, a member of Chris Ahern's lab, for his guidance and technical help on work involving oocytes and non-natural amino acids, and Gregory Dake (University of British Columbia) and student Arran Marais-Gilchrist for synthesis of polyamine blockers used throughout my projects. Another special thanks to the department secretary Wynne Leung for her help with any administrative issues throughout my degree.

Research in the lab is funded by Canadian Institutes of Health Research, Canada Foundation for Innovation, Natural Sciences and Engineering Research Council of Canada, and the Heart & Stroke Foundation of Canada.

## INTRODUCTION

Inwardly rectifying potassium (Kir) currents were discovered as early as the 1940s (Katz, 1949). They are named as such for the initial characteristic observations that only outward currents were inhibited. Kir channels do not exhibit intrinsic voltage-dependence or current kinetics of the classic voltage-dependent  $K^+$  currents in excitable cells first described by Hodgkin and Huxley (Hodgkin and Huxley, 1952). These voltage-gated potassium (Kv) channels are activated with depolarization and present with sigmoidal kinetics reflective of multiple pre-open states; Kir channels on the other hand are gated by intracellular molecules such as divalent cations and organic cationic ligands. With expression in a wide range of cell types, Kir channels contribute to electrical excitability of neurons and muscle cells, as well as relay external and internal signals for normal physiology of organs such as the heart and pancreas. A thorough understanding of the biochemical processes underlying Kir channel functions and how they are regulated will provide a foundation for innovating therapeutic approaches towards related diseases.

### **Kir channel structure and function**

There are seven families of inward rectifiers (Kir1-7) with a total of at least 15 different mammalian genes/subunits. They are functionally grouped into four categories:  $K^+$  transport channels (Kir1, 4, 7), classical Kir channels (strong rectifiers Kir2), G protein-gated channels (GIRK/Kir3), and ATP-sensitive channels ( $K_{ATP}$ /Kir6). A functional channel comprises 4 subunits and can be homo or heterotetrameric; heteromerization adds diversity to the channel's function but usually occurs among members of the same family (e.g. Kir2.1 with Kir2.2, Kir3.1 with Kir3.4)(Hibino et al., 2010). There is ample evidence supporting this stoichiometry for Kir channels (Raab-Graham and Vandenberg, 1998; Glowatzki et al., 1995; Yang et al., 1995; Inanobe et al., 1995), especially from crystallographic studies (Hansen et al., 2011; Whorton and MacKinnon, 2011; Nishida et al., 2007). An exception is the ATP-sensitive Kir6 family which co-assembles with auxiliary sulfonylurea receptor (SUR) subunits creating an octamer.

Similar to voltage-gated  $K^+$  and  $Na^+$  channels, Kir channels' pore-forming region consists of 2 transmembrane (TM)  $\alpha$ -helices from each subunit; these 2 N-terminal domains are linked via a re-entrant "P-loop" segment that makes the selectivity filter. Kir channels however are not gated by membrane

voltage *per se* due to the lack of additional TM helices, especially a voltage sensor containing basic amino acid residues arginine and lysine (Hansen et al., 2011;Whorton and MacKinnon, 2011). The TM domain (TMD) encloses the ion permeation pathway and isolates it from the hydrophobic membrane bilayer. The other major part of the channel is the cytoplasmic domain (CTD) which is largely composed of the C-terminal portion of each subunit. A unique structure of Kir channels is the interfacial or slide helix which is an  $\alpha$ -helix preceding the TM helices, and lies parallel to the plane of the membrane; as the name implies, this helix forms an interface between the TMD and CTD and probably facilitates transduction between the ligand binding site and channel gate. The CTD interacts with many intracellular ligands; thus transduction of these signals to channel gating is crucial for physiological processes.

#### *The transmembrane domain*

The architecture of the TM domain is well conserved among  $K^+$  channels from bacterial KcsA to mammalian Kv channels to Kir channels (Hibino et al., 2010). The 2 TM helices of a subunit are termed the outer helix (TM1) and inner helix (TM2) which directly faces the pore; the TM portion of the ion permeation pathway is commonly called the inner cavity which is roughly a spherical space 10 Å across. Interestingly there are two highly conserved glycine residues along TM2. Studies have suggested that the upper glycine acts as a “hinge” to allow flexibility of TM2. Firstly, the upper glycine G175 in Kir3.4 (a GIRK channel) was necessary for G protein-activation of the otherwise constitutively closed channel. The same study showed that substitution with the kink-inducing residue proline below G175 produced constitutively open channels (Jin et al., 2002). Secondly, in the heteromeric Kir4.1/Kir5.1 where the upper glycine is absent, introduction of glycine halfway along TM2 decreased channel opening (Shang and Tucker, 2008). These findings propose that bending of TM2 and the correlated low channel activity are likely due to the presence of the upper glycine hinge, and that channel activation, by G proteins for example, confers splaying of TM2 allowing opening of the ion permeation pathway. The role of the lower glycine in constriction of the pore is less clear but was suggested to contribute to tight packing of the bundle-crossing region (Shang and Tucker, 2008). However, there is evidence showing the importance of structural requirements in the bundle-crossing region to channel gating. Substitutions of bulky residues in this region with small residues (alanine, serine, glycine) rendered Kir3 channels constitutively active

(Claydon et al., 2003;Sadja et al., 2001). In particular, modeling indicated that V188 of TM2 in Kir3.2 may mediate inter-subunit interactions stabilizing a closed bundle-crossing, while the mutation V188G induces a conformation similar to that in the constitutively active Kir2.1 where these interactions are absent (Minor, Jr. et al., 1999;Yi et al., 2001). An implication from these structural hypotheses is that Kir3 channel opening upon activation is likely not due to the disappearance of TM2 bending, but rather due to the rotation of TM2 with respect to its helical axis twisting the bundle-crossing gate open (Yi et al., 2001). This may also explain the functional differences between channels that are gated by ligands (Kir3, Kir6), and those that are constitutively active in which control of TM2 movement is probably absent.

Opposing residues of the TM helices, especially at the bundle-crossing region, are crucial for some ligand-gating of Kir channels. The ability to hydrogen bond between the TM helices at this region (e.g. N94 in Kir3.2 TM1, K80 in Kir1.1 TM1) seems to be important for gating by ligands such as intracellular protons (pH) and membrane phosphatidylinositol 4,5-bisphosphate (PIP<sub>2</sub>) – having residues lacking hydrogen bonding ability at this position diminished acidification-induced channel inhibition and increased the rate of channel activation by PIP<sub>2</sub> (Rapedius et al., 2007). Moreover, there is a TM1 tryptophan and a TM2 lysine at the bundle-crossing gate that are highly conserved among eukaryotic Kir channels (W68 and K170 in Kir6.2)(Mannikko et al., 2011). Due to close proximity, it is highly likely that there is an interaction between the two residues that may affect gating in a similar way as the aforementioned hydrogen bond. On the other hand, recent Kir crystal structures (Hansen et al., 2011;Whorton and MacKinnon, 2011) strongly suggest that the two residues interact with PIP<sub>2</sub> and contribute to PIP<sub>2</sub>-induced opening of the bundle-crossing gate. Nonetheless, whether opposing TM helix residues interact with each other or cooperatively with ligands, they are necessary for directly transducing ligand binding to conformational changes that lead to the opening or closing of the bundle-crossing gate.

The selectivity filter of K<sup>+</sup>-selective channels is structurally conserved (Nishida et al., 2007). Although detailed studies of the Kir channel selectivity filter have yet to be done, its structure and function can be reasonably extrapolated from the well-studied bacterial channel KcsA. The filter is made of the K<sup>+</sup> channel signature amino acid sequence (Heginbotham et al., 1994) from each subunit, T-X-G-Y(F)-G where X varies, and lines the extracellular end of the ion permeation pathway (see Illustration 1,

in green). The main-chain carbonyl oxygen atoms of the 5 residues protrude into the pore and mimic the hydration shell (water molecules) surrounding a naked  $K^+$  ion (Morais-Cabral et al., 2001; Zhou et al., 2001). This highly stable interaction with  $K^+$  confers  $K^+$  channels with high selectivity; however, repulsion between adjacent  $K^+$  ions in the selectivity filter overcomes this electrostatic attraction to allow ion conduction (Doyle et al., 1998).

From crystal structures, it has been accepted that in a conducting pore's selectivity filter, there are 4 binding sites for  $K^+$  ions located in between the layers of oxygen atoms (8 oxygen atoms coordinating 1  $K^+$  ion); however,  $K^+$  ions are normally  $\sim 7.5$  Å apart and very rarely under 3.5 Å apart (diameter of  $K^+$  is 2.7 Å) suggesting that they are separated by a water molecule (Doyle et al., 1998; Morais-Cabral et al., 2001; Zhou et al., 2001). Thus a conducting selectivity filter alternates between a 1,3 and a 2,4 configuration holding 2  $K^+$  ions at a time. This structure is largely changed in a non-conducting state of the channel – the filter constricts in the middle and  $K^+$  ions are not observed at position 2 or 3 (Zhou et al., 2001). This conformation was observed in low- $K^+$  (<5mM) and can reflect the closed state of the channel where the filter is only exposed to extracellular  $K^+$ . Single-channel patch clamp recordings of Kir channels exhibit long bursts of opening separated by long periods of inactivity (slow gating) and flickering activity within bursts (fast gating); from mutagenesis studies and structural evidence, it is thought that slow gating corresponds to gating at the bundle-crossing, and fast gating corresponds to changes in the selectivity filter conformation in response to “seeing” low and high  $K^+$  (Yi et al., 2001; Choe et al., 2001; Trapp et al., 1998; Hibino et al., 2010).

The slide helix is a  $\sim 20$  residue segment connecting TM1 to the N-terminus which contributes to the CTD (see Illustration 1, in red). This helix that lies at the interface between membrane and cytoplasm is a structure unique to Kir channels and not found in KcsA (Doyle et al., 1998), calcium-gated  $K^+$  channels (Jiang et al., 2002), or voltage-gated  $K^+$  channels (Jiang et al., 2003; Long et al., 2005a). The importance of the slide helix is evident from the development of disease with slide helix mutations – mutations in Kir1.1 and in Kir2.1 produce a loss of function (LOF) either by decreasing channel expression or inhibiting conductance, and are associated with inherited Bartter syndrome (1997) and Andersen syndrome (Plaster et al., 2001; Bendahhou et al., 2003), respectively. Functional necessity of the

slide helix is unquestionable but molecular mechanisms behind disease-causing mutations may not be clear. For example, mutations of slide helix residues contributing to PIP<sub>2</sub>-binding in Kir2.1 are expected to impair channel function (Donaldson et al., 2003), but how mutations disturb slide helix-CTD interaction (Decher et al., 2007) or how they increase channel block (Tani et al., 2007) remains poorly understood. In Chapter III of this thesis, a functional screening of slide helix mutants in Kir6.2 will be described; however, until we determine the interacting partners of slide helix residues, their roles in Kir channel function and regulation will remain a mystery.

### *The cytoplasmic domain*

Structural details of Kir channel CTDs are available from crystal structures of soluble CTD complexes (Nishida and MacKinnon, 2002; Pegan et al., 2005; Inanobe et al., 2007) as well as of whole channels (Kuo et al., 2003; Nishida et al., 2007; Hansen et al., 2011; Whorton and MacKinnon, 2011). The CTD is made of both the N- and C-termini of the protein and forms the binding site for numerous intracellular ligands. The N-terminus is just a single  $\beta$ -strand ( $\beta$ A) that sits at the interface between CTDs of adjacent subunits (Hibino et al., 2010); it also combines with two other  $\beta$ -strands ( $\beta$ L,  $\beta$ M) in the C-terminus of an adjacent subunit to form a  $\beta$ -sheet. This inter-subunit association can occur between different subunits (e.g. C-terminus of Kir6.2 with N-terminus of Kir2.1) and is likely a common theme in all Kir channels important for CTD stability and channel function (Tucker et al., 1998). For example, a peptide fragment from the C-terminus of Kir3.1 is strongly associated with the N-terminus fragment of Kir3.1 or Kir3.4 and greatly enhances binding of G $\beta$  $\gamma$  subunits when compared with the C-terminus alone (Huang et al., 1997); this likely underlies high-affinity G protein-activation in Kir3 channels (Huang et al., 1995). Furthermore, this association between the N- and C-termini forms the cytoplasmic portion of the ion permeation pathway, making the pore of Kir channels much longer (>60 Å) than without a CTD (30-40 Å) (Nishida and MacKinnon, 2002). The additional length is physiologically relevant for Mg<sup>2+</sup> ions and polyamines which are intracellular pore-blockers of Kir channels – in this thesis, I will analyze the trajectory of polyamines through the Kir2.1 pore, from plugging the cytoplasmic pore to subsequent occlusion of the inner cavity.

An interesting structure in Kir channels is the G-loop which is a segment connecting two  $\beta$ -strands ( $\beta$ H,  $\beta$ I) in the CTD and it is the apex of the cytoplasmic pore (see Illustration 1, in orange)(Hibino et al., 2010). In the crystal structure of a KirBac3.1-Kir3.1 chimera (Nishida et al., 2007) as well as recent structures of chicken Kir2.2 (Hansen et al., 2011) and mammalian GIRK2 (Kir3.2)(Whorton and MacKinnon, 2011), it is clear that the G-loop may offer another level of gating by having at least two conformations – dilated or constricted. Indeed in Kir2.1, steric expansion mutations in the G-loop prevented ion conduction and LOF mutations in the G-loop have been associated with Anderson syndrome (Pegan et al., 2005). Recent structures showed that PIP<sub>2</sub>-binding opens the G-loop gate (see section below: Kir channel regulation, physiology, and pharmacology)(Hansen et al., 2011;Whorton and MacKinnon, 2011) and this at least partly underlies the necessity of PIP<sub>2</sub> for normal Kir channel function (Bendahhou et al., 2003;Hilgemann and Ball, 1996;Huang et al., 1998;Lopes et al., 2002).

For a visual representation of the Kir channel structure, see Illustration 1 below, where several important structural elements are highlighted.

As alluded to earlier, the CTD is under the influence of many ligands including nucleotides (e.g. ATP), PIP<sub>2</sub>, G proteins, and even protons (pH). It was shown that intracellular acidification (from pH 7.4 to 6.6) inhibited Kir2.3 activity but not Kir2.1 activity (Qu et al., 2000). Replacement of the Kir2.1 N-terminus with that of Kir2.3 conferred pH sensitivity; a 4-residue segment in the C-terminus of Kir2.3 that is different in Kir2.1 also conferred pH sensitivity when substituted, but only in the presence of the Kir2.3 N-terminus; finally, acidification increased binding between the N- and C-termini. These findings and further mutagenesis experiments suggested that histidine residues (pKa of 6) in the C-terminus are sensitive to a pH drop from 7.4 and perhaps induce conformational changes that promote channel closure via association between the N- and C-termini (Qu et al., 2000). Although the molecular mechanisms are unclear, evidence of pH- and G protein-gating of Kir channels strongly supports the critical role of the CTD, especially where the N- and C-termini associate, in channel gating. In the next section, we take a closer look at how Kir channels are gated differently by other ligands.

## **Kir channel regulation, physiology, and pharmacology**

A major regulatory mechanism in Kir channels is inward rectification, most notably of the strong inward-rectifier family Kir2. This process is due to the presence of  $Mg^{2+}$  ions and polyamines that act as intracellular open-pore blockers – they interact with the channel pore and physically block the permeation pathway (Lopatin et al., 1994; Matsuda et al., 1987). Inward rectification through Kir channels describes the physiological phenomenon where inward  $K^+$  current is large and relatively ohmic at hyperpolarizing membrane voltages (less than  $E_K$ , the  $K^+$  equilibrium potential) and outward current becomes progressively inhibited; this “turning-off” of  $K^+$  current is crucial in the heart and parts of the brain allowing the action potential to initiate from depolarization (Hagiwara and Takahashi, 1974; Miyazaki et al., 1974; Sakmann and Trube, 1984). Studies have shown a fast and slow component to physiological inward rectification – the fast corresponds to  $Mg^{2+}$  (Ishihara et al., 1989; Matsuda, 1988) and the slow to polyamines (Ficker et al., 1994; Fakler et al., 1995; Lopatin et al., 1994; Lopatin et al., 1995). Essentially, upon depolarization, polyamines (cellular metabolites of basic amino acids) enter and block Kir channels, and upon hyperpolarization, polyamines unblock. This block is thought to be a two-step process where polyamines interact with the CTD (shallow block) (Pegan et al., 2005; Kurata et al., 2007; Fujiwara and Kubo, 2006) followed by the TM inner cavity (deep block), both of which involve acidic pore-lining residues. It follows that not all Kir channels exhibit strong rectification, in light of their different physiological functions; Kir2 and some Kir3 subunits are strongly rectifying, while others such as Kir1 and 6 are weak, conducting large outward current. The acidic inner cavity residue (aspartate or glutamate) is often called the “rectification controller” due to its requirement for steep rectification (Matsuda et al., 2003; Wible et al., 1994; Xie et al., 2002; Lopatin et al., 1994); strong rectification can be reconstituted in weak rectifiers such as Kir1.1 and Kir6.2 by simply introducing an acidic pore-lining residue to the inner cavity (Kurata et al., 2004; Wible et al., 1994; Lu and MacKinnon, 1994). However, Kir3.2 lacks an acidic residue in the inner cavity but still shows strong rectification (Slesinger et al., 1996) suggesting that an electronegative cytoplasmic pore exerts a stabilizing effect on deep block and may be sufficient to generate rectification (Robertson et al., 2008). To further study rectification, Chapter I and II of this thesis

will focus on the molecular aspects of polyamine block in the well-characterized strong inward-rectifier Kir2.1.

Kir channel conductance is dependent on both intra ( $[K^+]_i$ ) and extracellular  $K^+$  concentration ( $[K^+]_o$ ), but only the  $[K^+]_o$ -dependence has been extensively studied. It has been repeatedly demonstrated through single-channel and slope conductance measurements that Kir conductance has a square root dependence on  $[K^+]_o$  of up to 150 mM (i.e.  $K^+$  increases 100x, conductance increases 10x) (Perier et al., 1994; Sakmann and Trube, 1984; Kubo et al., 1993; Lopatin and Nichols, 1996a). This is consistent with the Goldman-Hodgkin-Katz (GHK) theory on independent ion permeation through an open pore (Goldman, 1943). However, experimental deviations (Lopatin and Nichols, 1996a) from the GHK predictions (at more extreme voltages or  $[K^+]$ ) on  $[K^+]$ -dependence of conductance confirm the multi-ion pore model for  $K^+$  channels where  $K^+$  ions at different binding sites can interact with each other in the open Kir channel pore (Ciani et al., 1978; Hille and Schwarz, 1978; Sakmann and Trube, 1984). This model is further reinforced by crystal structures showing multiple  $K^+$  binding sites (Doyle et al., 1998; Nishida et al., 2007; Tao et al., 2009; Xu et al., 2009). The dependence on  $[K^+]$  is an intrinsic channel property – the increase in conductance may involve conformational changes in the selectivity filter (Zhou et al., 2001); even though changes in  $[K^+]$  may not be physiologically relevant in terms of Kir channel regulation, it shows that channel function can vary in the absence of any ligands or signals.

As mentioned earlier, the membrane phospholipid  $PIP_2$  is essential for normal Kir channel functioning. In excised patches, current runs down due to the loss of  $PIP_2$  but can be regenerated from ATP and phosphatidylinositol by lipid kinases (Hilgemann and Ball, 1996). Functional analyses suggested that  $PIP_2$  interacts with basic residues in the CTD (Lopes et al., 2002) which is a requirement for further regulation of the channel – heteromeric Kir3.1/Kir3.4 channels could not be activated by the  $G\beta\gamma$  subunit of G proteins after current run-down, but regained function after  $PIP_2$  was added; it was also found that  $G\beta\gamma$  stabilized the interaction between  $PIP_2$  and the channel (Huang et al., 1998). Significant advancement in our understanding of  $PIP_2$ -activation of Kir channels was made with recent crystal structures of  $PIP_2$ -bound Kir2.2 (Hansen et al., 2011) and Kir3.2 (Whorton and MacKinnon, 2011). The latter revealed details consistent with the aforementioned  $G\beta\gamma$ - $PIP_2$  synergy; it was observed that  $PIP_2$ -

binding open the bundle-crossing gate and using a constitutively active Kir3.2 mutant, it was inferred that G proteins open the G-loop gate but only when both G $\beta\gamma$  and PIP<sub>2</sub> are bound does the channel fully open and conduct ions. It was shown in both studies that the negative head-group of PIP<sub>2</sub> is stabilized at the bundle-crossing region (interface between membrane and cytoplasm) by a pocket of basic residues from both TM helices and the TM2-CTD linker, suggesting that PIP<sub>2</sub> “pulls open” the bundle-crossing gate. A consequence of this pulling is that the CTD moves towards the TMD allowing close interactions. This was also evident in the crystal structures and perhaps explains why PIP<sub>2</sub>-binding is required for channel regulation and transduction of ligand-binding in the CTD to gating at the TMD.

There are several other ways by which Kir gating is controlled via small molecules. As already discussed, acidification or a drop in intracellular pH can inhibit Kir channel activity (Kir1.1, Kir2.3, and Kir4.1 are more sensitive). The subunits Kir3.2 and Kir3.4 exhibit PIP<sub>2</sub>-dependent activation by intracellular Na<sup>+</sup> which is also evident in the crystal structure where it was suggested that Na<sup>+</sup>-binding induces conformational changes similar to those with G protein-binding (Whorton and MacKinnon, 2011). It can then be rationalized that Na<sup>+</sup>- and G protein-activation of the channel are synergistic (Petit-Jacques et al., 1999). An aspartate residue in the CTD is essential for this process – in Kir3.2, mutation of this aspartate (D226) to an asparagine abolished Na<sup>+</sup> sensitivity; furthermore, Na<sup>+</sup>-activation did not affect single-channel activity or activation through muscarinic receptors indicating that it is strictly a gating mechanism (Ho and Murrell-Lagnado, 1999). Another classic example of molecular gating of Kir channels is by nucleotides. The ATP-sensitive Kir6 family is expressed with the SUR subunit which is essential for channel trafficking (Zerangue et al., 1999; Bao et al., 2011); the Kir6 CTD directly interacts with ATP, causing inhibition of channel activity (Antcliff et al., 2005; John et al., 2003; Li et al., 2000; Proks et al., 1999; Reimann et al., 1999) whereas nucleotide diphosphates (e.g. ADP) bind SUR subunits, in the presence of Mg<sup>2+</sup>, to increase channel activity (D'hahan et al., 1999; Gribble et al., 1997; Matsuoka et al., 2000; Shyng et al., 1997b). More on the regulation of Kir6 channels will be discussed later (see section below: Kir6 – ATP-sensitive inward rectifiers).

The Kir3 family or GIRK is activated by G proteins and G protein-coupled receptors (GPCR) and thus contributes to the body's homeostatic response. In the heart where GIRK1 and 4 (Kir3.1,

Kir3.4)(Krapivinsky et al., 1995) play an important role in mediating inhibitory effects, acetylcholine (ACh) activates GIRK channels through the muscarinic  $M_2$  receptors producing the  $I_{K,ACh}$  current (Kurachi et al., 1986). Under basal conditions, the  $M_2$  receptor is coupled to the  $G\alpha\beta\gamma$  trimeric G protein complex (Gilman, 1987). When an agonist (e.g. ACh) activates the receptor,  $G\alpha$  separates from  $G\beta\gamma$  and can both associate with membrane effectors; GIRKs are activated by  $G\beta\gamma$  (Kurachi, 1995; Logothetis et al., 1987; Clapham and Neer, 1993; Ito et al., 1992) resulting in hyperpolarization of the membrane potential and reduced cellular excitability. Studies have shown that  $G\beta\gamma$ -binding to GIRKs occurs in the CTD, specifically where the N- and C-termini associate (Chan et al., 1997; He et al., 1999; Huang et al., 1995; Huang et al., 1997) and likely induce conformational changes that pull the channel open (Riven et al., 2003; Whorton and MacKinnon, 2011). Although the  $G\alpha$  subunit does not directly affect GIRK channel activity, it has been shown, through binding and functional assays, to associate with the  $G\beta\gamma$ -GIRK complex (Ivanina et al., 2004; Peleg et al., 2002; Slesinger et al., 1995). This suggests that prior to agonist-activation, inactive G protein-GIRK complexes are already formed; this allows a rapid response to agonist release and accounts for the rapid kinetics of agonist-activation observed *in vivo* (Peleg et al., 2002; Riven et al., 2006; Slesinger et al., 1995; Ivanina et al., 2004).

It is noteworthy that GIRKs are still subjected to other gating schemes in Kir channels including strong inward rectification. This has important implications on the intricate physiology of GIRK channels. With basal agonist-activation and low channel activity, GIRKs likely do not contribute as much to the “turning off” of repolarizing influence during an action potential or repolarization itself as constitutively active channels like Kir2. Upon agonist stimulation (i.e. parasympathetic response), more GIRK channels are open and therefore exhibit inward rectification, but at the same time suppress the excitability of cells (Burgen and Terroux, 1953) and slow down heart rate (Hutter and Trautwein, 1956; Wickman et al., 1998). Thus, while GIRKs’ role in beat-by-beat regulation of the heart may be masked by Kir2 channels, their unique ability to relay and amplify signals from the nervous system grants them control over long-term regulation of the heart. In the brain, GIRKs were shown to mediate inhibitory postsynaptic potentials (Misgeld et al., 1989; Thompson and Gahwiler, 1992; Thompson et al., 1992) and may play a role in controlling seizures (Signorini et al., 1997). With evidence for various other inhibitory roles in the brain

and pancreas, GIRK is the only Kir family indirectly gated by extracellular signals via intracellular ligands, allowing dynamic physiological processes.

Despite so much understanding of the structure and function of Kir channels, there are surprisingly few pharmacological agents that target them and none that are commonly used clinically. The cations  $Ba^{2+}$  and  $Cs^{+}$  are commonly used as Kir channel blockers (Franchini et al., 2004; Quayle et al., 1993; French and Shoukimas, 1985; Hille and Schwarz, 1978; Oliver et al., 1998), inhibiting current when applied externally. This process is voltage-dependent and block strengthens with hyperpolarization, the opposite to intracellular  $Mg^{2+}$  and polyamines. Also, increasing  $[K^{+}]_o$  decreases block by  $Ba^{2+}$  and  $Cs^{+}$  (Hagiwara et al., 1976; Hagiwara et al., 1978) suggesting an extracellular binding site for these ions. The only clinically relevant agents affecting Kir channel activity target the SUR subunit of Kir6 channels (see section below: Kir6 – ATP-sensitive inward rectifiers). Since Kir channels are so ubiquitously expressed, an effective therapeutic agent likely requires specificity to certain channel subunits and even then would probably have significant side-effects. However, the few pharmacological agents available can be useful for probing channel properties and function.

The structure of Kir channels determines their function (ion selectivity and permeation), and different Kir families exhibit different ligand-sensitivity. It is clear that gating of Kir channels, like any ion channel, dictates regulation and confers their physiological role. This thesis will explore two gating schemes and the underlying mechanisms: first, the voltage-dependent regulation of Kir2 by polyamines that exemplifies the rapid changes in channel conductance in constitutively active tissues such as the heart, and second, the regulation of Kir6 by ATP that reflects the slower transduction of ligand-binding in the CTD to conformational changes in the bundle-crossing gate converting biological signals to electrical activity. Before discussing the experiments and results, I will introduce more in detail the Kir2 and Kir6 families in terms of their unique characteristics among Kir channels that lead to their respective physiology and associated diseases.

## **Kir2 – prototypical strong inward rectifiers**

The Kir2 family of inward rectifiers are strongly sensitive to voltage-dependent polyamine block exhibiting very little outward current (Lopatin et al., 1994; Yamada and Kurachi, 1995). They are abundant in skeletal and cardiac muscles where they maintain resting membrane potential and shut off upon depolarization to allow an action potential. There are six members in this family: Kir2.1/2.2/2.3/2.4 or IRK1/2/3/4 (Kubo et al., 1993; Takahashi et al., 1994; Bond et al., 1994; Topert et al., 1998), Kir2.5 which was discovered in the crucian carp heart (Hassinen et al., 2008), and Kir2.6 which was discovered in human skeletal muscles and is transcriptionally regulated by thyroid hormones (Ryan et al., 2010). Kir2.1 shares between 60-70% amino acid sequence homology with the other subunits, with the TM domain (TM1, TM2, selectivity filter) being mostly conserved (Hibino et al., 2010). Although Kir2 subunits usually assemble as homotetramers (Tinker et al., 1996), members can mix to form heteromers *in vivo* (Schram et al., 2002) and exhibit mixed channel properties electrophysiologically (Preisig-Muller et al., 2002).

Strong rectification in Kir2 channels can be attributed to rings of pore-lining acidic residues (presumably bearing negative charges) with their side-chains pointing to the pore axis, allowing electrostatic attraction with positively charged polyamines (Kuo et al., 2003; Nishida and MacKinnon, 2002). The rectification controller, as previously mentioned, is an important determinant of high-affinity polyamine binding in the inner cavity (D172 in Kir2.1) producing block even with very low polyamine concentrations (Wible et al., 1994; Lopatin et al., 1994; Shin and Lu, 2005). However, there are four pore-lining acidic residues in the CTD (E224, D255, D259, E299) that are responsible for low-affinity interactions with polyamines and are also important for inward rectification (Pegan et al., 2005; Kurata et al., 2007; Guo and Lu, 2003) as mutations of any one produced marked outward current (Pegan et al., 2005). Having this two-step blocking process may be advantageous in that low-affinity block at the CTD increases the local polyamine concentration, facilitating subsequent entry into the inner cavity leading to high-affinity block (Kubo and Murata, 2001; Lopatin et al., 1995).

Kir2 channels are considered constitutively active because in the presence of PIP<sub>2</sub>, they are virtually always open. Unlike GIRK and Kir6 channels that possess a unique regulatory element (G proteins and

nucleotides, respectively), gating of Kir2 is only affected by common regulatory factors such as pH (see section above: Kir channel structure and function – the cytoplasmic domain) and phosphorylation. However, Kir2 channels differ in phosphorylation-dependence: Kir2.3 inhibition was associated with elevated protein kinase C (PKC) and the channel was shown to be phosphorylated at the N-terminus (Henry et al., 1996;Zhu et al., 1999); Kir2.1 was not affected by PKC but a splice variant Kir2.1b was inhibited (Henry et al., 1996;Karle et al., 2002); Kir2.2 seemed to be inhibited not by PKC, but by src kinases (Zitron et al., 2008); both Kir2.1 and Kir2.2 current were increased with protein kinase A (PKA)-activation (Zitron et al., 2004;Dart and Leyland, 2001). Unfortunately, the mechanisms behind Kir2 gating by protein kinases remain elusive; there has been some evidence suggesting that phosphorylation affects PIP<sub>2</sub>-binding as inhibition of Kir2.1 and Kir2.3 by PKC was enhanced with weaker channel-PIP<sub>2</sub> affinity (Du et al., 2004). Nonetheless, this shows that through protein kinases, Kir2 channels may also be regulated via receptor-dependent pathways and extracellular signals, much like GIRKs via G proteins.

#### *Channel localization*

Aside from the CTD's role in ligand regulation of Kir channels, it also contains amino acid sequences responsible for channel export from the endoplasmic reticulum (ER)(Hibino et al., 2010;Ma et al., 2001). This export signal in Kir2 channels is F-C-Y-E-N-E (Ma et al., 2001;Stockklausner et al., 2001) and is likely different among Kir families. From the ER, channels end up in the Golgi and export from the Golgi to the plasma membrane seems to depend largely on two groups of residues in the CTD: in Kir2.1, R44/R46 in the N-terminus and a 4-residue sequence starting with Y242, as mutations in these elements resulted in channel retention in the Golgi (Stockklausner and Klocker, 2003;Hofherr et al., 2005). However, the trafficking of Kir2 channels to the cell surface is likely multifactorial; some disease-causing LOF mutations in Kir2.1 (V302M, deletion of S95-F98 in TM1, and deletion of S314-Y315 in the CTD) lead to channel retention in the cytoplasm (Plaster et al., 2001;Tristani-Firouzi et al., 2002;Bendahhou et al., 2003). Whether these mutations directly prevent membrane localization of channels or cause folding defects-induced retention and degradation, the fact remains that regulation of Kir2 trafficking is no trivial matter and a LOF can potentially be rescued by forced channel expression.

### *Physiological roles in major organs*

Perhaps the most well-defined role of Kir2 channels is in the heart where they produce the cardiac current  $I_{K1}$  which is abundant in Purkinje fibres and ventricular/atrial myocytes (Beeler, Jr. and Reuter, 1970;Kurachi, 1985;McAllister and Noble, 1966) but not present in pacemaker cells (Noma et al., 1984); it has been shown specifically that Kir2.1, Kir2.2, and Kir2.3 but not Kir2.4 are expressed in human hearts (Wible et al., 1995;Raab-Graham et al., 1994;Wang et al., 1998). There are three main functions of  $I_{K1}$  (Hibino et al., 2010): large  $K^+$  conductance near  $E_K$  clamps the resting membrane potential (RMP) close to  $E_K$ ; inhibition of outward current at more depolarized voltages (inward rectification) prevents  $K^+$  efflux from interfering with the action potential; repolarization by Kv channels “reactivates”  $I_{K1}$  allowing acceleration of repolarization and reestablishment of RMP. Thus,  $I_{K1}$  (encoded by Kir2 genes) is essential for the generation and time course of the cardiac action potential.

$I_{K1}$  in animal models is likely attributable to Kir2.1/Kir2.2 heteromers (Zaritsky et al., 2001;Zobel et al., 2003) with Kir2.1 being the crucial subunit. Cardiac myocytes from Kir2.1 knockout mice could not establish a stable RMP and produced spontaneous action potential firings; they also showed longer action potentials (Zaritsky et al., 2001). Interestingly, these mice did not experience arrhythmias associated with abnormal pacemaking, reinforcing the absence of  $I_{K1}$  in nodal cells.

Kir2 channels are also expressed in the vasculature (Adams and Hill, 2004;Nilius and Droogmans, 2001). In endothelial cells, Kir2 channels maintain a negative RMP which is necessary for blood flow-induced  $Ca^{2+}$  influx and consequently  $Ca^{2+}$ -dependent NO production which leads to vasodilatation (Kwan et al., 2003;Wellman and Bevan, 1995); indeed, shear stress activates Kir2 currents (Olesen et al., 1988) which may underlie shear stress-induced endothelial secretion of NO and vascular smooth muscle relaxation. This indicates a potentially key regulatory role of endothelial Kir2 channels in maintaining vascular tone. In vascular smooth muscles, evidence suggests that a mild increase in  $[K^+]_o$ , rather than depolarization, increases Kir2 conductance causing hyperpolarization of muscle cells and is associated with cerebral and coronary arterial dilatation (Knot et al., 1996;McCarron and Halpern, 1990;Nelson et al., 1995). It is possible that in the brain, increased  $K^+$  secretion from astrocytes due to high neuronal activity relaxes vascular smooth muscles causing cerebral arterial dilatation – this generates a

compensatory increase in blood flow to highly active brain regions (Filosa et al., 2006). This  $[K^+]_o$ -dependence is reminiscent of that discussed previously (see section above: Kir channel function, physiology, and pharmacology).

Biochemical assays in animal models have shown expression of Kir2 channels in neurons throughout the brain (Horio et al., 1996;Karschin et al., 1996;Pruss et al., 2005) and skeletal muscles (Kubo et al., 1993;Perier et al., 1994;Takahashi et al., 1994); they were also found in human skeletal muscles (Raab-Graham et al., 1994). Unfortunately, the physiological significance of Kir2 channels in these organs remains unclear. It is believed that they play an important role in establishing a negative RMP crucial for cellular excitability (Hibino et al., 2010); for example, in the Kir2.1 LOF disease Andersen's syndrome, periodic paralysis (Plaster et al., 2001) may be due to a depolarized RMP causing  $Na^+$  channel inactivation and inhibition of action potential firing. There is a correlation between increasing Kir2.1 expression and the differentiation (Konig et al., 2004) and development (Fischer-Lougheed et al., 2001) of human skeletal myoblasts; it is believed that gradual hyperpolarization of myoblasts due to Kir2.1 permits  $Ca^{2+}$  influx necessary for development.

### *Diseases*

A well-known Kir2-associated channelopathy is Andersen's syndrome. It is an autosomal dominant genetic disorder caused by LOF mutations in Kir2.1 (Plaster et al., 2001). Its clinical features are cardiac arrhythmias due to prolongation of the action potential (long QT syndrome, LQT7), periodic muscle paralysis, and abnormal facial and digital bone structures (Tawil et al., 1994). Many associated mutations either disrupt channel interactions with  $PIP_2$  or impair channel trafficking. For example, mutation of a basic residue in the binding site of  $PIP_2$ , R218Q/W, causes a loss of  $PIP_2$  sensitivity which likely underlies the LOF phenotype; other disease-causing mutations in the CTD such as G300V and E303K also seemed to decrease  $PIP_2$ -binding but are not part of the  $PIP_2$  binding site (Plaster et al., 2001;Lopes et al., 2002). As mentioned previously, mutations preventing proper trafficking of channels to the membrane are associated with Andersen's syndrome (Bendahhou et al., 2003). The lack of physiological contribution from Kir2.1 can rationalize the symptoms of Andersen's syndrome: weakening of cardiac action potential repolarization causes LQT; depolarized RMP leads to elevated  $Na^+$  channel inactivation

and skeletal muscle inactivity; elevated pH in the bone matrix due to the lack of Kir-dependent H<sup>+</sup> secretion prevents proper bone modelling by osteoclasts, possibly causing the disease-associated bone deformities (Hibino et al., 2010).

Several other pathological conditions have been suggested to involve Kir2 channels, albeit the evidence is preliminary. Cholinergic activation of M<sub>1</sub> muscarinic receptors greatly inhibits activity of channels containing Kir2.3 subunits and this suppression was implied to be involved in abnormal neuronal networks of Parkinson's disease (Shen et al., 2007;McNeill et al., 1988). On another note, high cholesterol decreases Kir2 currents in Chinese Hamster Ovary cells as well as in human endothelial cells (Romanenko et al., 2004;Romanenko et al., 2002); hypercholesterolemia has been shown in pigs to depolarize RMP via Kir channel inhibition (Fang et al., 2006b). These imply a role of Kir channels in the pathology of endothelial dysfunction and vascular diseases associated with hypercholesterolemia.

The correlation between Kir2 channels and the aforementioned diseases is no doubt worth further investigation. However, there is another pathological phenomenon associated with Kir2 channels that can be studied on a molecular level and can be explained with electrophysiology: a form of short QT syndrome (SQT3) caused by a gain of function (GOF) mutation in Kir2.1. Opposite to LQT, SQT shortens the cardiac action potential and is associated with a high incidence of arrhythmias and cardiac death (Schimpf et al., 2005). The SQT3 form has been linked to the Kir2.1 mutation D172N (Priori et al., 2005;El et al., 2009) which neutralizes the rectification controller important to polyamine block; this mutation weakens inward rectification (Wible et al., 1994;Lopatin et al., 1994) thereby augmenting action potential repolarization. Since inward rectification in Kir2 channels seems fundamental to many of their physiological roles as well as pathological mechanisms such as with SQT3, Chapter I and II of this thesis will examine the biophysics of polyamine block and its molecular determinants in Kir2.1. This will provide further understanding to inward rectifier function and one of its major gating schemes.

## **Kir6 – ATP-sensitive inward rectifiers**

$K_{ATP}$  channels are octameric protein complexes composed of 4 pore-forming Kir6 channel subunits and 4 auxiliary SUR subunits. The name  $K_{ATP}$  comes from the fact that Kir6 channels are sensitive to and closed by ATP (exception in smooth muscles); the SUR can bind nucleotide diphosphates (NDPs) such as ADP inducing Kir6 opening (Ashcroft, 1988; Terzic et al., 1995; Tung and Kurachi, 1991). Thus,  $K_{ATP}$  channels respond to cellular metabolism and affect membrane excitability. Expression of either Kir6 channels or SUR subunits alone does not produce Kir6-specific currents (Inagaki et al., 1995b; Aguilar-Bryan et al., 1995). The physiological necessity of SUR assembly with Kir6 channels for expression of currents displays its importance for not only regulation but also expression of the channel. The SUR is a member of the ATP-binding cassette (ABC) protein superfamily; it has 2 cytoplasmic nucleotide-binding domains (NBDs) which bind and hydrolyze ATP (Bienengraeber et al., 2000; Matsuo et al., 2000) and 3 TMDs (TMD0 – TM1-5, TMD1 – TM6-11, TMD2 – TM12-17). There are two Kir6 (Kir6.1, Kir6.2) and three SUR (SUR1, SUR2A, SUR2B) subunits; combinations of channel and SUR are more or less tissue specific.

Unlike Kir2 channels,  $K_{ATP}$  channels are insensitive to polyamine block and exhibit very weak inward rectification (Shyng et al., 1997a; Kurata et al., 2004) due to the lack of an acidic rectification controller (N160 in Kir6.2) as well as the absence of rings of acidic residues in the cytoplasmic pore (Robertson et al., 2008). This highlights the differential gating schemes and physiological roles between Kir2 and Kir6 channels.

The major regulatory mechanism of  $K_{ATP}$  channels is through intracellular nucleotides. Interestingly, the effect of ATP on channel activity depends on  $Mg^{2+}$ . It was shown with various channel/SUR combinations that ATP alone inhibited channel activity more potently than in the presence of  $Mg^{2+}$  (Mg-ATP) (Ashcroft and Kakei, 1989; Kajioka et al., 1991; Findlay, 1988). Furthermore, rundown of current can be reversed by Mg-ATP but not with non-hydrolyzable ATP analogs (Findlay, 1987; Ohno-Shosaku et al., 1987; Takano et al., 1990). However, this is common to all Kir channels (Huang et al., 1998) and is not specific to  $K_{ATP}$ ;  $Mg^{2+}$  is necessary for phosphorylation of phosphatidylinositol to generate  $PIP_2$  via ATP-dependent lipid kinase – the activating effect of Mg-ATP is partly due to  $PIP_2$ . On

the other hand,  $Mg^{2+}$  is also required for the activation of  $K_{ATP}$  channels by NDPs; without  $Mg^{2+}$ , NDPs enhance ATP-inhibition (Dunne and Petersen, 1986; Lederer and Nichols, 1989; Findlay, 1987). This  $Mg^{2+}$ -dependence suggests that NDPs (e.g. ADP from ATP-hydrolysis) bind at a different site as ATP to exert its stimulatory effect (Terzic et al., 1994; Tung and Kurachi, 1991).

The dual regulation by ATP and NDPs affects slow gating – in single-channel recordings, ATP prolongs intervals of channel closure and shortens bursts of channel opening (flickering), and vice versa for NDPs (Alekseev et al., 1998). This means that ATP-binding in  $K_{ATP}$  channels stabilizes the closed state and destabilizes the open state while NDPs do the opposite. The ATP binding site is located in the Kir6 CTD at the interface of the N- and C-termini (Antcliff et al., 2005; Haider et al., 2005; Trapp et al., 2003); it is likely that up to 4 ATP molecules can bind one Kir6 channel to synergistically inhibit channel activity, but 1 ATP has been shown to suffice for channel closure (Craig et al., 2008). Moreover, ATP-induced channel closure is inhibited by  $PIP_2$  which can be explained by the close proximity of  $PIP_2$  and ATP binding sites (Baukrowitz et al., 1998; Shyng and Nichols, 1998) – binding of either ligand probably changes local conformation altering the binding pocket of the other. On the other hand, NDPs (in the presence of  $Mg^{2+}$ ) exert their stimulatory effect by binding to the NBDs of SUR (D'hahan et al., 1999; Gribble et al., 1997; Matsuoka et al., 2000). From studies on other ABC proteins and their NBDs, it is known that the 2 NBDs dimerize and form two ATP binding pockets; this is followed by ATP hydrolysis in the presence of  $Mg^{2+}$  (Hollenstein et al., 2007). It has been suggested that nucleotide-bound NBDs transition from a closed channel-associated state to an open channel-associated state (Yamada et al., 2004). This implies that ATP binds the NBDs but is immediately hydrolyzed to ADP; ADP and other NDPs probably activate the channel by stabilizing the NBDs in the open channel-associated state (Zingman et al., 2001). The  $Mg^{2+}$ -dependence of NDP-activation of  $K_{ATP}$  channels likely reflects the necessity of NBDs' hydrolytic ability to regulation by nucleotides.

Although there is ample evidence for Kir6 channel regulation through ligand-binding in the SUR, the molecular mechanisms remain largely unknown. It is believed that SUR's TMD0 associates with the N-terminus and TM1 helix of Kir6 (Babenko and Bryan, 2003; Fang et al., 2006a); specifically the cytosolic linker L0 at the N-terminus of SUR's TMD1 connects Kir6/TMD0 to the rest of the SUR

(Babenko and Bryan, 2002). Therefore it is rational to believe that ligand-binding in the SUR controls channel gating by inducing conformational changes that are coupled to Kir6 via L0 and TMD0.

A functional  $K_{ATP}$  channel requires SUR subunits. However, truncated Kir6.2 channels, where the last 26 residues of the C-terminus are deleted, are functional and can be expressed without SURs (Tucker et al., 1997). The deleted region contains the amino acid sequence R-K-R which signals retention in the ER; the same sequence is found in SUR1 (Zerangue et al., 1999). This suggests that in wild-type  $K_{ATP}$ , both retention signals are hidden when Kir6 and SUR associate, allowing proper channel trafficking.

### *Physiological roles in major organs*

$K_{ATP}$  channels consisting of Kir6.2 and SUR1 are abundantly expressed in pancreatic  $\beta$ -cells (Inagaki et al., 1996; Inagaki et al., 1995a). They are essential for transducing high blood glucose to insulin secretion (Ashcroft and Kakei, 1989; Ashcroft and Rorsman, 1989): a postprandial increase in blood glucose increases metabolism and the ATP:ADP ratio in  $\beta$ -cells. The rise in ATP and drop in ADP synergistically inhibit  $K_{ATP}$  activity which depolarizes the membrane. L-type voltage-gated  $Ca^{2+}$  channels are then activated causing  $Ca^{2+}$ -mediated fusion of insulin-containing vesicles to the membrane. Thus,  $K_{ATP}$  channels respond to and fine-tune blood glucose concentration and mediate its absorption and metabolism.

In the heart, it is unclear whether Kir6.2 is expressed with SUR1 or SUR2A (Hibino et al., 2010). One possible role of cardiac  $K_{ATP}$  channels is preconditioning in which brief myocardial ischemia is introduced to ready the heart for severe ischemia in the future (Murry et al., 1986; Yellon and Downey, 2003). In support of this, the protective effect of preconditioning is absent in Kir6.2-knockout mice (Gumina et al., 2003; Suzuki et al., 2002) and when  $K_{ATP}$  channel blockers are used in animal models (D'Alonzo et al., 1992; Gross and Auchampach, 1992; Schulz et al., 1994). The underlying mechanisms are unknown but likely involve many downstream signalling pathways (Yellon and Downey, 2003). Data from many studies using mice strongly suggest a cardio-protective effect of  $K_{ATP}$  channels under cardiac stress or excessive adrenergic influence (Zingman et al., 2002; Tong et al., 2006; Liu et al., 2004; Kane et al., 2006). Although the cardiac roles of  $K_{ATP}$  channels are speculative, their activity seems inarguably

beneficial; it is possible that channel regulation by nucleotides is involved – ischemia decreases the ATP:ADP ratio, promoting  $K_{ATP}$  opening.

$K_{ATP}$  channels are also found in vascular smooth muscles and the brain. The smooth muscle form is likely Kir6.1 with SUR2B (Isomoto et al., 1996; Yamada et al., 1997) which is quite insensitive to ATP. This renders them almost constitutively active, similar to Kir2 channels, and play a role in maintaining a negative RMP and promote smooth muscle relaxation and vasodilatation. The regulation of vascular tone by  $K_{ATP}$  channels is largely mediated via vasodilators such as prostaglandin, and vaso-constrictors such as endothelin, serotonin, and histamine (Quayle et al., 1997); how these agents affect channel activity is elusive. On the other hand,  $K_{ATP}$  channels containing either Kir6.2 or Kir6.1 are expressed in the hypothalamus and they retain glucose/ATP sensitivity (Ashford et al., 1990; Routh, 2002); much like in pancreatic  $\beta$ -cells, a rise in glucose increases the ATP/ADP ratio which closes  $K_{ATP}$  channels and promotes excitation – this may be involved in hypothalamic control over wakefulness, energy expenditure, and appetite. During ischemia or hypoxia,  $K_{ATP}$  channel opening also suppresses neuronal excitability in the substantia nigra pars reticulata (Jiang et al., 1994; Yamada et al., 2001) which inhibits seizure propagation (Depaulis et al., 1994; Iadarola and Gale, 1982); this neuronal protective effect seems physiologically relevant as Kir6.2 knockout mice were especially susceptible to seizure after a brief period of hypoxia (Yamada et al., 2001).

### *Diseases*

A major role of  $K_{ATP}$  channels is to control insulin secretion in response to increased blood glucose. It follows that a LOF mutation in  $K_{ATP}$  can cause membrane depolarization and hyper-secretion of insulin. Indeed, many LOF mutations in SUR1 (Huopio et al., 2000; Thomas et al., 1995) and Kir6.2 (Ashcroft, 2005; Reimann et al., 2003; Thomas et al., 1996) are associated with inherited persistent hyperinsulinemic hypoglycaemia of infancy (PHHI) which causes irreversible brain damage. Mutations in SUR1 can either prevent  $K_{ATP}$  trafficking or assembly, or if in the NBDs, produce channels with impaired sensitivity to Mg-ADP (Ashcroft, 2005; Dunne et al., 2004; Yan et al., 2004); either way these mutations lead to diminished channel activity. Unfortunately, PHHI patients with  $K_{ATP}$  mutations are often irresponsive to

drugs that open  $K_{ATP}$  channels (KCO) such as diazoxide and require surgery to lower insulin secretion and boost blood glucose (Hibino et al., 2010).

A polar opposite of PHHI is reflected by GOF mutations in either Kir6.2 or SUR1 causing neonatal diabetes (congenital type 1 diabetes) where constitutive  $K_{ATP}$  activity hyperpolarizes pancreatic  $\beta$ -cells suppressing insulin secretion (Ashcroft, 2005). As this disease phenotype is most probably associated with a loss of ATP-inhibition, Kir6.2 mutations account for ~50% of permanent neonatal diabetes (Edghill et al., 2004; Sagen et al., 2004). In severe Kir6.2 mutations, neonatal diabetes accompanies other debilitating conditions such as developmental delay, muscle weakness, and epilepsy. The importance of ATP-inhibition of  $K_{ATP}$  channels is reflected by the positive correlation between the extent of loss of ATP-sensitivity and disease severity (Ashcroft, 2005). Most patients can be treated with sulfonylureas which inhibit the SUR thereby inhibiting channel activity, or with insulin injections in severe cases.

Mutations in Kir6.2 that cause neonatal diabetes generally fall under two categories: those that disrupt ATP-binding directly and those that disrupt ATP-inhibition without affecting binding *per se*. In the former case for example, disease-causing mutations I182V and R201C/H occur near the ATP-binding site in the Kir6.2 CTD likely altering binding pocket conformation (Gloyn et al., 2004; Gloyn et al., 2005; Proks et al., 2004). In the latter case, mutations such as Q52R and V59M/G occur in the slide helix and are associated with severe disease phenotype (Proks et al., 2004; Proks et al., 2005). This reinforces the previously mentioned notion that the slide helix is crucial for coupling of ligand-binding in the CTD to gating at the TMD – when this coupling is disrupted, binding of ATP becomes futile leading to its complete loss of sensitivity. In the last part of the thesis, I will study the role of the Kir6.2 slide helix in channel inhibition by ATP. Screening of slide helix mutations may suggest a model in which channel regulation by ligand-binding is achieved via TMD-CTD coupling.

With clearer perspectives on the importance of the different gating mechanisms of Kir2 and Kir6 channels to their physiological roles, the rest of the thesis is divided into 3 chapters exploring first, inward rectification in Kir2.1 which contributes to cardiac excitability and normal heart rhythm, and second,

ATP-induced inhibition of Kir6.2 which underlies the homeostatic response of insulin secretion to the metabolic state of the body:

Chapter I: *Blockade of the inward rectifier Kir2.1 by a series of sterically expanded polyamine analogs.* Blockers with progressively expanded terminal amines were tested to see their voltage-dependence of block, kinetics, and  $[K^+]_o$ -dependence. Findings will suggest whether polyamines require entry into the selectivity filter to produce steep voltage-dependence. A 3-state 2-step model of polyamine block was tested for its viability in predicting experimental results.

Chapter II: *Chemical basis for high-affinity polyamine block in the inner cavity of Kir2.1.* Channels were modified with MTS reagents forcibly introducing amines into the inner cavity to see their effects on the blocking affinity and unblocking kinetics of spermine and various diamine analogs. Results will reveal details of spermine's deep binding site including the interactions between it and D172 (rectification controller). The disease mutant D172N was used to further examine the importance of hydrogen bonding in high-affinity block.

Chapter III: *Transduction of ligand-binding to channel gating in the ATP-sensitive inward rectifier Kir6.2.* Slide helix residues were singly mutated to observe the effect on channel inhibition by ATP and gating kinetics. Several CTD residues that potentially interact with the slide helix were also mutated. Non-functional mutants were rescued using a novel pH-dependent forced gating. This screen will determine interfacial residues important for ligand transduction and may suggest a model of coupling between the CTD and the TMD gate.

## Illustrations

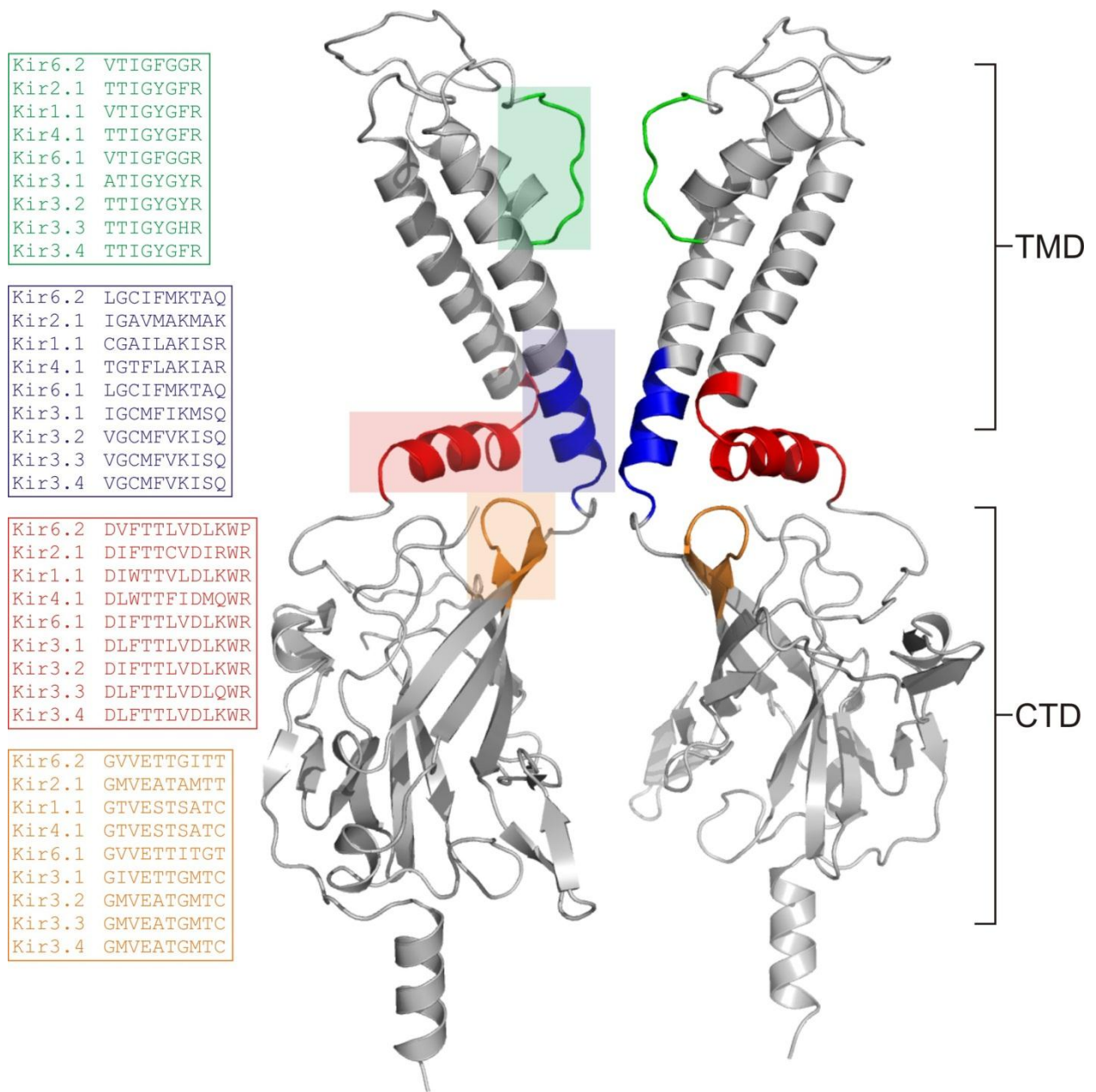


**ILLUSTRATION 1. Structural representation of a Kir channel.** Two of four subunits of a Kir channel are shown, comprising a transmembrane domain (TMD) and a cytoplasmic domain (CTD). Several important structural elements are highlighted: selectivity filter (green), bundle-crossing gate (blue), slide helix (red), and G-loop (orange). Amino acid sequence alignments of these regions are shown for 9 eukaryotic Kir channels. Note the highly conserved residues: signature sequence T-X-G-Y(F)-G of the selectivity filter, a lysine (K) in M2 at the bundle-crossing gate, most of the slide helix residues including a tryptophan (W) at the bundle-crossing region, and most of the G-loop residues.

## CHAPTER I

### Blockade Of The Inward Rectifier Kir2.1 By A Series Of Sterically Expanded Polyamine Analogs

Strongly-rectifying channels exhibit a large macroscopic conductance at hyperpolarized voltages, but are silenced at depolarized voltages, due to voltage-dependent block by intracellular polyamines (Ficker et al., 1994; Lopatin et al., 1994; Lopatin et al., 1995; Fakler et al., 1995). Understanding the molecular basis of polyamine block is an essential step to describe the function of strong rectifiers and how channel mutations may lead to diseases (Priori et al., 2005; El et al., 2009). Voltage-dependent channel block was associated with blocker entry into the TM electric field four decades ago (Woodhull, 1973). Since then, studies have repeatedly supported the idea that endogenous polyamines enter the Kir channel pore, but were associated with a large charge movement that could not be accounted for solely by blocker movement through the field (effective valence exceeded blocker valence). This “excess” charge is attributed to the displacement of permeating  $K^+$  ions coupled to polyamine movement through the pore (Hille and Schwarz, 1978; Oliver et al., 1998; Pearson and Nichols, 1998; Spassova and Lu, 1998).

Polyamine block comprises a weakly voltage-dependent blocking step followed sequentially by a more steeply voltage-dependent transition to a high-affinity binding site (Lopatin et al., 1995; Shin and Lu, 2005). Shallow block involves stabilization of polyamines in the cytoplasmic pore by acidic residues, notably E224, D255, D259, and E299 (Wible et al., 1994; Pegan et al., 2005; Kurata et al., 2007; Guo and Lu, 2003) as well as the aromatic residue F254 (Xu and Lu, 2004; Shin et al., 2005). The steeply voltage-dependent “deep” binding site depends primarily on a single acidic residue in the inner cavity, D172 in Kir2.1 (Wible et al., 1994; Xie et al., 2002; Matsuda et al., 2003). Several studies probing the nature of the inner cavity spermine (an endogenous polyamine) binding site have indicated a deep locale, likely between the rectification controller and selectivity filter (John et al., 2004; Kurata et al., 2004; Kurata et al., 2010b; Chang et al., 2003). A persisting question is just how deep the inner cavity binding site lies, and whether steep voltage-dependence of polyamine block requires blocker interactions with the selectivity filter. Experiments using a sterically expanded polyamine analog (1,10-bis-trimethylaminodecane, or decamethonium) have demonstrated that the voltage-dependence of polyamine

block remains virtually unaltered by methylation of the terminal amines, suggesting that the blocker does not enter the spatially constrained selectivity filter (Shin and Lu, 2005). However, in the context of other studies suggesting a somewhat compliant/mobile filter (Noskov et al., 2004), we asked whether the methylated termini were sufficient to exclude selectivity filter binding of the bis-TMA-C10 blocker. In the present study we have directly tested this question with a series of progressively larger polyamine analogs.

Each sequential voltage-dependent blocking step involves coupled movements of ions occupying the channel pore, and so it is not surprising that the apparent polyamine affinity depends strongly on the concentrations of permeant ions present (Lopatin and Nichols, 1996b; Hagiwara et al., 1976). Polyamine block is especially sensitive to  $[K^+]_o$ , although the molecular basis for this sidedness is not well understood. It has been suggested that polyamines may compete directly with potassium ions for occupancy of binding sites on the intracellular side of the selectivity filter, although this has been difficult to test.

In this study, we demonstrate that steric expansion of the termini of polyamine blockers does not abolish the steep voltage-dependence or the  $[K^+]_o$ -dependence of polyamine block of Kir channels. Our findings illustrate that sterically expanded blockers exhibit considerably slower kinetics (both binding and unbinding), and their kinetic properties imply significant effects on at least two barriers for movement through the channel pore. These observations reinforce the notion of coupled ion movement as a determinant of steeply voltage-dependent channel blockade, and refine our structural description of the deep spermine binding site in Kir channels.

## **Materials and methods**

### *Kir2.1 channel constructs*

All experiments were done using IRK1J, a mouse Kir2.1 construct where six out of thirteen endogenous cysteines were mutated (C54V, C76V, C89I, C101L, C149F, C169V) to prevent channel function alteration from cysteine oxidation, while maintaining wild-type function and polyamine-induced inward rectification (Lu et al., 1999; Chang et al., 2005). For the rest of the text, results for IRK1J are

interpreted as equivalent to that for Kir2.1. The IRK1J template DNA was provided by R.-C. Shieh (Institute of Biomedical Sciences, Taipei, Taiwan).

### *Cell culture*

TSA cells were cultured in a 50 ml polystyrene tissue culture flask (Becton Dickinson Labware) with DMEM high glucose 1x growth media (Invitrogen) containing 10% FBS and 1% penicillin-streptomycin. Cells were incubated at 37°C with 5% CO<sub>2</sub>. Cells were transfected with IRK1J cDNA (1-1.5 µg per 35 mm dish) and GFP cDNA (240 ng per 35 mm dish) using Lipofectamine 2000 transfection reagent (Invitrogen). After 24 hrs, transfected cells were split onto sterile glass cover slips, followed by electrophysiology 16-48 hours later.

### *Electrophysiology*

Inside-out patch clamp experiments were performed at room temperature using a multi-lane perfusion system for rapid solution exchange (Kurata et al., 2011). Data were typically filtered at 1 kHz, digitized at 10 kHz, and stored directly onto computer hard drive using Clampex software (Axon Inc.). Glass pipettes were pulled to a resistance of 1-2 MΩ. All experiments were done at room temperature. In most experiments, symmetrical pipette/external solutions were used: 140 mM KCl, 1 mM EGTA, 1 mM K<sub>2</sub>EDTA, 4 mM K<sub>2</sub>HPO<sub>4</sub>, pH 7.3 (using 1 mM KOH and 1 mM HCl). For experiments using different K<sup>+</sup> concentrations, the concentration of KCl in the solution was adjusted, maintaining all other components. Spermine (FLUKA chemicals, Sigma-Aldrich) and analogs synthesized in house (University of British Columbia, Vancouver, Canada) were stored as 10 mM stocks (dissolved in 150 mM K<sup>+</sup> recording solution, with pH adjusted to 7.3).

### *Modeling of polyamine block in Kir2.1*

Results were analyzed based on a 3-state 2-step model of polyamine block introduced previously (Shin and Lu, 2005; Kurata et al., 2007). The channel was modeled into an open (O) state and 2 blocked (OB1, OB2) states. The equilibrium between O and OB1 is described by the equilibrium constant  $K_1 = k_1[B]/k_{-1}$ , where  $k_1$  and  $k_{-1}$  are forward and backward rate constants, and [B] is the polyamine concentration; similarly, the equilibrium between OB1 and OB2 is described by  $K_2 = k_2/k_{-2}$ . The rate

constants are described by the standard exponential function  $k_x(V)=k_x(0mV)e^{(z\delta FV/RT)}$ ; equilibrium constants can then be described as the ratio of the two rate functions,  $K_x(V)=K_x(0mV)e^{(z\delta FV/RT)}$  where  $K_x(0mV)=k_x(0mV)/k_{-x}(0mV)$  and  $z\delta=z\delta_{k1}-z\delta_{k-1}$ . The algebraic solution to this model (see Fig. 6A) is  $G=1/(1+K_1[B]+K_1[B]K_2)$ , where G is the normalized conductance. This two-component equation was fitted to experimental data through least sum of squares using Microsoft Solver.

## Results

### *Role of the selectivity filter in steeply voltage-dependent high-affinity block*

To explore polyamine interactions with the selectivity filter, and to ask whether steeply voltage-dependent high-affinity block requires polyamine entry into the filter, we synthesized and characterized a family of sterically expanded structural analogs of spermine (Fig. 1A). These analogs lack the two central amines but are comparable in length to spermine. 1,10-diaminodecane (diamine decane) has primary terminal amines much like spermine; subsequent analogs have quaternized terminal amines: bis-trimethylamine (bis-TMA-C10), bis-quinuclidine (bis-QUIN-C10, a “cyclized” TEA moiety), and bis-triethylamine (bis-TEA-C10). Two models of polyamine interactions with the selectivity filter and/or inner cavity were considered. In the “cavity” model, polyamines are excluded from the sterically constricted selectivity filter. In this model, the voltage-dependence ( $z\delta$ ) associated with spermine block should be relatively insensitive to steric modifications of blocker termini (Fig. 1B, top row). In the “filter” model, polyamines directly displace selectivity filter ions to generate a significant portion of the valence of block, leading to a prediction that the larger analogs (certainly bis-TEA-C10; tetraethylammonium diameter  $\sim 8.5$  Å) would be sterically excluded from the filter (diameter  $\sim 4.5$  Å), resulting in a measurably lower  $z\delta$  (Fig. 1B, bottom row). It is noteworthy that the bis-quinuclidine compound does not have linear extensions of the blocker termini (that might enter the restricted space of the selectivity filter), adding an additional structural constraint to this analog.

Using voltage-step recordings from inside-out membrane patches, we generated conductance-voltage (G-V) curves for all four analogs and spermine (Fig. 2A). All analogs showed similar affinity (weakened relative to spermine), with no clear trend related to blocker size. Among the analogs, diamine decane had the highest affinity, and bis-TMA-C10 the lowest; the two larger alkylated analogs (bis-QUIN

and bis-TEA) were intermediate in their affinity (Fig. 2B,C). Larger blockers, especially bis-TEA-C10, were very slow to achieve steady state current at lower depolarizing voltage (Fig. 2A, bottom right). Therefore, a longer voltage step protocol was used to accurately generate steady state G-V curves and yield reliable  $z\delta$  values. With this experimental attention to attaining steady state blockade, all four analogs generated a comparably steep  $z\delta$  value (Fig. 2B, Table 1). In summary, despite large steric differences in the blocker termini, no major changes in affinity or effective valence were observed for the series of sterically expanded polyamine analogs. This collection of observations seems most consistent with a “cavity” model, in which steep voltage-dependence of polyamine block does not depend upon blocker entry into the selectivity filter.

#### *Effects of internal and external $K^+$ on polyamine block*

To further examine whether polyamines interact with the selectivity filter, we examined the effects of changing  $[K^+]_i$  or  $[K^+]_o$  on channel block by the largest analog bis-TEA-C10. It has been recognized that there is a strong relationship between polyamine block and the  $K^+$  reversal potential (Lopatin and Nichols, 1996b; Hagiwara et al., 1976). However, an important detail of this relationship is that the effects of potassium exhibit strong sidedness. Changes in reversal potential due to changes in  $[K^+]_o$  dramatically alter polyamine affinity, whereas changes in  $[K^+]_i$  have little or no effect. We have previously speculated that this sidedness might arise due to competitive interactions between extracellular ions and spermine in selectivity filter binding sites (Kurata et al., 2010b). With the sterically expanded family of blockers, we were able to directly test this possibility. Specifically, if extracellular ions indeed compete with polyamines, then bis-TEA-C10 would likely exhibit weak sensitivity to changes in  $[K^+]_o$ .

We tested the potency of Kir2.1 channel block by bis-TEA-C10 in various  $K^+$  gradients, again using extended voltage step protocols to ensure steady state channel block. We observed that, similar to spermine in previous studies, block by bis-TEA-C10 was markedly reduced with increased  $[K^+]_o$  (Fig. 3A). Notably, at the same reversal potential (0 mV), but different  $K^+$  concentrations (50in:50out vs 300in:300out), bis-TEA-C10 exhibited significantly different potency: much higher voltages are required in 300 mM  $K^+$  conditions to generate substantial channel block (Fig. 3A). At a given  $[K^+]_i$ , changes in external (pipette)  $K^+$  had dramatic effects on blocker potency. In contrast at either  $[K^+]_o$ , alterations of

internal  $K^+$  had little effect on blocker potency. These findings are strongly reminiscent of the previously described  $[K^+]_o$ -dependence of spermine, and suggest that bis-TEA-C10 and spermine interact with  $K^+$  ions in a similar fashion. Since the large analog bis-TEA-C10 is likely unable to enter the selectivity filter, these findings indicate that the  $[K^+]_o$ -dependence of polyamine block is not due to direct competition with ions for a site in the filter. Lastly, an interesting observation from the G-V curves (Fig. 3A) was that the shallow component at hyperpolarizing voltages, due to low-affinity block in the cytoplasmic domain (Kurata et al., 2007;Shin et al., 2005), was more apparent with low  $K^+$  concentrations (see Chapter I Discussion).

We also examined the effects of potassium concentrations on kinetics of bis-TEA-C10 unbinding. Previous work has demonstrated that unbinding rates of spermine are dependent on both  $[K^+]_i$  and  $[K^+]_o$  (Lopatin and Nichols, 1996b;Matsuda et al., 2010). Similar to effects on spermine, increasing internal  $K^+$  from 50 mM to 300 mM (-45 mV shift in  $E_K$ ) decelerated the unbinding rate, suggesting that the blocker was locked in by  $K^+$ ; increasing external  $K^+$  from 50 mM to 300 mM (+45 mV shift in  $E_K$ ) accelerated blocker unbinding (Fig. 3B,C). Overall, these data are consistent with the idea that polyamines compete with  $K^+$  ions throughout the channel pore, and that polyamine occupancy of the selectivity filter is not essential to observe strong  $K^+$ -dependence of block.

#### *Kinetics of polyamine block in Kir2.1*

In addition to measuring steady state properties of blockade, we also characterized the kinetics of block and unblock for the sterically expanded polyamine analogs, for the purpose of evaluating their properties in the context of a kinetic model (see Fig. 6A). Blocking time constants,  $\tau$ , were obtained from exponential fits of the decay of current after pulsing from -50 mV to various depolarizing voltages. Voltage-dependent rate constants,  $k$ , were derived as a function of blocker concentration, using multiple combinations of blocker concentrations and voltages, as described elsewhere (Kurata et al., 2007;Shin and Lu, 2005). There was considerable slowing of blocking rate for larger polyamine analogs, with bis-TEA-C10 blocking 2-3 orders of magnitude slower than diamine decane (Fig. 4A). This observation is consistent with an intuitive notion of steric hindrance or an increased energetic barrier for a larger blocker to enter the inner cavity. This size-dependence of blocking rate was observed at all voltages (Fig. 4B)

although a further observation was the emergence of a biphasic nature of the rate-voltage plots for larger blockers. This biphasic characteristic is reminiscent of the effects of Kir2.1 inner cavity modification on the kinetics of spermine block, where the voltage-dependence of the spermine blocking rate steepens at intermediate voltages (Kurata et al., 2010b).

Unbinding time constants were similarly derived from exponential fits of the recovery of current at hyperpolarizing voltages, after a prepulse to +60 mV to elicit channel blockade. Similar to the blocking rate, there was considerable deceleration of blocker unbinding with larger polyamines (Fig. 5A). Blocker unbinding was independent of concentration (Fig. 5B), but steeply voltage-dependent (Fig. 5C). Overall, these blocker properties are internally consistent: all of the blockers had relatively similar affinities (Fig. 2), but dramatically different blocking rates accompanied by similar changes in unbinding rates. Thus, the observation of size-dependent unbinding rates further reinforces the notion of steric hindrance to entry and exit from the inner cavity.

#### *Simulation and modeling of polyamine block in Kir2.1*

We used a previously described 3-state 2-step model of polyamine block to analyze steady state and kinetic data related to the sterically expanded polyamine blockers (see Chapter I Materials and methods). In this model, blockers interact with the channel in two sequentially linked steps. The first blocking step generates a “shallow” blocked state (OB1), conceptualized to involve a low-affinity polyamine binding site within the cytoplasmic domain, with little charge displacement. Subsequently, polyamines enter a deep blocked state with steep voltage-dependence, conceptualized to involve blocker interactions with the inner cavity, stabilized especially by interactions with rectification controller D172 (Nichols and Lopatin, 1997; Lu, 2004). Each transition is described by a rate constant,  $k_x(V)$  each with a respective voltage-dependence,  $z\delta_x$ . The first blocking step (governed by  $k_1(V)$  and  $z\delta_1$ ) is also concentration-dependent as it describes interactions of the channel with the intracellular pool of polyamines (Fig. 6A). As previously described (Shin and Lu, 2005; Kurata et al., 2010b), virtually all of these parameters can be constrained by experimentally derived values (Table 2). Estimates of  $z\delta_1$  and  $k_1(0mV)$  can be extracted from exponential fits of blocking rate/voltage plots;  $z\delta_2$  and  $k_2(0mV)$  can be assigned values based on unbinding rate/voltage plots. Also,  $K_1(0mV)$  and  $K_2(0mV)$  (and associated valences) could be estimated from

steady-state G-V curves of high concentrations of blockers, and based on the relationship  $K_x(0\text{mV})=k_x(0\text{mV})/k_{-x}(0\text{mV})$ , we derived  $k_{-1}(0\text{mV})$ ,  $k_2(0\text{mV})$ , and  $z\delta_{-1}$ ,  $z\delta_2$ . As unbinding rates for diamine decane were too fast to accurately measure, experimental values for  $k_2(0\text{mV})$ ,  $k_{-2}(0\text{mV})$ ,  $z\delta_2$  and  $z\delta_{-2}$  were not derived.

The sterically expanded polyamine analogs exhibited several features that we hoped could be accounted for by the kinetic model. Firstly, many of the blockers exhibited a clear biphasic nature to the voltage-dependence of blocking rate (Fig. 4B). Secondly, the voltage-dependent blocking rates approached different saturating values, with considerably slower block (~2 orders of magnitude) observed for the largest blocker analogs. Specifically, the largest blockers appeared to exhibit an initial phase (at intermediate voltage) with considerably steeper voltage-dependence of blocking rates relative to smaller blockers, and transitioned to a shallower “plateau” at the most depolarized voltages. We were especially interested by the biphasic blocking rates, because a previous study demonstrated that modification of some pore-lining residues generated a similar biphasic voltage-dependence of block, which could be modeled in a straightforward manner by heightening the energetic barrier for blocker entry into the deep binding site (Kurata et al., 2010b). We examined whether the steric expansion of blocker termini acts similarly as a barrier for blocker entry from the shallow cytoplasmic binding site into the deep inner cavity binding site.

Simulation of currents, followed by the same analysis as the experimental data, resulted in clear biphasic voltage-dependence of blocking rates (fits in Fig. 4B). Model simulations were first performed with experimentally constrained rate constants and effective valences. We slightly adjusted model parameters to better recapitulate the data, but overall the final model parameters closely matched the initial experimental constraints (Table 3).

To explore the overall decrease in blocking rates with increasing blocker size as well as the biphasic nature of the plots, we decomposed the sequential blocker binding model and explored the effects of altering rates of each individual transition. With very high  $k_x(0\text{mV})$  and  $k_{-x}(0\text{mV})$  values describing spermine kinetics taken from a previous study (Kurata et al., 2010b), the blocking rate vs voltage plot was more or less linear (on a log scale), lacking a biphasic nature (Fig. 6B). This voltage-

dependence of blocking rate was consistent with what we saw with diamine decane, the fastest and smallest blocker in our scan of sterically expanded analogs. Maintaining the equilibrium constant  $K_1(0\text{mV})$  while decreasing both rate constants  $k_1(0\text{mV})$  and  $k_{-1}(0\text{mV})$  (by equal factors), the rate plot shifted downward, but maintained linearity (Fig. 6Bi). This observation arises because the O-OB1 step is rate-limiting and dictates the kinetics of block over the simulated voltage range. In contrast, maintaining  $K_2(0\text{mV})$  while decreasing both  $k_2(0\text{mV})$  and  $k_{-2}(0\text{mV})$  produced the biphasic characteristic, with a steepening of the voltage-dependence of blocking rate at lower depolarizing voltages (Fig. 6Bii), but reaching the same saturating rate (dictated by the O-OB1 equilibrium). Considered together, these observations indicate that description of the effects of steric expansion of blocker termini (i.e. biphasic voltage-dependence of block, and progressive slowing of the “saturating” blocking rate) requires changes to the rates governing both blocking transitions in the model.

## Discussion

In strong inward rectification of Kir channels, polyamine blockers traverse a long ( $>70 \text{ \AA}$ ) pore, displacing multiple  $\text{K}^+$  ions accounting for the steep voltage-dependence of block (Xu et al., 2009; Pegan et al., 2006; Nishida et al., 2007; Hansen et al., 2011). Sufficient kinetic models of spermine block have simplified the trajectory of the blocker into two binding sites: a peripheral site located in the CTD and whose occupancy is weakly voltage-dependent, and a deep site in the inner cavity that exhibits very steep voltage-dependence (Lopatin et al., 1995; Shin et al., 2005; Kurata et al., 2010b). In the present study, we used a family of sterically expanded polyamine blockers to probe pore dimensions restricting blocker movement, and to determine blocker features essential for steeply voltage-dependent block.

*Does the selectivity filter play a role in mediating polyamine block?*

Our first application of the sterically expanded analogs was to evaluate the possibility that steeply voltage-dependent block requires polyamine entry into the selectivity filter. A previous study took a similar approach to this question by comparing the blocking properties of spermine and bis-TMA-C10 (Shin and Lu, 2005). They found that bis-TMA-C10 (named bis-QA<sub>C10</sub> in their study, also referred to as decamethonium) exhibited the same voltage-dependence as spermine ( $z\delta$  of 4.5 and 4.6 respectively), and

concluded that steep voltage-dependence did not require spermine entry into the filter. Another similar study used variably alkylated quaternary amines and also demonstrated identical voltage-dependence (Spasova and Lu, 1998). We expanded these approaches to include additional diamine blockers with even larger terminal radii, motivated by the idea that some studies have suggested considerable flexibility of the selectivity filter (Noskov et al., 2004) that might accommodate (even partially) the termini of bis-TMA-C10. The additional blockers in our study are much larger and thus more unlikely to enter the selectivity filter. Furthermore, the bis-quinuclidine compound does not have any free alkyl extensions that might migrate into the filter and displace occupant ions. Overall, we observed that the entire series of analogs in our study exhibited virtually indistinguishable effective valences of block relative to spermine (Table 1).

We also observed that the characteristic  $[K^+]_o$ -dependence of spermine block (Hagiwara et al., 1976; Lopatin and Nichols, 1996b) is preserved for even the largest polyamine analogs. This finding suggests that the  $[K^+]_o$ -dependence does not arise from direct competition between ions and polyamines in the selectivity filter. A more consistent explanation is that blockers in the inner cavity region are affected by external ions over a long distance, with ion effects being transmitted through a column of occupant ions in the filter. However, the details of permeation and the molecular mechanism underlying  $[K^+]_o$ -dependence of polyamine block remain unclear and will continue to be investigated. Another interesting observation from these experiments was that the shallow blocking component was much more apparent with low internal  $K^+$ . This is highly consistent with the notion that blocking cations and polyamines compete with  $K^+$  ions all along the channel pore – with high internal  $K^+$ , blockers were unable to maintain their low-affinity interaction with the acidic cytoplasmic residues. Overall, these findings provide strong evidence that polyamines can achieve steeply voltage-dependent block without entering the selectivity filter, and that coupled ion movement is likely sufficient to generate the entire voltage-dependence of high-affinity block.

#### *Localization of polyamine blockers in the Kir channel inner cavity*

Numerous previous studies have worked towards mapping polyamine binding sites using charge introduction (with MTS modifying reagents) in the Kir channel inner cavity. Introduction of positive

charges deep in the inner cavity (between the rectification controller and the selectivity filter) causes dramatic reduction of polyamine affinity (Kurata et al., 2004). Furthermore, occupancy of spermine “protects” (slows the MTS modification rate of) cysteines substituted in this deep region of the inner cavity, while cysteines substituted on the cytoplasmic side of the rectification controller are only protected by long polyamine analogs (Chang et al., 2003; Kurata et al., 2006). Lastly, a recent study in Kir2.1 channels demonstrated that introduction of positive charges at shallow positions on the cytoplasmic side of the inner cavity had no effect on spermine affinity, but introduced kinetic barriers to blocker migration (Kurata et al., 2010b). Overall, these findings strongly support the notion that spermine occupies a deep position in the inner cavity.

Is it possible to resolve the idea of a deep binding site with findings that spermine need not enter the selectivity filter to generate steeply voltage-dependent block? For reasons that are not always clear, interpretation of blocker binding data generally depicts spermine and other polyamine analogs as fully extended linear structures (Guo and Lu, 2003; Shin and Lu, 2005; Chang et al., 2003; John et al., 2004). However, these are extremely flexible compounds with numerous torsionable bonds and a large conformational space that can be occupied. For example, previous attempts at docking spermine into models of Kir channel pores generated predominantly coiled and kinked structures of spermine (Kurata et al., 2008), and there is little reason to doubt that the diamine analogs used here (with fewer charges than spermine) will not occupy similar non-linear conformations that can be accommodated in the Kir inner cavity. An obvious future direction, explored in the next chapter, will be to use similar MTS-reagent mapping approaches on the sterically expanded polyamine blockers to derive some structural constraints on their binding sites, and compare these to spermine.

#### *Modeling polyamine block with a 3-state 2-step model*

We tested the viability of a previously described sequential model of polyamine block in predicting the unique biphasic feature of blocking kinetics for the largest polyamine analogs. A simple way to interpret the biphasic nature is to understand that there is a voltage-dependent balance between two blocking steps, O-OB1 and OB1-OB2, and the overall relaxation is affected by both rates. Their relative contributions will vary, because of their disparate effective valences. Transition from O to OB1 at the

low-affinity CTD binding site had shallow voltage-dependence and that from OB1 to OB2 at the high-affinity inner cavity site had steep voltage-dependence. Therefore, at the highest voltages examined, the O-OB1 transition becomes rate-limiting and controls the blocking rate of the system. At intermediate voltages the OB1-OB2 rate becomes much slower, and while it does not map linearly to the relaxation rate of the whole system, its contributions generate a deviation from a linear blocking rate/voltage relationship (on log scale). The most straightforward conclusion to draw from these findings is that steric expansion of the blocker termini affects multiple barriers encountered as the blocker migrates through the Kir channel pore. The simulations demonstrated that the biphasic rate plots for the analogs can be reproduced by increasing the energetic barriers of both blocking steps, indicative of the steric barrier introduced by bulky terminal amine groups.

## Conclusion

In this study, we discerned detailed biophysical aspects of polyamine block in the inward rectifier Kir2.1. Polyamines can achieve the characteristic steep voltage-dependence of block without having to enter the selectivity filter of the channel where most of the membrane field is dissipated. High-affinity block was relieved by increasing  $[K^+]_o$ , indicating that competition with a polyamine for the internal binding site of the filter is not required to generate the  $[K^+]_o$ -dependence of polyamine block. Finally, kinetic modeling revealed that a previously described 3-state 2-step model can be extended to describe the sterically expanded family of polyamine blockers used in this study, and demonstrated that migration of these blockers is hindered at several locations along the length of the channel pore.

## Tables and figures

**TABLE 1. Voltage-dependence ( $z\delta$ ) of polyamine block in Kir2.1.** Conductance-voltage curves (Figure 2) were fitted with Boltzmann parameters and  $z\delta$  was derived. Voltage-dependence was nearly the same among analogs.

Polyamine	Diamine decane	Bis-TMA-C10	Bis-QUIN-C10	Bis-TEA-C10
$z\delta \pm \text{SEM (n)}$	$4.2 \pm 0.1 (10)$	$4.6 \pm 0.1 (6)$	$4.4 \pm 0.1 (10)$	$4.4 \pm 0.1 (7)$

**TABLE 2. Parameters for a 3-state 2-step model of polyamine block of the inward rectifier Kir2.1.** Blocking ( $k_1$ ,  $k_2$ ), unblocking ( $k_{-1}$ ,  $k_{-2}$ ) rate constants, and voltage-dependence ( $z\delta_1$ ,  $z\delta_{-1}$ ,  $z\delta_2$ ,  $z\delta_{-2}$ ) for 3 polyamines are tabulated. All  $k$  values were rates at 0 mV,  $k(0\text{mV})$ . Exp = experimentally derived, Sim = simulation parameters. Some parameters for diamine decane could not be derived from data.

	Diamine decane		Bis-TMA-C10		Bis-QUIN-C10		Bis-TEA-C10	
	Exp	Sim	Exp	Sim	Exp	Sim	Exp	Sim
$k_1$ ( $\mu\text{M}^{-1}\text{s}^{-1}$ )	$2.4 \times 10^2$	$2.4 \times 10^2$	39	39	1.0	1.0	0.49	0.49
$k_{-1}$ ( $\text{s}^{-1}$ )	$1.4 \times 10^2$	$2.4 \times 10^2$	$1.4 \times 10^5$	$2.0 \times 10^4$	$4.0 \times 10^2$	$4.0 \times 10^2$	$1.6 \times 10^2$	$1.0 \times 10^2$
$z\delta_1$	0.14	0.14	0.22	0.22	0.56	0.58	0.45	0.45
$z\delta_{-1}$	-0.37	-0.37	-0.56	-0.22	-0.14	-0.22	-0.16	-0.22
$k_2$ ( $\text{s}^{-1}$ )	-	25	$8.3 \times 10^2$	$2.2 \times 10^2$	25	5.5	3.1	3.0
$k_{-2}$ ( $\text{s}^{-1}$ )	-	25	16	15	1.4	1.4	0.29	0.30
$z\delta_2$	-	1.5	1.7	1.8	1.2	2.4	1.6	2.4
$z\delta_{-2}$	-	-2.1	-1.7	-1.5	-1.5	-1.6	-1.7	-1.7

**TABLE 3. Ratio of experimental to simulation parameters.** All  $k$  values compared were rates at 0 mV,  $k(0\text{mV})$ . Ratios closer to 1 indicate a better match. Some parameters for diamine decane could not be obtained from experimental data.

	Diamine decane	Bis-TMA-C10	Bis-QUIN-C10	Bis-TEA-C10
$k_1$	1.0	1.0	1.0	1.0
$k_{-1}$	0.58	7.0	1.0	1.6
$z\delta_1$	1.0	1.0	0.97	1.0
$z\delta_{-1}$	1.0	2.5	0.64	0.73
$k_2$	-	3.8	4.5	1.0
$k_{-2}$	-	1.1	1.0	0.97
$z\delta_2$	-	0.94	0.5	0.67
$z\delta_{-2}$	-	1.1	0.94	1.0

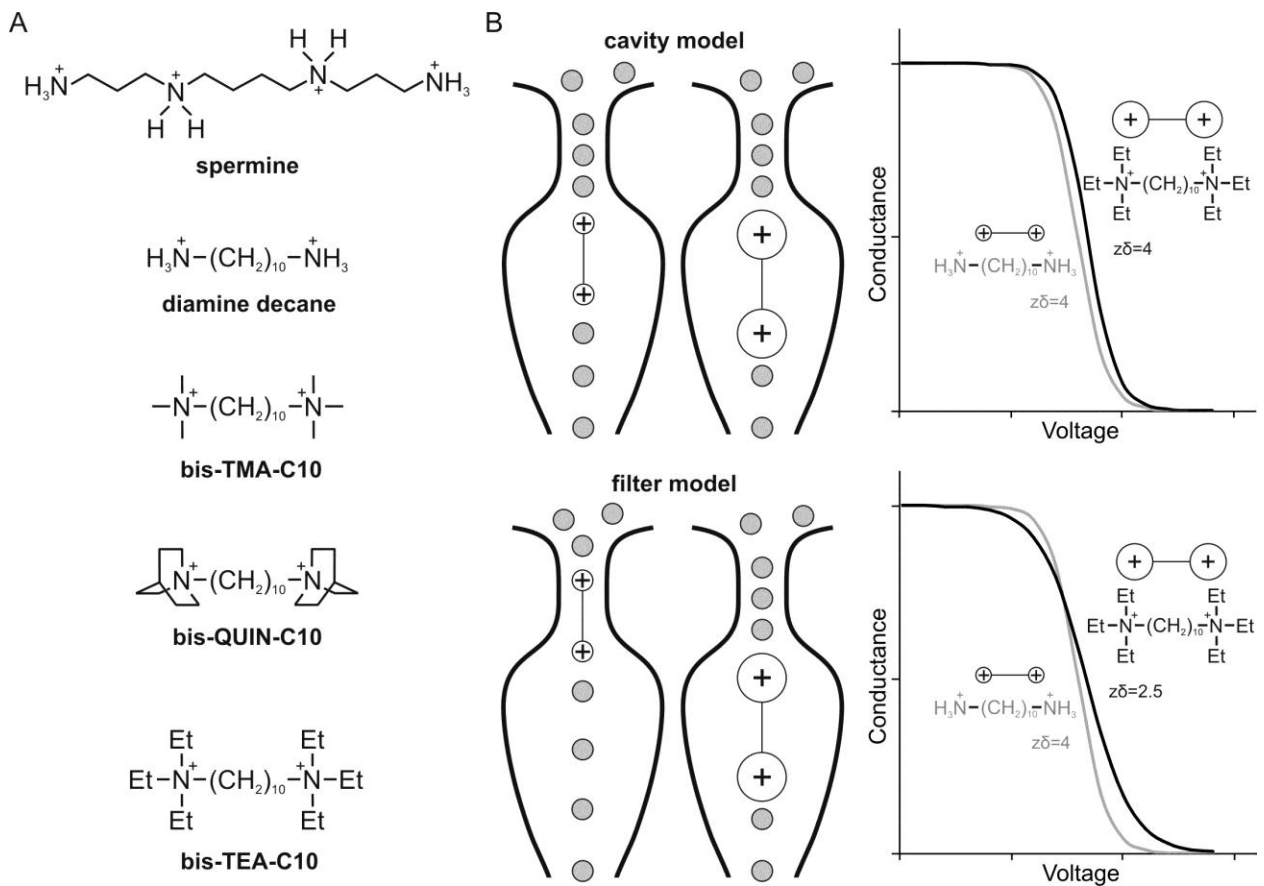


**FIGURE 1. Determination of the position of polyamine binding site in the Kir2.1 inner cavity.** *A.* Structures of polyamine analogs used to probe the location of the binding site. Naturally occurring spermine is shown for comparison. *B.* Schematics showing two models of polyamine binding. Gray circles represent K<sup>+</sup> ions. In the cavity model, increasing the blocker's terminal amine size does not affect binding, reflected by the same voltage dependence ( $z\delta$ ) among analogs. In the filter model, increasing blocker size eventually prevents binding in the sterically constrained selectivity filter, reflected by a lower  $z\delta$ . Representative plots to the right show arbitrary  $z\delta$  and that very similar  $z\delta$  can be clearly differentiated.

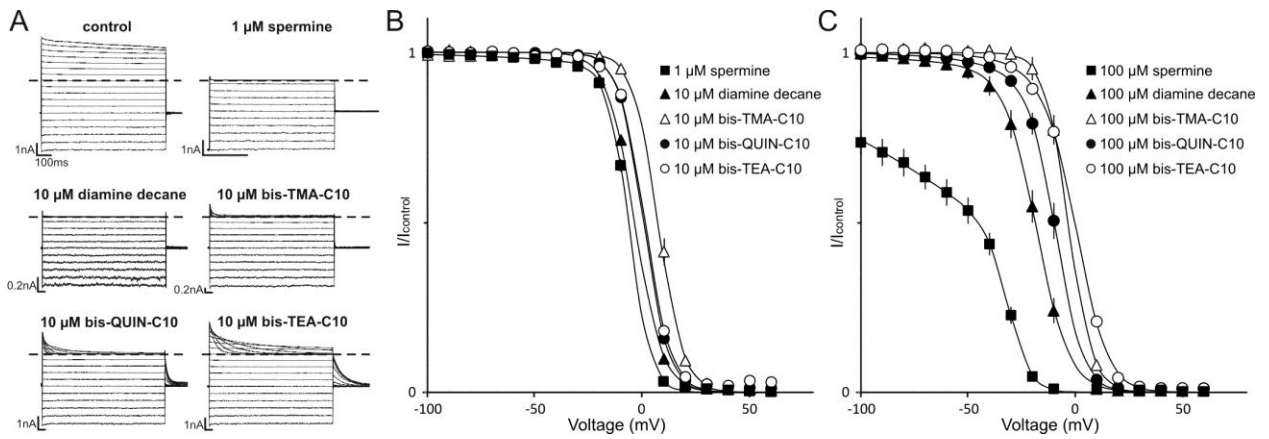


**FIGURE 2. Conductance-voltage relationship for polyamine block in Kir2.1.** A. Current traces from inside-out patches. Voltage-steps were in increments of +10mV starting from -100mV; holding potential was -50mV. Dashed line represents the reversal potential of 0mV. Control solution had no polyamines. Outward currents were blocked but more slowly with larger polyamines. When the steady state was not achieved, as for example with bis-TEA-C10, a longer protocol was used. B. Conductance-voltage curves (mean  $\pm$  SEM, n = 3-6) showing the same voltage-dependence (Table 1) among analogs. Spermine was more potent than the analogs. C. Conductance-voltage curves (mean  $\pm$  SEM, n = 5) with a high concentration of polyamines showing the development of a shallow phase.

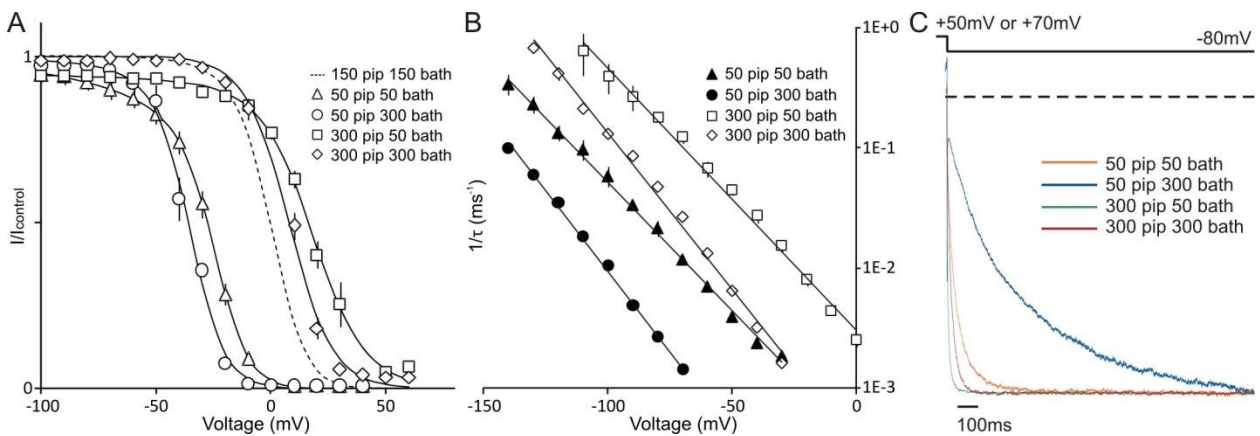


**FIGURE 3. Effects of varying internal and external  $K^+$  concentrations on polyamine affinity and unbinding kinetics.** 100  $\mu$ M Bis-TEA-C10 was used for these experiments. 50 and 300 represent  $K^+$  concentrations in mM; pip = pipette/external solution, bath = bath/internal solution. A. Conductance-voltage curves (mean  $\pm$  SEM, n = 3-4) showing that affinity depended largely on external  $K^+$  concentration. For reference, dashed line represents best-fit curve for symmetric  $K^+$  concentration of 150 mM. B. A plot of unblocking rate vs voltage (mean  $\pm$  SEM, n = 3-4). Lines are best-fit curves. C. Overlays of normalized current traces from inside-out patches showing time course of unblock. Channels were blocked at a depolarizing voltage and then stepped to -80 mV. Dashed line represents the reversal potential of 0 mV.

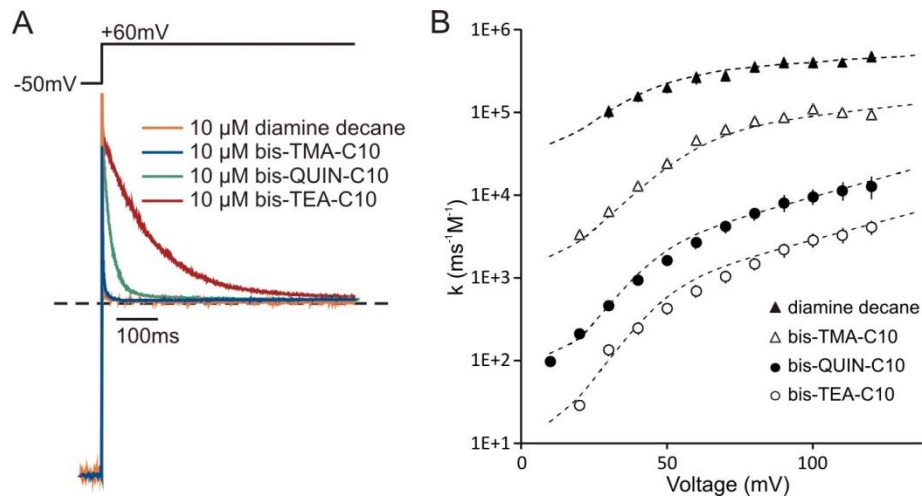


FIGURE 4. **Polyamine blocking kinetics in Kir2.1.** *A.* Overlays of normalized current traces from inside-out patches showing the time course of polyamine block. The membrane voltage was held at -50 mV and then stepped to +60 mV. Dashed line represents the reversal potential of 0 mV. Larger blockers blocked more slowly. *B.* A plot of concentration-normalized blocking rate vs voltage (mean  $\pm$  SEM,  $n = 3-14$ ). Dashed lines are simulated data generated from a 3-state 2-step model where parameters were constrained based on experimental data.

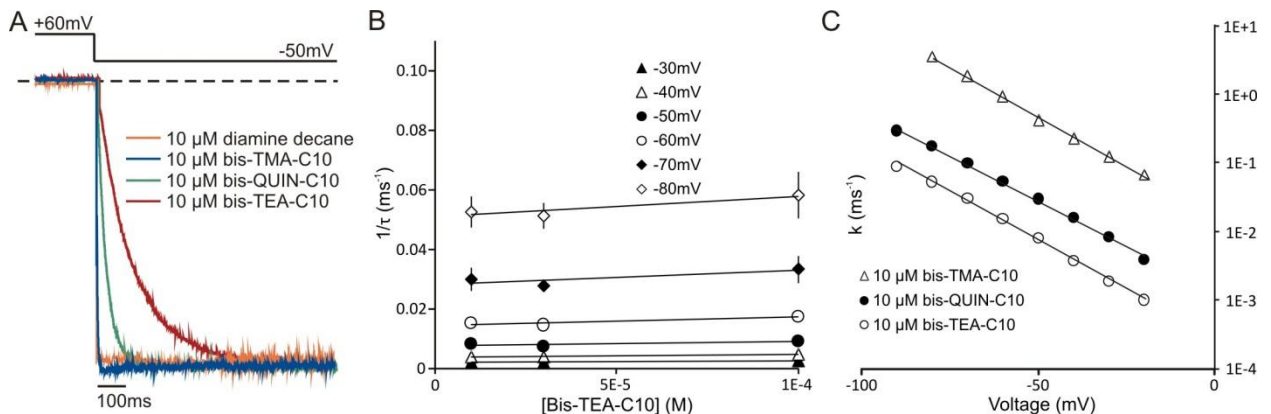


FIGURE 5. **Polyamine unbinding kinetics in Kir2.1.** *A.* Overlays of normalized current traces from inside-out patches showing time course of polyamine unblock. Channels were blocked at +60 mV and then stepped to -50 mV. Dashed line represents the reversal potential of 0 mV. Larger blockers unblocked more slowly. *B.* A plot of unblocking rate vs blocker concentration (mean  $\pm$  SEM,  $n = 4-5$ ). Bis-TEA-C10 is shown here to indicate that unblocking rates were concentration-independent. Lines are best-fit curves. *C.* A plot of unblocking rate vs voltage (mean  $\pm$  SEM,  $n = 4-6$ ). Rates for diamine decane were too fast to accurately measure and therefore not available. Lines are best-fit curves.

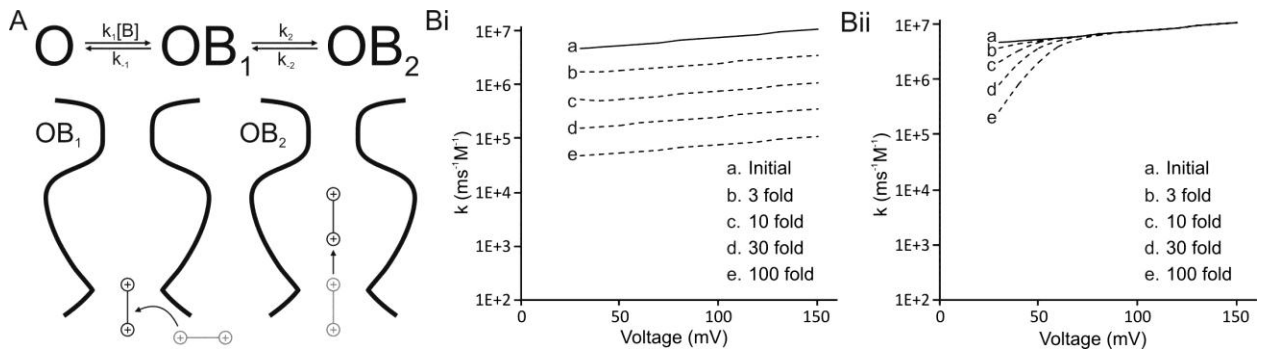


FIGURE 6. A 3-state 2-step model of polyamine block. A. Schematic model showing 3 channel states, open (O) and 2 open-blocked (OB1,2); polyamine blocking and unblocking kinetics are dictated by the four voltage-dependent rate constants where the first blocking step is also dependent on blocker concentration [B]. Bi. Control simulations were done starting with very fast rates (solid line). Progressively slower rates (dashed lines) were achieved by decreasing  $k_1$  and  $k_{-1}$  by the same factor (x-fold). Bii. By decreasing  $k_2$  and  $k_{-2}$  by the same factor (x-fold), the biphasic nature was generated.

## CHAPTER II

### Chemical Basis For High-Affinity Polyamine Block In The Inner Cavity Of Kir2.1

Polyamine block in Kir2.1 is well described by kinetic models involving at least two transitions. The initial low-affinity blocking step involves weakly voltage-dependent interactions with pore-lining acidic (E224, D255, D259, E299) and aromatic (F254) residues in the CTD (Pegan et al., 2005; Kurata et al., 2007; Fujiwara and Kubo, 2006). This is followed by a steeply voltage-dependent transition to a high-affinity binding site that depends strongly on the presence of an aspartate in the inner cavity, D172 (Matsuda et al., 2003; Wible et al., 1994; Xie et al., 2002; Lopatin et al., 1994). There is ample evidence that D172 is crucial for high-affinity block, but less is known about the specific chemical interactions between this residue and polyamines. Overall, a pore-lining acidic side-chain in the inner cavity appears to be necessary and sufficient to produce high polyamine sensitivity (Kurata et al., 2004). Weak rectifiers possess a neutral side-chain at the rectification controller (N171 in Kir1.1 and N160 in Kir6.2), but strong rectification can be reconstituted by substitution of an acidic side-chain at this position or elsewhere in the inner cavity (Shyng et al., 1997a; Wible et al., 1994; Lu and MacKinnon, 1994).

A generally accepted hypothesis is that electrostatic interactions underlie high-affinity polyamine binding in the inner cavity, presuming that D172 carries a negative charge at physiological pH. However, there is no reliable measurement of the pKa of this pore-lining aspartate, and it is notable that close proximity of acidic side-chains can dramatically alter their pKa (Lindman et al., 2007; Khurana et al., 2011). Most convincingly, single-channel recordings of the inherently cation-selective nAChR pore have demonstrated significant pKa shifts of substituted acidic side-chains well into the physiological pH range (Cymes and Grosman, 2011). Thus, many questions persist relating to whether D172 is predominantly charged (deprotonated) in the inner cavity environment, and what role other chemical forces may have in mediating high-affinity block.

In this study, we investigated the chemical details of polyamine block of Kir2.1 channels, with a focus on examining the role of hydrogen bonding between D172 and polyamine blockers. A series of methanethiosulfonate (MTS) reagents were used to introduce positive amine moieties one helical turn

below (i.e. closer to the cytoplasmic side) D172 to explore whether disruption of hydrogen bonding capability compromises polyamine block. We also synthesized and characterized the inward rectification properties of a hydrogen bond-deficient spermine analog to dissect the contributions of electrostatic and hydrogen bond interactions between D172 and the polyamine blocker. Our findings highlight the importance of chemical interactions between blockers and pore-lining residues.

## **Materials and methods**

### *Kir2.1 channel constructs*

All experiments were done using the IRK1J background channel. Construct preparation is the same as described in Chapter I. MTS modification experiments were done using IRK1J dimers with F254A (in both subunits, to abolish low affinity polyamine block) and I176C (in one subunit, to control the stoichiometry of MTS modification and prevent complete rundown of current). IRK1J dimers were constructed by PCR amplification of the appropriate mutant subunits to introduce a 6X-glycine linker sequence and BamHI restriction site at the C terminus of the first subunit in the dimer, and a BamHI site at the N-terminus of the second dimeric subunit. The subunits were subcloned into pcDNA3.1(-) in the pattern EcoRI – IRK1J[F254A] – 6X glycine – BamHI – IRK1J[I176C][F254A] - HindIII. The resulting tetrameric channel has F254A on four subunits and I176C on two subunits. Point mutations (D172N, I176C, F254A) were generated by PCR amplification of overlapping fragments in the region of the desired mutation, followed by subcloning into pcDNA3.1(-). All mutations and constructs were verified by restriction endonuclease digestion and third party DNA sequencing (Genewiz).

### *Cell culture*

TSA cells were transfected with channel cDNA (1-1.5 µg per 35 mm well) and GFP (250 ng/well) for ~24 hours using Lipofectamine 2000 (Invitrogen) or FuGENE 6 transfection reagents (Roche). Transfected cells were split onto sterile glass cover slips for easier transfer into the electrophysiological recording chamber and recordings were performed 16-48 hours later. TSA cells were cultured in DMEM high glucose growth media (Invitrogen), supplemented with 10% FBS and 1% penicillin-streptomycin, and incubated at 37C with 5% CO<sub>2</sub>.

## *Electrophysiology*

Inside-out patch clamp experiments were performed at room temperature in an ‘oil-gate’ chamber designed to enable rapid solution exchange, and prevent solution mixing (Kurata et al., 2011; Cannell and Nichols, 1991). Data were typically filtered at 2 kHz, digitized at 10 kHz, and stored directly onto the computer hard drive using Clampex software (Axon Inc.). Glass pipettes were pulled from soda-lime glass to a resistance of 1-2 M $\Omega$ . Pipette/external solution and bath/internal solution were: 140 mM KCl, 1 mM EGTA, 1 mM K<sub>2</sub>EDTA, 4 mM K<sub>2</sub>HPO<sub>4</sub>, pH 7.3 (using 1 mM KOH and 1 mM HCl). Polyamines were either purchased from commercial suppliers (spermine, 1,10-diaminedecane, decamethonium, from Fluka/Sigma-Aldrich), or synthesized in house at the University of British Columbia. Polyamines were maintained in frozen 10 mM stocks (in standard recording solutions, adjusted to pH7.3) and diluted to appropriate concentrations each experimental day. MTS reagents (Toronto Research Chemicals Inc.) were prepared as 10 mM stocks each experimental day, and were kept on ice throughout the day. Before each application, MTS reagents were diluted 10x in the standard recording solution and pipetted into one lane of the recording chamber. Channel modification was catalyzed by depolarizing voltage steps, until induced current reduction reached a clear steady state. Due to significant current rundown from MTS modification (~80% from MTSET, 70% from MTSED, 60% from MTSEM, and 40% from MTSEA), only inside-out patches with sizable currents (>2 nA at -80 mV in unmodified channels) were used for experiments.

## *Analysis*

Results were analyzed based on a 3-state 2-step model of polyamine block introduced previously (Shin and Lu, 2005; Kurata et al., 2007). The channel has an open (O) state and 2 blocked (OB<sub>1,2</sub>) states. Equilibrium between O and OB<sub>1</sub> is described by the equilibrium constant  $K_1 = k_f[B]/k_{-1}$ , a ratio of forward and backward rate constants, where [B] is the polyamine concentration; similarly, the equilibrium between OB<sub>1</sub> and OB<sub>2</sub> is described by  $K_2 = k_2/k_{-2}$ . Conductance-voltage curves that appeared to lack a shallow component were fitted with the function  $G = 1/(1 + K[B])$ ; if there was a shallow component, the curves were fitted with the two-component function  $G = 1/(1 + K_1[B] + K_1[B]K_2)$ . Equations were fitted to

experimental data through least sum of squares using Microsoft Solver. Throughout the text, data are presented as mean  $\pm$  S.E.M.

### *Molecular modelling*

Starting with the 'open' Kir2.2 (+ diC8-PIP<sub>2</sub>, pdb 3SPI), we built modified cysteine residues at residue I177 (equivalent to Kir2.1 I176) in two diagonally opposed subunits, to reflect the stoichiometry of channel modification used in the experiments. Schrodinger Maestro was used for all modification of molecular models. Structures containing introduced modified side chains were minimized until convergence using the Impact application of Maestro.

## **Results**

### *Effect on spermine affinity from I176C modification by MTS amines*

Previous reports have described the effects of MTS modification of numerous pore-lining residues on spermine block in Kir2.1 (Kurata et al., 2010b). The effects of modification of position I176C, one helical turn below the D172 rectification controller, depend on the chemical properties of the modifying reagent. Specifically, MTSEA (a primary, titratable amine) modification of I176C significantly reduces spermine affinity. In contrast, MTSET (a quaternary, permanently charged amine) modification of the same position has virtually no effect on spermine affinity, but hinders spermine entry into and exit from a deep inner cavity binding site (Kurata et al., 2010b). These divergent effects of MTSEA and MTSET, which introduce similar charges, but with different chemistry, motivate the idea that electrostatics are not the sole/primary determinant of polyamine blocker interactions in the Kir channel inner cavity.

We have further dissected the effects of MTS modification on spermine affinity with two additions to these previous reports. Firstly, we have examined the effects of I176C modification in the context of the F254A mutation, which strongly diminishes the weakly voltage-dependent component of spermine block arising from low-affinity interactions with the CTD (Shin et al., 2005). This manipulation isolates the deep binding equilibrium, allowing for clearer assessment of the effects of MTS modification. Secondly, we have examined an entire series of MTS modifiers, with progressive methylation of MTSEA, to MTSEM (secondary amine), MTSED (tertiary amine), and finally MTSET (quaternary amine) (Fig.

7A). These compounds have a progressively weaker propensity to donate a hydrogen bond, thus a weaker propensity to interact with carboxylate side-chains (Mavri and Vogel, 1994).

Modification of I176C with the methylated series of MTS reagents resulted in a range of disparate effects on spermine affinity and the kinetics of spermine block. In unmodified channels, spermine (100  $\mu$ M) inhibited outward current almost completely (Fig. 7B). We observed significant loss of spermine sensitivity after I176C modification with MTS reagents with the greatest potential for donating hydrogen bonds (MTSEA or MTSEM) (Fig. 7B,C). This was most apparent at intermediate voltage (-20 mV, -10 mV), where block of unmodified channels was nearly complete, but significant inward current was observed in channels modified with MTSEA or MTSEM (Fig. 7B). In contrast, channels modified with MTSED or MTSET were more potently inhibited by spermine at intermediate voltages. These different outcomes are emphasized by G-V curves, demonstrating that MTSEA or MTSEM modified channels require significantly more depolarized voltages to achieve the same extent of spermine block as seen in MTSED or MTSET modified channels (Fig. 7C).

The panel of MTS modifying reagents also had distinct effects on spermine unbinding rates, measured with hyperpolarizing steps to -50 mV following a depolarizing pulse (+30 mV) sufficient to block channels (Fig. 8). Specifically, MTSEA and MTSEM had no discernible impact on spermine unbinding, which remained extremely fast. However, both MTSED and MTSET modification dramatically slowed spermine unbinding by a comparable amount. Similar slowing of spermine unbinding has been reported in wild-type (WT) Kir2.1-I176C dimers (with F254), with the cytoplasmic shallow binding site still intact (Kurata et al., 2010b). These effects of cysteine modification cluster much like effects on steady state spermine block (above), with MTSEA/M having clearly different effects from MTSED/T. The slow spermine unbinding rate in I176C-MTSET modified channels can be well-modeled by increasing the energetic barrier between the shallow and deep binding sites, resulting in a slower blocker entry into and exit from the deep site (Kurata et al., 2010b). In contrast, rapid spermine unbinding and weaker spermine affinity in MTSEA/M modified channels indicate disruption of deep spermine binding.

### *Energy-minimized models of dimeric MTS modified channels*

We generated energy-minimized models of MTSEA and MTSET modified channels based on recently reported crystal structures of the closely related chicken Kir2.2 channel (Hansen et al., 2011). For both MTSET (Fig. 9A) and MTSEA (Fig. 9B), one introduced an amine oriented close to the D172 rectification controller, while the other pointed down and away towards the cytoplasmic side of the inner cavity. Although the overall arrangement of the modifiers was similar, several salient features are notable. Most importantly, the MTS reagents were nestled between two D172 residues from adjacent subunits, allowing for a “bidentate” interaction with D172. This interaction will be much more prominent for MTSEA (or MTSEM, each with the potential to engage in multiple hydrogen bonds), and this is reflected in the minimized model, as the MTSEA amine was oriented in very close proximity ( $<3.5$  Å) from each of its partner D172 side-chains. In contrast, the MTSET amine was oriented slightly closer to the center of the pore (farther away from each D172); due to a weakened electrostatic attraction with delocalized charge of the quaternary ammonium, and potentially steric clashes preventing the bulky modifier from closely engaging D172 (each D172 carries a charge of -1 in the model). Overall, the predicted interaction of MTS modifiers with D172 side-chains from two neighbouring subunits is consistent with our experimental observation of the similar effects of MTSEA and MTSEM, but different when compared to MTSET (which cannot hydrogen bond) or MTSED (which cannot simultaneously engage neighbouring D172 residues). This is consistent with previous work suggesting that the potent effects of MTSEA reflect the similarity between the primary amine of the MTSEA moiety, and the terminal primary amines of spermine. Specifically, since MTSEA will mimic the chemical features of the spermine terminal amines, it will most effectively compete for the detailed inner cavity interactions (such as ionized hydrogen bonding with D172) essential for high-affinity polyamine block.

### *A hydrogen bond-deficient methylated spermine analog*

Our findings demonstrate that the charge of the MTS modifier does not determine its effect on spermine blocking potency and kinetics. Rather, the effects of the modifiers appear to be related to their ability to engage carboxylate side-chains of D172, potentially forming ionized hydrogen bonds. To further explore the chemical determinants of spermine interactions in the Kir2.1 inner cavity, we

synthesized and characterized a hydrogen bond-deficient analog decamethylspermine (Me<sub>10</sub>-spermine, Fig. 10A). Me<sub>10</sub>-spermine (1 μM) inhibited IRK1J channels less potently than spermine (1 μM), with a 24 ± 2 mV shift in the V<sub>1/2</sub> of block (Fig. 10B,C). Furthermore, Me<sub>10</sub>-spermine block exhibited a smaller effective valence compared to spermine.

We also examined the effects of spermine and Me<sub>10</sub>-spermine in Kir2.1[D172N] channels, a frequently used mutation that weakens spermine binding in the deep inner cavity binding site (Fig. 10B,C)(Wible et al., 1994;Lopatin et al., 1994). Although the substituted asparagine amide functional group retains a propensity to accept hydrogen bonds (through the amide carbonyl), it will be unable to form ionized hydrogen bonds proposed to mediate interactions between D172 and spermine. Furthermore, the N-H bonds of the amide functional group possess a dipole moment that may cause a hydrogen bond “clash” with other hydrogen bond donors like from spermine. As expected, the D172N mutation considerably weakened spermine block (some outward currents were apparent in 1 μM spermine, Fig. 10B, bottom middle). However, Me<sub>10</sub>-spermine block was largely unchanged in D172N relative to WT channels (Fig. 10B, right). These properties are most apparent in G-V curves (Fig. 10C) with the V<sub>1/2</sub> of spermine block shifted by (21 ± 1) mV by the D172N mutation, while Me<sub>10</sub>-spermine block was shifted by only (4 ± 3 mV). The principal implication of this experiment is that charge interactions are likely not the sole contributors to high-affinity polyamine block because the blockers were affected very differently when the influence of the potential D172 charge was removed. Furthermore, in the absence of an ionized hydrogen bonding partner, spermine and Me<sub>10</sub>-spermine inhibited the channel with similar potency.

#### *Effect of MTS modification on polyamine analogs*

We further investigated polyamine interactions in the Kir channel inner cavity by examining the effects of MTS modification (in I176C dimeric channels) on the blocking properties of numerous spermine analogs. An initial prediction for these experiments is that hydrogen bond-deficient analogs might have a less disparate response to MTSEA vs MTSET. We examined Me<sub>10</sub>-spermine, and also a series of diamine analogs with varying methylation of their terminal amines: 1,10-diaminodecane (diamine decane), 1,10-bis-trimethylaminodecane (bis-TMA-C10, also known as decamethonium), and 1,10-bis-triethylaminodecane (bis-TEA-C10) (Fig. 11A). In raw current records, it was apparent that for

all of the analogs examined, block was considerably weakened and in many cases, significant outward current appeared after MTSET modification (Fig. 11B). This was significantly different from spermine block, which was only marginally affected in MTSET modified channels (compare with Fig. 7B,C). Inspection of mean data in G-V curves clarifies that MTSET and MTSEA modification produced similar shifts in Me<sub>10</sub>-spermine affinity, consistent with the notion that the inability of Me<sub>10</sub>-spermine to hydrogen bond renders this blocker less sensitive to the chemical differences between MTSET and MTSEA modifiers. With all of the diamine analogs, MTSET consistently weakened block more prominently than MTSEA (Fig. 11C). This observation diverges significantly from the effects of these modifying reagents on spermine block (Fig. 7), suggesting important differences between the interactions of spermine vs diamine analogs with the Kir inner cavity.

We also examined the effects of MTS modification on unbinding rates of the polyamine analogs. As previously mentioned, spermine unbinds very slowly after MTSET modification of I176C (Fig. 8). In contrast, this was not observed for the diverse analogs examined. Me<sub>10</sub>-spermine was the only analog that exhibited any convincingly slow unbinding after MTSET modification, although unlike spermine, slow kinetics only accounted for a small fraction of the tail current amplitude (Fig. 12). Unlike the dramatic slowing of spermine unbinding, MTSET caused very little slowing of the unbinding rates of diamine analogs. For analogs with inherently slow unbinding kinetics (i.e. bis-TEA-C10), we could convincingly resolve that modification modestly accelerated blocker unbinding (Fig. 12, bottom right). These findings generate two important implications. Firstly, the different effects of MTS modification on diamine analogs relative to spermine indicate that this method reveals some important differences in specific details of binding of these polyamines in the Kir channel pore. Secondly, the blocker-specific effects of MTS modification indicate that their effects are primarily due to interactions with channel blockers, rather than indirect effects arising from reduced K<sup>+</sup> permeation (see Chapter II Discussion).

## Discussion

In many excitable tissues, inward rectification is essential to remove the repolarizing influence of Kir channel opening around the RMP, and allow action potential generation. The essential physiological role of inward rectification is revealed in some forms of short QT syndrome (SQT3) in which mutations

like D172N generate a GOF phenotype and accelerate the rate of repolarization of the cardiac action potential (Priori et al., 2005; El et al., 2009). In this study, we used synthetic spermine analogs and the disease mutant channel D172N to probe the chemistry behind high-affinity polyamine block. We have also investigated the interactions of spermine and other polyamine analogs with tethered amine “competitors” in the Kir channel inner cavity, to study the detailed blocker-channel interactions underlying inward rectification.

Our results suggest a model to explain different functional outcomes of MTS modification experiment involving spermine (Fig. 13A) vs various diamine analogs (Fig. 13B). Spermine is stabilized deep in the inner cavity by the ring of D172 side-chains, and this is likely enabled by the multiple charged amines in this unique blocker. When MTSEA is introduced one helical turn below, it efficiently interacts with D172 carboxylates (competing with spermine), but does not directly interact with deeply bound spermine to perturb its stability. This proposal of an “indirect” mechanism for the effects of MTS reagents on spermine is motivated by the observation that the effects of I176C modification are highly chemistry-dependent, as MTSET had virtually no effect on spermine affinity (Fig. 7B,C). The direct implication of this observation is that the deep spermine binding site does not significantly overlap with Kir2.1 residue 176, and that the effects of MTS modification of 176 depend on the modifying reagent’s interactions with the rectification controller, rather than the blocking polyamine. Since the quaternary amine of MTSET does not interact well with D172, it cannot disrupt spermine binding by this “indirect” destabilization mechanism. However, this bulky modifier can “lock in” deeply bound spermine leading to extremely slow spermine unbinding (Fig. 8, 13A). This dichotomy between MTSEA and MTSET effects was not observed for the diamine analogs or Me<sub>10</sub>-spermine (Fig. 11, 12). Since diamine analogs bind with lower affinity in the deep site, we suggest that they may transition to a lower position in the inner cavity, overlapping frequently with I176C. MTS modifiers at I176C will directly interact with these lower affinity blockers, causing a decrease in affinity that is relatively independent of the chemical features of the modifier (Fig. 13B).

### *D172N and a hydrogen bond-deficient blocker provide insight into molecular mechanism*

To investigate the importance of the hydrogen bonding propensity of the blocker, we synthesized and characterized Me<sub>10</sub>-spermine, a hydrogen bond-deficient analog closely related to spermine. Relative to spermine, Me<sub>10</sub>-spermine inhibited WT Kir2.1 channels with both a weaker affinity (reflected by a right-shifted V<sub>1/2</sub>) and a smaller effective valence (reflected by a shallower slope of the G-V curve). Several factors can contribute to the lower affinity of Me<sub>10</sub>-spermine, including steric effects of permethylation, or delocalization of charge across multiple methyl groups. However, we find results from the D172N mutant channel to be the most informative. Most importantly, coulombic interactions in the inner cavity are virtually eliminated, but this had barely detectable effects on potency of Me<sub>10</sub>-spermine block. This finding suggests that despite its significant positive charge (+4), direct charge-charge interactions with D172 play a minor role in determining Me<sub>10</sub>-spermine affinity for the channel - Me<sub>10</sub>-spermine affinity is the same with or without D172. Spermine, in contrast, would be capable of forming ionized hydrogen bonds with D172, and so we speculate that the weakening of this chemical interaction by the D172N mutation is the primary cause of the weakened spermine affinity.

As described previously, the Kir2.1 polyamine binding site is somewhat “resilient” in the sense that relatively high affinity blockade is preserved even in the absence of an inner cavity carboxylate (Lopatin et al., 1994;Wible et al., 1994). In contrast, Kir6.2 channels exhibit virtually complete spermine insensitivity in the absence of an aspartate or glutamate in the inner cavity (Shyng et al., 1997a). This difference is likely due to the richly electronegative pore of the Kir2.1 CTD that exerts a stabilizing effect on deep blocker binding (Robertson et al., 2008). Kir6.2 channels contrast significantly: with N160 in the inner cavity and the absence of these CTD residues (S225 N242 G243 N247 in Kir6.2 instead of E224 F254 D255 D259 in Kir2.1 respectively), there is complete absence of spermine sensitivity (Shyng et al., 1997a;Kurata et al., 2004).

### *Chemical interaction of MTS modifiers and polyamine analogs*

Analogous to the differences between spermine and Me<sub>10</sub>-spermine, the panel of MTS reagents had a gradient of hydrogen bonding ability, and thus might interact differently with the rectification controller carboxylate side-chains. Much like Me<sub>10</sub>-spermine however, other features might contribute to weaker

“competition” for D172 binding by MTSET relative to MTSEA, including greater steric bulk and charge delocalization across methyl groups yielding a less focused charge. However, these confounding factors appear to be minor contributors when examined in the context of the multiple polyamine analogs used in this study. Most notably, Me<sub>10</sub>-spermine responded similarly to both MTSET and MTSEA modification of I176C. This observation indicates that when the hydrogen bonding propensity of spermine is removed, MTS modification has a similar effect regardless of bulk or charge delocalization. Phrased another way, these data indicate that because Me<sub>10</sub>-spermine cannot hydrogen bond, it is indifferent to which MTS reagent is introduced.

In contrast to spermine, blockade by the diamine analogs is clearly perturbed by MTSET, suggesting that the diamines may occupy space near I176C more frequently than spermine. An important implication of these data is confirmation that the slow unbinding of spermine (after MTSET modification) is not due to an indirect effect of ion permeation. One uncertainty arising from previous reports of dramatically slowed spermine kinetics (Kurata et al., 2010b) was that these effects arose from slower ion permeation (which is coupled to spermine block) after MTSET modification. If this was the case, all blockers would be predicted to exhibit substantial deceleration of unbinding. However, we demonstrate here that MTSET modification did not slow unbinding of diamines (instead, accelerated unbinding was observed where kinetics were possible to record). This seems best explained by frequent occupancy of a slightly shallower site by diamines resulting in direct interaction with MTS adducts at I176C (either MTSEA or MTSET). In this scenario, effects of modification on blocker affinity depend mostly on coulombic and steric interactions with MTS reagents, not their chemical properties (e.g. hydrogen bonding propensity).

## **Conclusion**

We have developed tools to probe the chemical details underlying high-affinity polyamine block of inward rectifier K<sup>+</sup> channels. We determined that formation of polarized hydrogen bonds is an important contributor to high-affinity polyamine block. Firstly, a hydrogen bond-deficient spermine analog (Me<sub>10</sub>-spermine) has weakened affinity relative to spermine, and is also insensitive to neutralization of D172 in the inner cavity (indicating a minor role for coulombic interactions). Secondly, MTS reagents with

stronger hydrogen bonding ability disrupted spermine block, while Me<sub>10</sub>-spermine blockade was insensitive to the hydrogen bonding propensity of the modifying reagent. These findings raise the possibility that direct charge interactions may not be essential for high-affinity spermine binding, motivating further investigation of the protonation state of the inner cavity aspartates in strong inward rectifiers.

## Tables and figures

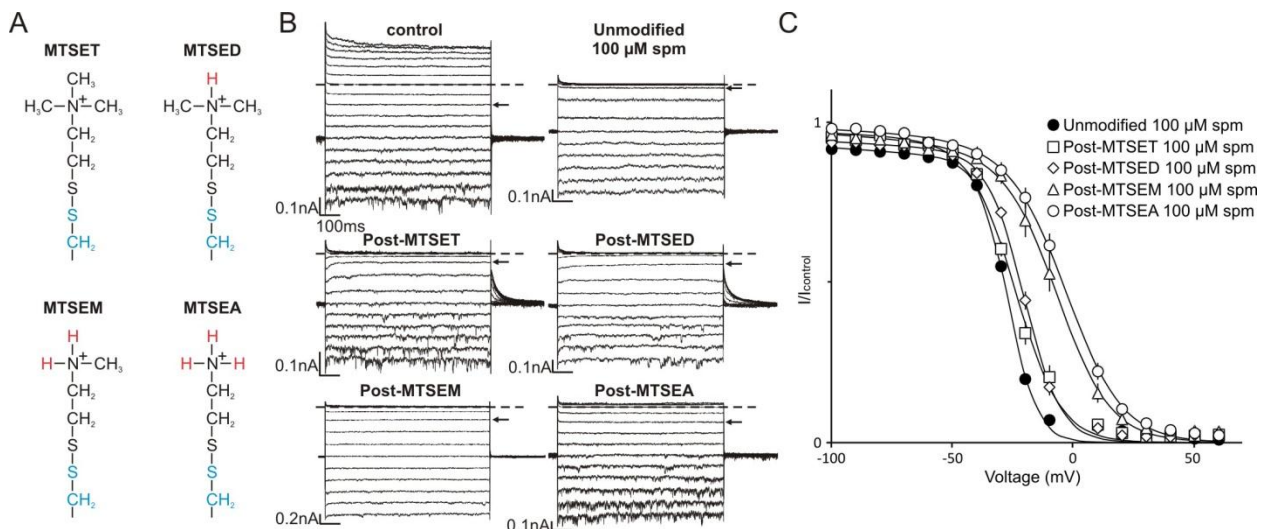


**FIGURE 7. Effects of MTS modification on spermine block in Kir2.1.** F254A I176C construct was used. **A.** Structures of MTS reagents used to modify residue I176C shown in blue. From MTSET to MTSEA, there is a progressive increase in hydrogen bonding capability indicated by increasing number of red hydrogen atoms. **B.** Current traces from inside-out patches. Voltage-steps were in increments of +10 mV starting from -100 mV; holding potential was -50 mV. Dashed line represents the reversal potential current at 0 mV. Control trace is representative showing the absence of polyamines and all other traces were recorded with 100 μM of spermine (spm). Arrows indicate steady state current at -20 mV showing progressive relief of block with MTS reagents having higher hydrogen bonding capability. **C.** Conductance-voltage curves (mean ± SEM, n = 3-6) showing the progressive decrease in spermine affinity across the series of MTS modifications of I176C.

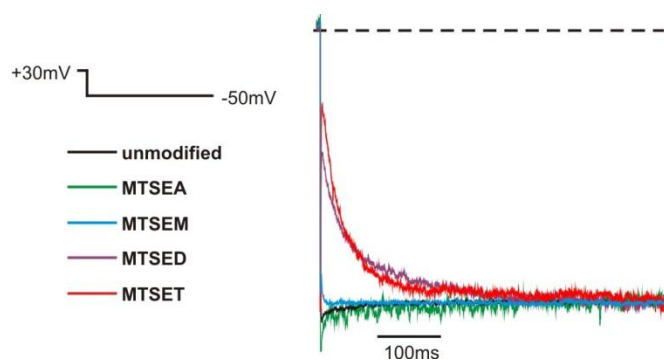


**FIGURE 8. Spermium unbinding kinetics after MTS modification.** F254A I176C construct was used. Tail current traces from inside-out patches were overlaid. Steady state block was achieved before stepping to -50 mV to observe the time course for blocker unbinding. Dashed line represents the reversal potential current at 0 mV. MTSEA and MTSEM minimally affected spermium unbinding (green and blue traces) while MTSED and MTSET dramatically slowed down unbinding rate (purple and red traces).

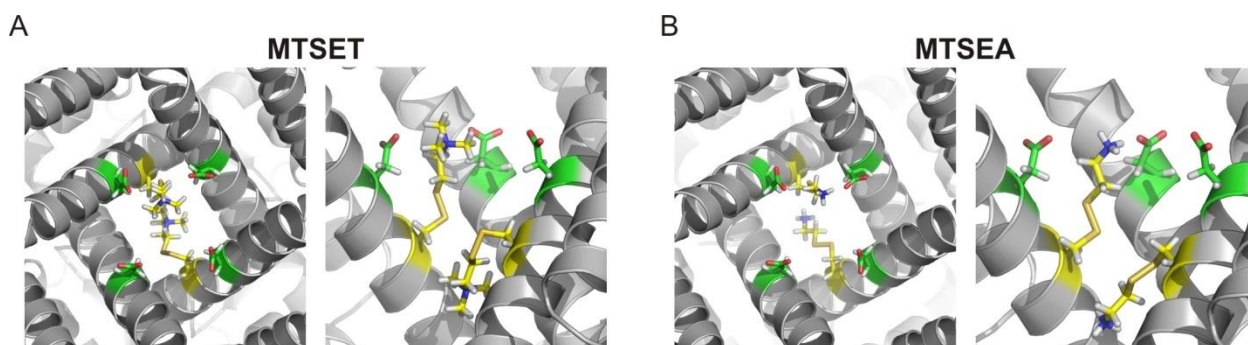


**FIGURE 9. MTS interactions with D172 in the inner cavity of Kir2.1.** Energetically minimized structural models showing how *A.* MTSET and *B.* MTSEA interact with D172 carboxylate side-chains (green). The left model in both sets is a top down view; the right is a side view with one channel subunit omitted. Methyl groups shield MTSET's nitrogen atom from D172. MTSET also seems to be less aligned with adjacent D172 side-chains than MTSEA.

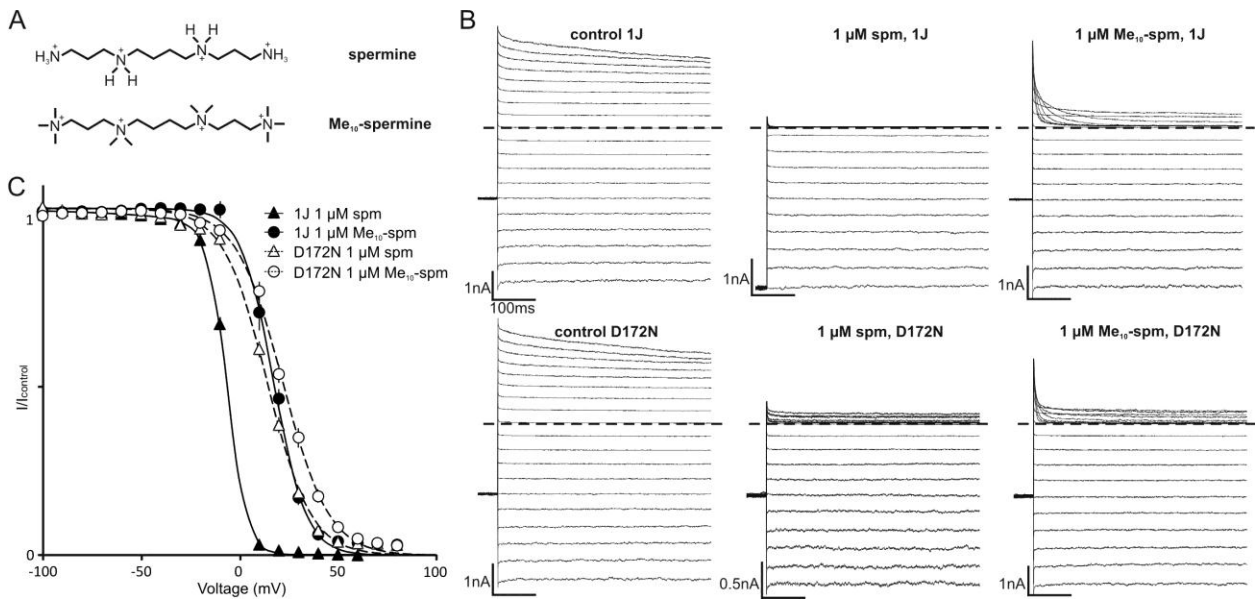


**FIGURE 10. High-affinity polyamine block in the D172N mutant.** *A.* Structures of spermine (spm) and its hydrogen bond-deficient analog decamethylspermine (Me<sub>10</sub>-spm). *B.* Current traces from inside-out patches. Voltage-steps were in increments of +10 mV starting from -100 mV; holding potential was -50 mV. Dashed line represents the reversal potential current at 0 mV. 1J represents the wild-type IRK1J channel. Control trace is representative showing the absence of polyamines. Traces in the presence of a blocker are representative and not necessarily from the same patch. D172N produced a greater effect with spermine than with the analog. *C.* Conductance-voltage curves (mean ± SEM, n = 4-5) showing that D172N produced a greater shift in spermine affinity than in Me<sub>10</sub>-spm affinity.

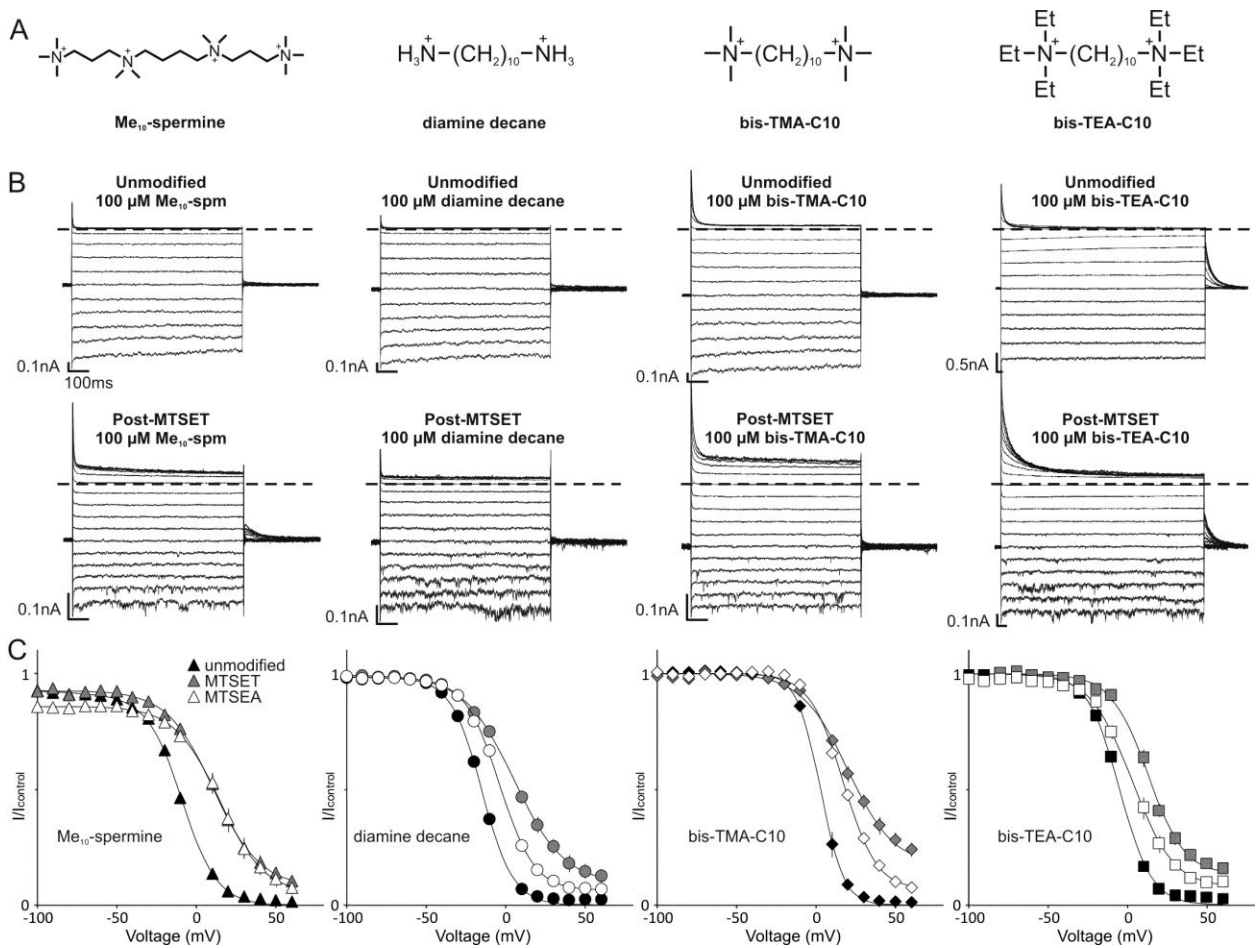


**FIGURE 11. Effects of MTS modification on polyamine block in Kir2.1.** F254A I176C construct was used. **A.** Structures of diamine analogs that are of similar length as spermine. **B.** Current traces from inside-out patches. Voltage-steps were in increments of +10 mV starting from -100 mV; holding potential was -50 mV. Dashed line represents the reversal potential current at 0 mV. Pre- and post-modification traces for each blocker are representative and not necessarily from the same patch. MTSET modification of I176C markedly decreased affinity of decamethylspermine ( $\text{Me}_{10}\text{-spm}$ ) and diamine analogs, and had varying effects on kinetics. **C.** Conductance-voltage curves (mean  $\pm$  SEM,  $n = 3\text{-}4$ ) for polyamine analogs. Black data points are for unmodified, gray for MTSET, and white for MTSEA.

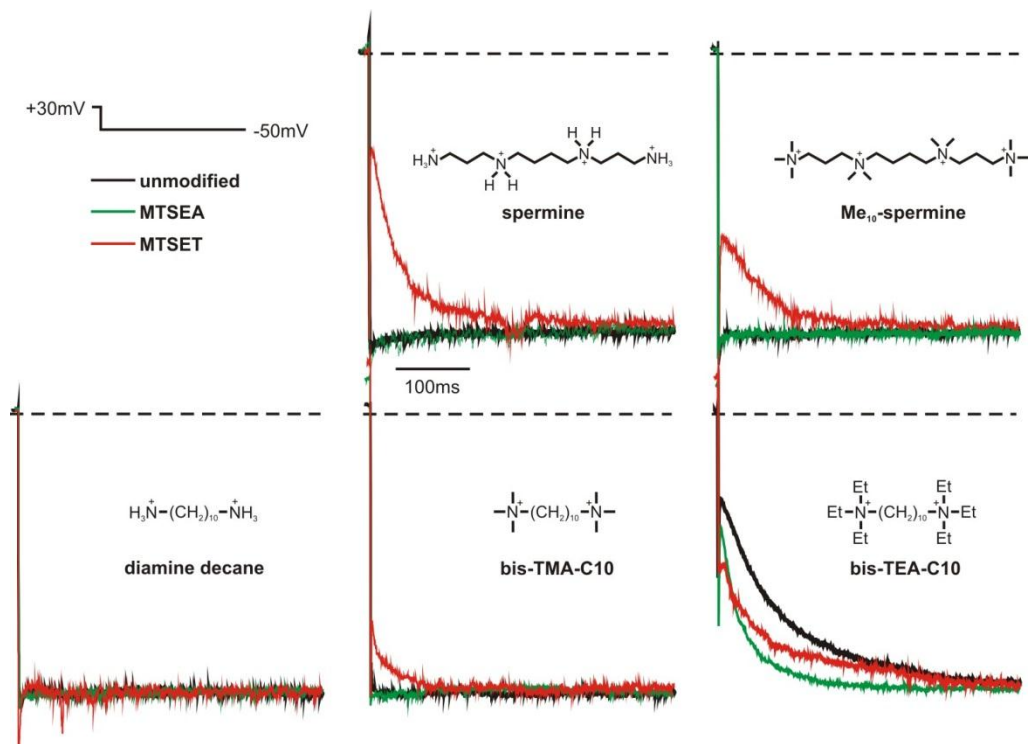


**FIGURE 12. Polyamine unbinding kinetics after MTS modification.** F254A I176C construct was used. Tail current traces from inside-out patches were overlaid. Steady state block was achieved before stepping to -50 mV to observe the time course for blocker unbinding. Dashed line represents the reversal potential current at 0 mV. MTSEA minimally affected blocker unbinding (green traces) except for bis-TEA-C10 where it increased unbinding rate. MTSET slowed down unbinding rate (red traces) for spermine and Me<sub>10</sub>-spermine but minimally affected the diamine analogs.

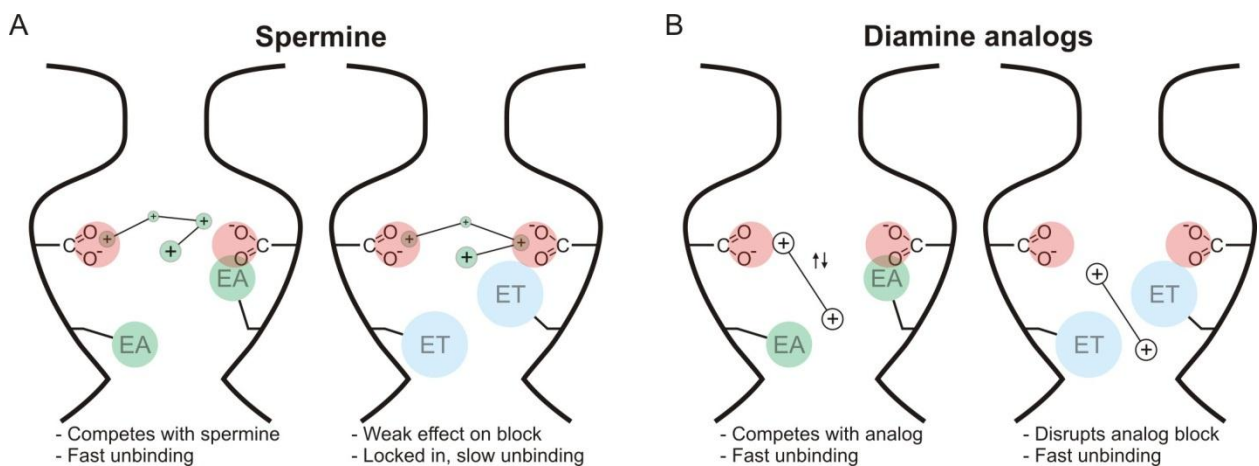


**FIGURE 13. Unique characteristics of spermine binding in the inner cavity.** Schematics showing our proposed explanation for observed results of high-affinity polyamine block. **A.** Spermine binds stably and deep in the inner cavity. The strong competitor MTSEA weakens spermine affinity while the weaker competitor MTSET minimally affects it. Spermine being locked in by the bulky MTSET elicits slow unbinding. **B.** Diamine analogs bind “loosely” in the inner cavity. Partial binding in a shallow position renders them susceptible to physical interference by MTSET. Analogues are no longer locked in by MTSET therefore eliciting fast unbinding.

## CHAPTER III

### Transduction Of Ligand-Binding To Channel Gating In The ATP-Sensitive Inward Rectifier Kir6.2

In addition to voltage-dependent block by  $Mg^{2+}$  and polyamines, some Kir channels are regulated by ligand-dependent gating that controls conformational changes around the helix bundle-crossing (in the TMD), and potentially a second auxiliary gate in the cytoplasmic G-loop (Pegan et al., 2006;Khurana et al., 2011;Hansen et al., 2011;Whorton and MacKinnon, 2011;Bavro et al., 2012). These ligand-dependent gating mechanisms act physiologically to influence or trigger cellular depolarization. One very well-known example is regulation of heart rate by the sino-atrial node  $I_{K,ACH}$  current (mediated by GIRKs)(Logothetis et al., 1987). A second example is regulation of glucose-stimulated insulin secretion by  $K_{ATP}$  channels – the pancreatic  $K_{ATP}$  isoform comprises Kir6.2 and SUR1 subunits, and is the model for ligand-dependent regulation used in the present study (Inagaki et al., 1995a;Aguilar-Bryan et al., 1995). When intracellular ATP concentrations are low,  $K_{ATP}$  channels exhibit significant open probability, causing membrane hyperpolarization and inhibition of insulin secretion. However, after a meal, glucose metabolism elevates intracellular ATP, leading to inhibition of  $K_{ATP}$  channels and membrane depolarization, triggering  $Ca^{2+}$  influx essential for insulin secretion.

In place of the voltage-sensing domain that typifies the voltage-gated Kv channel family, the Kir channel pore module is coupled to a CTD that extends the ion permeation pathway and serves as a ligand binding site for regulatory molecules like  $G\beta\gamma$  subunits (in Kir3 channels) or ATP (in Kir6 channels)(Whorton and MacKinnon, 2011;Nishida et al., 2007). In addition, all Kir channels require binding of  $PIP_2$  for channel activity, and recent crystallographic studies have demonstrated that the binding site for this essential phospholipid is formed predominantly by positively charged side-chains in the C-terminal end of the pore-lining M2 helix (Hansen et al., 2011;Whorton and MacKinnon, 2011).

This modular architecture necessitates a mechanism for transduction of ligand-binding to the channel gate. The observation of a transverse interfacial helix (slide helix) in Kir channel structures has provoked considerable speculation regarding its role as a mediator of coupling between the CTD and TMD, that is analogous to the S4-S5 linker as a coupling element for voltage-sensor movement and

channel gating in voltage-dependent ion channels (Long et al., 2005b; Lu et al., 2002; Batulan et al., 2010). Guided by recently reported structures of eukaryotic Kir channels, we have taken a systematic approach to investigate the role of the slide helix, and identify features that are essential for transduction of ligand-binding to the channel gate – the transduction of ATP-binding to closure of the Kir6.2 gate.

## **Materials and methods**

### *K<sub>ATP</sub> channel constructs*

All mutant channel constructs were generated from a mouse WT Kir6.2 gene expressed in the pcDNA3.1(-) plasmid (Invitrogen). All channel constructs had a C-terminal GFP tag fused to the Kir6.2 C-terminus by a 6X-glycine linker. Point mutations were introduced by overlapping PCR-based methods, followed by subcloning of desired fragments into pcDNA3.1(-), and verification by restriction endonuclease digestion and sequencing. SUR1 (hamster) and FLAG-SUR1 (a gift from Show-Ling Shyng, OHSU, Portland, Oregon) were expressed in the pECE vector.

### *Cell culture and electrophysiology*

COSm6 cells were maintained in culture in a 5% CO<sub>2</sub> incubator at 37 °C in DMEM supplemented with 10% FBS and penicillin/streptomycin. Cells were transfected with channel constructs and hamster SUR1 using either Fugene (Roche) or Lipofectamine 2000 (Invitrogen). Recordings were done 2-3 days following transfection.

For continuous recordings, data were filtered at 1 kHz, digitized at 5 kHz, and stored directly on a computer hard drive using Clampex software (Axon Inc.). For voltage-step recordings, data were filtered at 2 kHz and sampled at 10 kHz. The standard pipette (extracellular) and bath (cytoplasmic) solutions had the following composition: 140 mM KCl, 1 mM K-EGTA, 1 mM K-EDTA, and 4 mM K<sub>2</sub>HPO<sub>4</sub>. The solution pH was adjusted with KOH or HCl to the desired level. Because the recording solutions are not very strongly buffered, pH was verified each experimental day for each experimental solution, with particular attention to the addition of solutes that can affect solution pH (in this case, particularly ATP). Solutions were delivered at room temperature by pressure-driven flow (syringe pump) through a multi-

barrelled solution delivery turret, driven by the RSC-200 (BioLogic) rapid solution exchanger to enable solution jumps. Chemicals were purchased from Sigma-Aldrich or Fisher.

#### *Non-radioactive Rb efflux assay*

COSm6 cells were transiently transfected with SUR1 and various Kir6.2 mutants with Fugene (Roche) or Lipofectamine 2000 (Life Technologies), and efflux assays were performed after 2 days. Cells were loaded for 1 hour with Rb loading media (in mM: RbCl, 5.4; NaCl, 150; CaCl<sub>2</sub>, 2; NaH<sub>2</sub>PO<sub>4</sub>, 0.8; MgCl<sub>2</sub>, 1; glucose, 5; HEPES, 25; pH7.4), washed quickly (2X) with PBS, and incubated in assay buffer (in mM: 118 NaCl, 118; CaCl<sub>2</sub>, 2.5; KH<sub>2</sub>PO<sub>4</sub>, 1.2; KCl, 4.7; NaHCO<sub>3</sub>, 25; MgSO<sub>4</sub>, 1.2; HEPES, 10; pH 7.4) with metabolic inhibitors (2.5 µg/mL oligomycin, 1 mM 2-deoxy-D-glucose). Aliquots of the assay buffer were removed at multiple time points (5, 10, 20, 40 minutes) and the Rb concentration in the supernatant was determined by flame atomic absorption spectroscopy using the Aurora Biomed ICR8000 instrument. Rubidium efflux was normalized to total loaded Rb (determined by measuring Rb left in lysed cells at the end of the assay). For simplicity, only data from the 40 minute time point are presented.

#### *Western blot detection of K<sub>ATP</sub> channel surface expression*

COSm6 cells in 6-well plates were transfected with Kir6.2 channel cDNA (600 ng) and FLAG-tagged SUR1 (1.2 µg in the pECE vector). After 3 days of incubation, western blotting was carried out on total cell lysates, using 7.5% SDS-PAGE, followed by transfer to nitrocellulose membrane and labeling with mouse anti-FLAG primary antibody (Sigma-Aldrich) and HRP-conjugated goat anti-mouse secondary antibody (ABM, Vancouver, Canada). Blots were visualized by ECL methods (Femto ECL detection kit, Pierce) using a FluorChem SP gel imager (Alpha Innotech).

## **Results**

#### *Functional scan of the Kir6.2 slide helix*

The modular structure of Kir channels comprises a canonical pore-forming TMD, and a CTD (Fig. 14A). The TMD interfaces with the CTD via the N-terminal transverse slide helix, and the C-terminal extension of the pore-lining M2 helix, which also makes significant contacts with PIP<sub>2</sub>. We first investigated the functional role of the slide helix in ligand-dependent gating with a mutagenic scan,

extended to include what we have termed helix Sb (10 slide helix residues preceding the pore M1 helix) and helix Sa (10 residues preceding helix Sb) (Fig. 14B). This subdivision of the slide helix is based on a  $\sim 80^\circ$  kink apparent in the most recent eukaryotic Kir crystal structures (Fig. 14A)(Hansen et al., 2011;Whorton and MacKinnon, 2011), and it is noteworthy that helix Sb is highly conserved among the eukaryotic Kir channels while helix Sa is more divergent (Fig. 14B).

We initially scanned overall functionality of Kir6.2 slide helix mutants (co-expressed with SUR1) using a non-radioactive Rb efflux assay (Fig. 15A). Under conditions of metabolic inhibition (2-deoxy-D-glucose + oligomycin) to activate  $K_{ATP}$  channels, robust Rb efflux was observed through most helix Sa mutants, but several (6 out of 10) helix Sb mutants exhibited significant or complete loss of channel activity (Fig. 15A). These deficiencies are likely not the result of gross defects in folding or trafficking, based on inspection of SUR1 maturation with SDS-PAGE. As described elsewhere, cell-surface maturation and glycosylation of SUR1 (dependent on SUR1 interaction with Kir6.2) generates a high molecular weight band, while immature “core” glycosylated SUR1 comprises a lower molecular weight band (Fig. 15B)(Zerangue et al., 1999;Schwappach et al., 2000;Yan et al., 2007). All Kir6.2 slide helix mutants examined appeared to confer maturation of SUR1 (Fig. 15C), indicating that these mutations do not disrupt folding or trafficking of the  $K_{ATP}$  complex. Further evidence against gross folding defects arises from our ability to apply a functional rescue approach to all slide helix mutants.

#### *Functional rescue of slide helix mutants by a “forced gating” mechanism*

Due to the LOF phenotype of most helix Sb mutants, we were challenged to find a way to further investigate the functional role of this important motif. We adopted an approach to rescue channel function with a recently described “forced gating” mechanism (Khurana et al., 2011). A glutamate substitution at the hydrophobic Kir channel bundle-crossing (F168E mutation in Kir6.2) generates channels that are pH-sensitive and open upon alkalization, presumably due to mutual repulsion of the introduced side-chains. A similar mechanism of mutual repulsion has been described for activating mutations in KirBac channels (Bavro et al., 2012;Paynter et al., 2010). Despite this perturbation of the helix bundle-crossing, Kir6.2[F168E] channels retain a largely normal intact ATP-sensing mechanism (Fig. 16A, detailed differences are described by (Khurana et al., 2011)). We observed that every deleterious Kir6.2 slide helix

mutation could be functionally rescued with the F168E mutation, and currents could be enhanced with alkaline pH. This rescue mechanism allowed us to compare functional effects of mutations at all slide helix positions. This analysis includes multiple mutations that might have been disregarded as LOF, and thus never interrogated.

We determined the  $IC_{50}$  for ATP-inhibition of the channel for each slide helix mutant (on the Kir6.2[F168E] background, at pH 8, because currents are considerably larger at this pH) (Fig. 16). It is noteworthy that activity and ATP-sensitivity of Kir6.2[F168E] channels are pH-sensitive, so it was essential to meticulously adjust pH in all solutions to ensure that effects did not arise from slight variations in pH (rather than ATP concentration). Exemplar sweeps measuring ATP-sensitivity in slide helix mutants are depicted (Fig. 16A), in which patches were formed and excised in pH 7.3, switched to pH 8 to demonstrate the F168E-mediated pH-dependence, and stepped sequentially through several ATP concentrations at pH 8. Effects of pH and ATP were all rapid, stable, and fully reversible (Fig. 16A).

Two clusters of residues had prominent effects on ATP-inhibition. The first set (I49A, R50A) has been previously described and lies close to the well-described ATP binding site, likely contributing to binding of the ATP  $\gamma$ -phosphate (Antcliff et al., 2005; Proks et al., 1999). More interesting was the cluster of mutants (D58A, F60A) in the “kink” region of the slide helix (at the helix Sa and Sb junction, Fig. 14A). These positions are predicted to lie  $>20 \text{ \AA}$  from the putative ATP binding site, and are thus unlikely to make any direct contacts with ATP (Antcliff et al., 2005); an F60Y mutation has been identified previously in neonatal diabetes (Mannikko et al., 2010). The D58 position had the largest effect but has been largely unexplored, although mutations of the analogous position in Kir2.1 have been shown to cause LOF (similar to our findings in Kir6.2, Fig. 15A), and linked to Andersen syndrome (Decher et al., 2007). The D58A mutation profoundly reduced ATP-sensitivity, with very little inhibition observed even in 10 mM ATP, compared with the F168E background channel that exhibited an ATP  $IC_{50}$  of  $\sim 30 \text{ }\mu\text{M}$  (Fig. 16B) which is comparable to that in WT Kir6.2 (Khurana et al., 2011). Furthermore, the effects of the D58A mutation are significantly greater than the effects of mutations at positions identified by sequencing of Kir6.2 from neonatal diabetic patients (R50, Q52, G53, R54, V59, F60, T61) (Nichols,

2006). By rescuing non-functional mutant channels, these experiments reveal a fundamental and previously unrecognized component of the ATP-dependent gating mechanism.

#### *Kinetic features of Kir6.2[F168E] channels and impact of slide helix mutations*

Notably, in addition to rescuing LOF mutants, the Kir6.2[F168E] mutation imparts a weakly voltage-dependent gating phenomenon that is absent in WT Kir6.2 channels (Kurata et al., 2010a). Membrane hyperpolarization causes time-dependent opening of these channels, and kinetic features persist clearly in inside-out patches after washout of endogenous polyamines (Fig. 17A). Therefore, this voltage-dependence appears to be an intrinsic property of Kir6.2[F168E] mutant channels (rather than a consequence of block by residual polyamines). These properties are similar to a previously reported polyamine-independent voltage-dependence in Kir6.2[L157E] channels, but with opposite polarity (Kurata et al., 2010a). In addition, varying pre-pulse voltages significantly alters tail current magnitude in a typical channel activation protocol (unpublished data), suggesting that voltage is altering the distribution of open and closed states. The voltage-dependent kinetic features of Kir6.2[F168E] offered a unique additional approach to compare the effects of slide helix mutations on channel function.

Most slide helix mutants (including the strongly disruptive I49A and R50A ATP binding site positions) had little or no effect on gating kinetics, with hyperpolarization-dependent channel opening remaining intact and similar to the [F168E] background channel (Fig. 17A). Only two slide helix mutations (D58A, T61A) near the slide helix kink markedly accelerated the kinetics of voltage-dependent channel opening, although they did not affect the intrinsic rectification of the current-voltage relationship (Fig. 17A). Again, the D58 position stood out in this comparison of slide helix positions, as kinetics in Kir6.2[F168E][D58A] channels were far too rapid to resolve (Fig. 17A,B – we would estimate that in well-formed inside-out patches we can confidently resolve time constants of ~0.4 ms, and so  $2.5 \text{ ms}^{-1}$  was included as a lower limit for  $1/\tau_{\text{step}}$  presented for D58A channels).

#### *A keystone role for the slide helix “aspartate anchor”*

While multiple slide helix mutations abolish function (Mannikko et al., 2010; John et al., 2005; Shimomura et al., 2006; Koster et al., 2005; Koster et al., 2008), comparisons enabled by our

functional rescue approach highlight a uniquely important role for residue D58 in Kir6.2 channel function. In rescued channels, mutation of this position had the most substantial effects on channel ATP-sensitivity (far greater than identified disease-related slide helix mutations) and also dramatically accelerated the voltage-dependent gating kinetics imparted by the Kir6.2[F168E] mutation. We further investigated the importance of D58 by introducing additional mutations at this position. The D58 position exhibits an extremely stringent amino acid tolerance: even the most conservative mutations examined (D58E and D58N) were unable to generate functional channels (Fig. 18A), although they were trafficked to the cell-surface (Fig. 18B) and could be rescued with the [F168E] background (D58N, D58A, D58E, D58Q). All D58 mutants characterized by patch clamp exhibited severe disruption of ATP-sensitivity and gating kinetics (see exemplar data for D58E in Fig. 18C,D).

Based on these findings, residue D58 stands out as an essential “anchor” – the most functionally important slide helix residue for coupling between the TMD and CTD of Kir6.2. This aspartate anchor exhibits very high sequence conservation among both eukaryotic and prokaryotic Kir channels (Fig. 14A). We filtered the Pfam “pan-IRK” sequence alignment to remove channels that lacked a selectivity filter-like sequence, or lacked N-/C-termini outside the core K<sup>+</sup> channel pore module. Within this subset of Kir-like sequences, ~96% contained an aspartate homologous to D58 of Kir6.2 (compared to 86% with the selectivity filter GYG tyrosine). This high degree of conservation is consistent with the inability of any D58 mutants to remotely approximate WT function in Kir6.2 (Fig. 18), and suggests an important role for the aspartate anchor across the entire Kir family.

To explain our findings, we propose a hypothetical working model for the role of D58 (Fig. 19). In channels where the D58 TMD-CTD anchor is in place, gating kinetics are slow, likely because conformational changes of the TMD and CTD are linked, resulting in a significant energetic barrier to opening (Fig. 19A). With mutations that disrupt ATP-binding (e.g. I49A, R50A), but preserve the TMD-CTD anchor, ATP-inhibition is weakened but gating kinetics remain slow (Fig. 19B). In contrast, disruption of the TMD-CTD anchor by mutations to D58 abolishes ATP-inhibition (because ligand-dependent conformational changes are not effectively transduced to the TMD bundle-crossing gate), and gating kinetics (because conformational changes of the TMD are no longer linked to the CTD) (Fig. 19C).

### *Contacts between residue D58 and the CTD*

Kir6.2 position D58 stands out as a functional lynchpin that couples the CTD and TMD of Kir channels. We further investigated residues within the CTD that might interact with D58. Inspection of recent eukaryotic Kir channel structures demonstrates that the D58 side-chain is positioned especially close to R206, a residue that is also strongly conserved among all Kir channels (~90% identity in the alignments described above). However, numerous other nearby side-chains form adjacent clusters of positive charges that could also be important binding partners for D58 (specifically K207 in the CTD, and H175 R176 R177 in the TMD-CTD linker) (Fig. 20A). We neutralized each cluster of positive charges (R206A/R207A double mutant, and H175A/R176A/R177A triple mutant), again using the F168E background because R206 and R177 mutations preclude expression of functional channels (Shyng et al., 2000). Surprisingly, despite the close proximity of D58 and R206 in crystal structures, neutralization of R206 and/or K207 does not recapitulate the effects of D58 mutations. Kir6.2[F168E][R206A][K207A] channels exhibit only slightly perturbed ATP-sensitivity (Fig. 20B,C), although charge reversal with R206D was able to more significantly disrupt ATP-inhibition. All R206 mutations exhibited accelerated gating kinetics relative to the Kir6.2[F168E] background, but they were clearly slower than the D58 mutants and can be confidently resolved in patch clamp recordings (Fig. 21A,B).

In contrast, the Kir6.2[F168E][H175A][R176A][R177A] triple mutant dramatically disrupted ATP-inhibition (and in fact, often appeared to cause mild ATP-stimulation of channel activity). By decomposing this effect further with individual point mutants, we could attribute the disruption of ATP-sensitivity almost entirely to the R177A mutation, as both H175A and R176A were well-inhibited by ATP (Fig. 20B,C). Furthermore, Kir6.2[F168E][H175A][R176A][R177A] channels exhibited accelerated gating kinetics, although again not as rapid as the D58 mutants. Both R176A and R177A point mutations exhibited accelerated gating kinetics (Fig. 21A,B). Overall, these findings indicate that the effects of mutating the essential D58 anchor cannot be recapitulated by any single structurally-rationalized CTD mutant, although R177 appears to be highly important for transduction of ligand-binding.

## Discussion

Inwardly-rectifying K<sup>+</sup> channels translate activity of important metabolic and signalling pathways into changes in membrane voltage. This function relies on transduction of ligand-binding in the CTD to changes in the stability of the channel gate in the TMD. Despite diversity in the signalling molecules that regulate various Kir channels, conservation of architecture and primary sequence suggests that fundamental aspects of channel gating will be similar among different Kir channels.

Mutation of many residues in the interfacial slide helix abolishes channel function, preventing systematic characterization of the determinants of ligand-dependent gating (Fig. 15). However, a forced gating approach (using electrostatic repulsion to force open the helix bundle-crossing gate) overcame this experimental barrier, allowing us to dissect and compare the functional importance of each slide helix residue. Notably, our findings highlighted positions that appear to be highly intolerant of mutations, and would be impossible to characterize without this functional rescue. Despite the fairly significant inter-domain contacts available for transduction of ligand-binding, it is somewhat surprising that the coupling mechanism converged predominantly on a single slide helix residue, Kir6.2 position D58, which we have described as an aspartate anchor between the TMD and CTD. Disruption of this highly conserved anchor uncouples the TMD and CTD – ATP no longer inhibits the channel (Fig. 16A) and non-natural gating kinetics imparted by the F168E mutation are markedly accelerated (Fig. 17A). D58 mutants were the only channels in our scan to exhibit these properties together. We have suggested that the conformational changes underlying the voltage-dependent gating of Kir6.2[F168E] channels involve motions of both the CTD and TMD, and that disrupting the coupling mechanism (allowing the TM gate to operate independently) will diminish the energetic barrier for gating transitions. Although our understanding of the gating mechanism for F168E channels is incomplete, there is no question that the gating phenotype of D58 mutant channels is profoundly disrupted relative to all other mutations in the slide helix scan.

The demonstration of the essential role of the D58 position adds important functional information to recently reported structures of Kir2.2 (in complex with PIP<sub>2</sub>) and Kir3.2 (Hansen et al., 2011; Whorton and MacKinnon, 2011). These structures suggest that the D58 equivalent residue forms a salt bridge interaction with a nearby arginine (R206 in Kir6.2) in the βC-βD loop. However, our functional results

indicate that this is likely not the only important interaction in this vicinity, since neutralization of R206 (and/or its neighbour K207) failed to replicate the effects of D58 mutations on ATP-sensitivity or gating kinetics. Rather, neutralization of R177 had the most significant effect on transduction of ATP-binding (Fig. 20). While the essential role of D58 stands out in our findings, its interacting partners in the CTD remain less clearly defined.

One hypothesis stemming from these results is that the D58 side-chain might dynamically interact with multiple residues in the CTD, with R206 and R177 being obvious candidates. It is noteworthy that the D58 side-chain is “sandwiched” between the  $\beta$ C- $\beta$ D loop (containing R206) and the C-terminal extension of the M2 helix. This C-terminal extension contains important PIP<sub>2</sub>-binding residues (H175 and R176 in Kir6.2 analogous to K199 and K200 in the Kir3.2 crystal structure) as well as R177 which is identified in our study as essential for transduction of ligand-binding. This suggests a possible structural rationale for the known effects of PIP<sub>2</sub> on the channel’s ATP-sensitivity (Shyng and Nichols, 1998;Baukrowitz et al., 1998), arising from changes in the orientation of R177 in response to PIP<sub>2</sub>-binding. This close assembly of residues from both the TMD and CTD appears to be a critical locus for assembly of the two modules and is likely important for allosteric transmission of multiple ligand-dependent binding signals to the channel gate.

It is notable that the design of the Kir channel ligand transduction mechanism involves a non-covalent interface between the sensing (ligand-binding) and gating domains. In contrast, the S4 voltage-sensor in Kv channels is closely tethered to the gating/pore-forming domain and is thought to directly exert forces on the channel gate through the S4-S5 linker (Long et al., 2005b;Long et al., 2007). It has been suggested that this mechanism requires a second anchor point, proposed to involve a link between the extracellular side of the S1 helix and the pore module (Lee et al., 2009). At present, the details underlying force transmission between the Kir channel cytoplasmic ligand-binding domain and the channel pore are uncertain. By analogy to the model proposed for Kv channel gating, it seems likely that a second essential TMD-CTD anchor will emerge, enabling some torque to be exerted on the pore by differential motions of two pore-sensor contact points.

In many ways, the identification of Kir-associated channelopathies has significantly shifted the focus of investigation of Kir channel function towards the characterization of disease-related mutants. However, without probing more deeply into the mechanisms underlying the deleterious effects of LOF mutations like D58A, many essential features of channel gating could be overlooked. Mutations at multiple slide helix positions (R50, Q52, G53, V59, F60) have been shown to disrupt ATP-sensitivity and are associated with neonatal diabetes, pointing to the slide helix as an important motif in ligand-dependent gating. However, a complete description of D58 as the essential coupling element for ATP-inhibition has remained obscure because of the necessity of this anchor position for channel function – any mutation results in a dead or silent phenotype. Similarly, mutation of the equivalent position in Kir2.1 (D71V/N) has been reported to cause LOF and Andersen’s syndrome (Plaster et al., 2001), but further insight into the functional role of this position has been impossible without an experimental intervention to rescue channel function (Decher et al., 2007).

## **Conclusion**

Our “forced gating” approach has provided novel insights into channel assembly and gating, previously not measurable due to deleterious effects of slide helix mutations on channel activity. Our findings reveal that a highly conserved aspartate anchor plays an overwhelmingly central role in the transmission of ligand-binding to the channel gate, with multiple potential interacting residues in the CTD.

Tables and figures

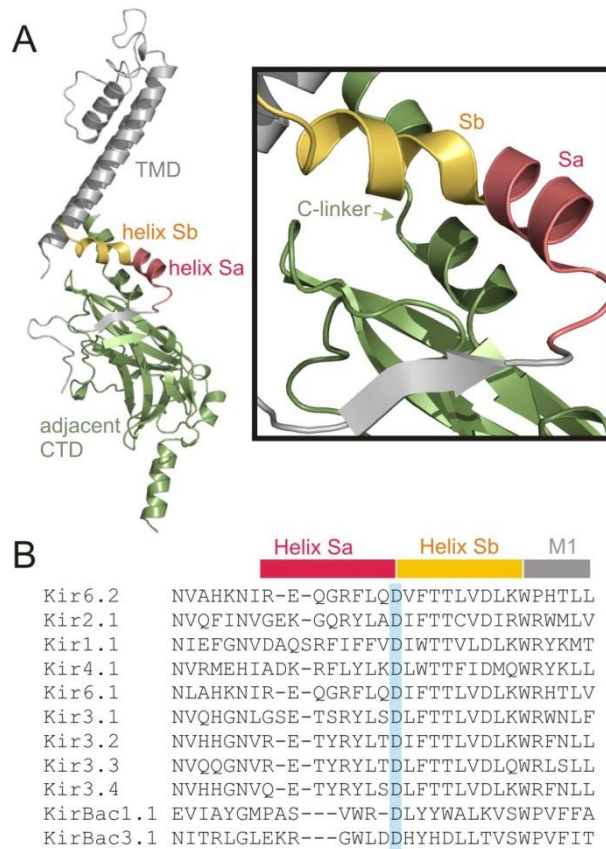


**FIGURE 14. Structural organization of Kir channels.** *A.* Kir channel structure highlighting the interface between the N-terminal half of one subunit (silver, with the interfacial ‘slide’ helix highlighted in red and yellow), and the C-terminal half of an adjacent subunit. The magnified image illustrates the close approach of the interfacial slide helix with the C-terminal extension of the M2 helix, and the cytoplasmic  $\beta$ C- $\beta$ D loop. *B.* Alignment of multiple Kir channel slide helix segments. The highlighted position corresponds to residue D58 at the transition between helices Sa and Sb.

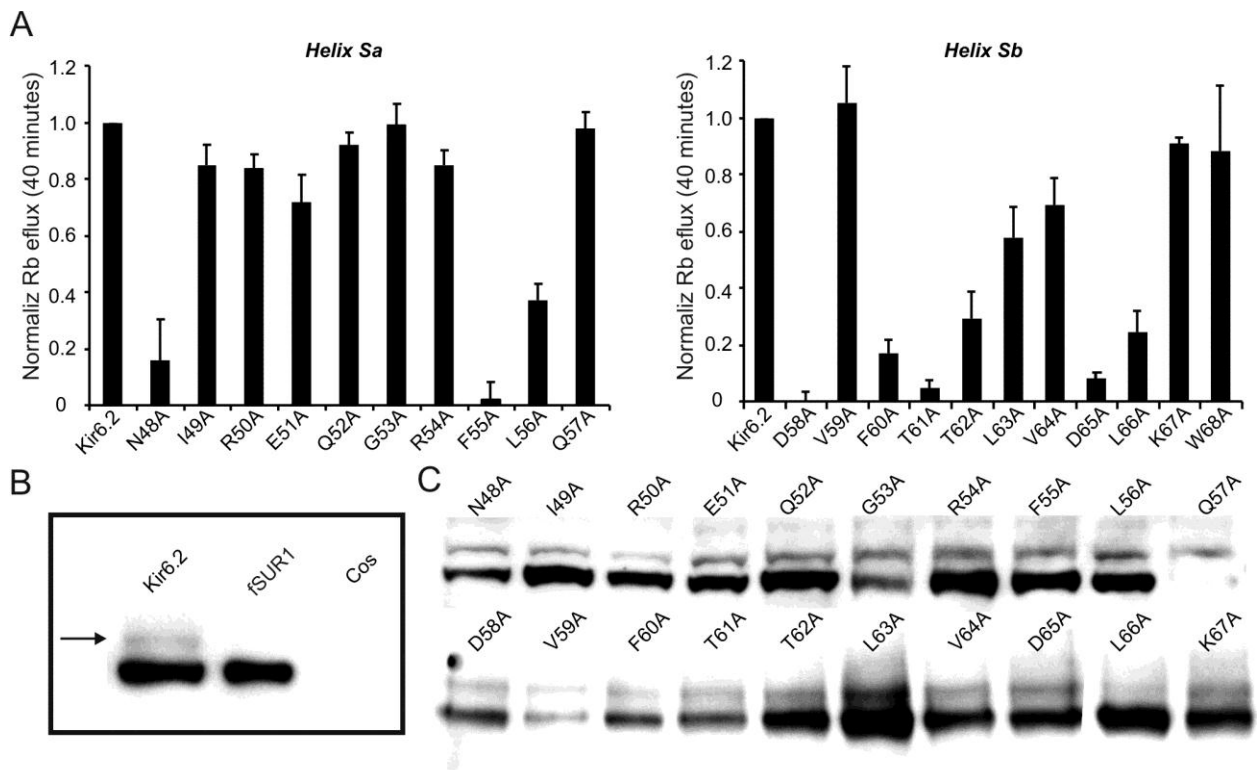


**FIGURE 15. Systematic scan of channel activity and expression of Kir6.2 slide helix mutants.** **A.** A non-radioactive rubidium efflux assay was used to determine channel activity of Kir6.2 mutants (co-expressed with SUR1, in CosM6 cells). Rubidium efflux from pre-loaded cells was measured by atomic absorption spectrometry to determine the percentage of loaded  $Rb^+$  released during a 40-minute incubation. **B.** Western blots to probe trafficking of the  $K_{ATP}$  channel complex. Total cell lysates from CosM6 cells transfected with FLAG-SUR1 alone or with WT Kir6.2 were probed with an Anti-FLAG antibody. Co-transfection of SUR1 and Kir6.2 is required for the appearance of a higher molecular weight (mature glycosylated) band. **C.** Western blots for cell lysates after transfected with FLAG-SUR1 and indicated slide helix mutations.

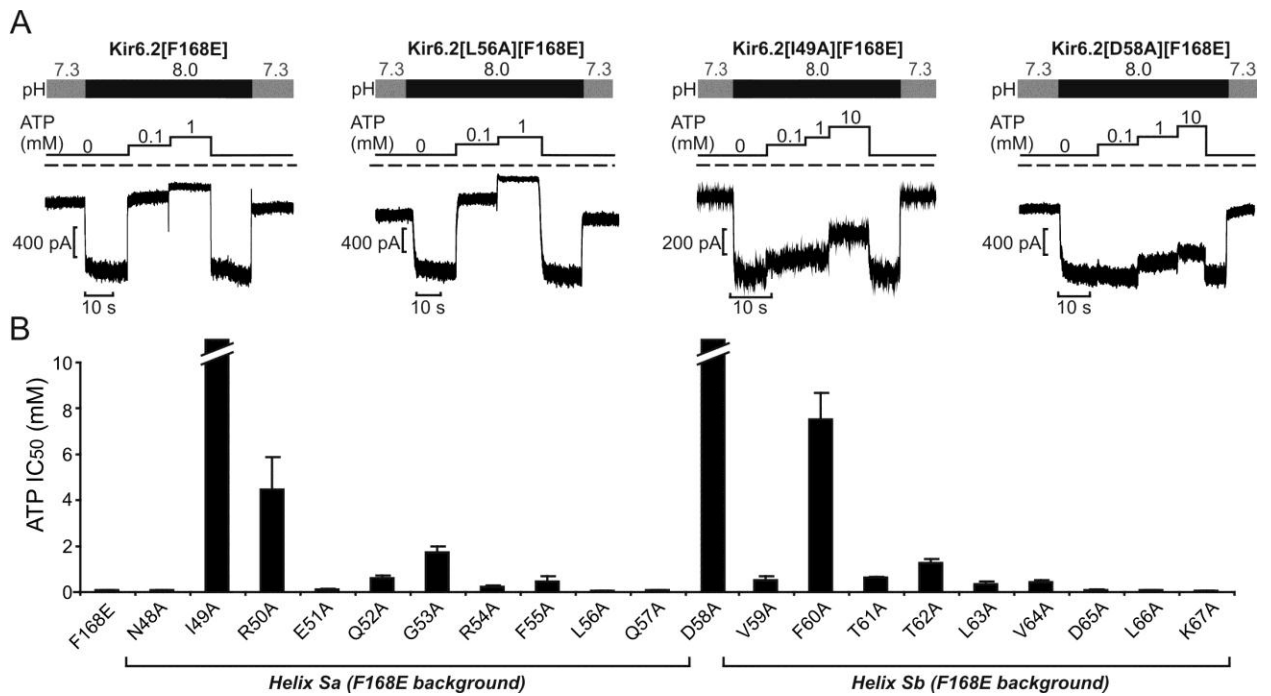


**FIGURE 16. ATP-sensitivity of Kir6.2 slide helix mutant channels.** *A.* Continuous inside-out patch clamp recordings at -50mV for CosM6 cells expressing Kir6.2[F168E] and exemplar Kir6.2[F168E] slide helix mutants (all co-expressed with SUR1). Dashed line represents zero current. Internal pH and ATP concentrations were switched as indicated, with a rapid solution exchange device. *B.* IC<sub>50</sub> for ATP-inhibition of slide helix mutants on the Kir6.2[F168E] background (ATP-inhibition was recorded at internal pH 8.0). The broken bars for I49A and D58A indicate IC<sub>50</sub> concentrations considerably higher than the largest ATP concentration (10 mM) tested.

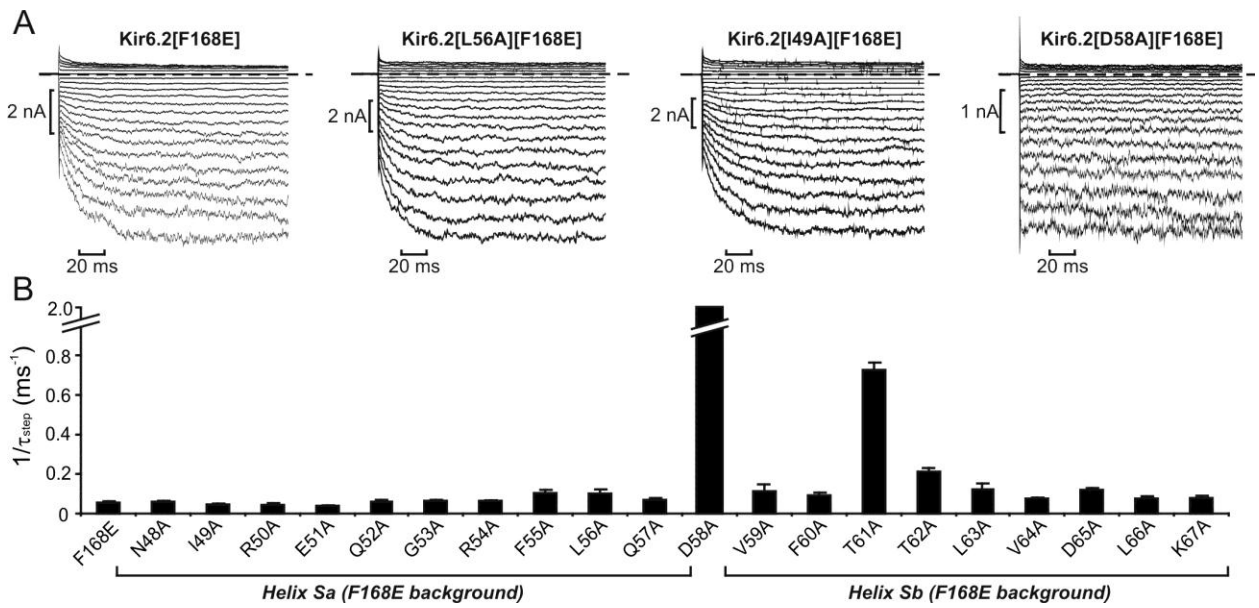


**FIGURE 17. Effects of slide helix mutations on the unique kinetic features of Kir6.2[F168E] channels.** *A.* Inside-out patch recordings from CosM6 cells expressing Kir6.2[F168E] and various exemplar Kir6.2[F168E] slide helix mutants (all co-expressed with SUR1). Patches were pulsed between -150 mV and +50 mV in 10 mV steps; holding potential was 0 mV. Dashed line represents zero current. *B.* Activating components of current after voltage steps to -150 mV were fit with a single exponential equation to extract the time constant  $\tau_{\text{step}}$  at pH 8. The broken bar for D58A indicates that channel opening was too rapid to confidently resolve.

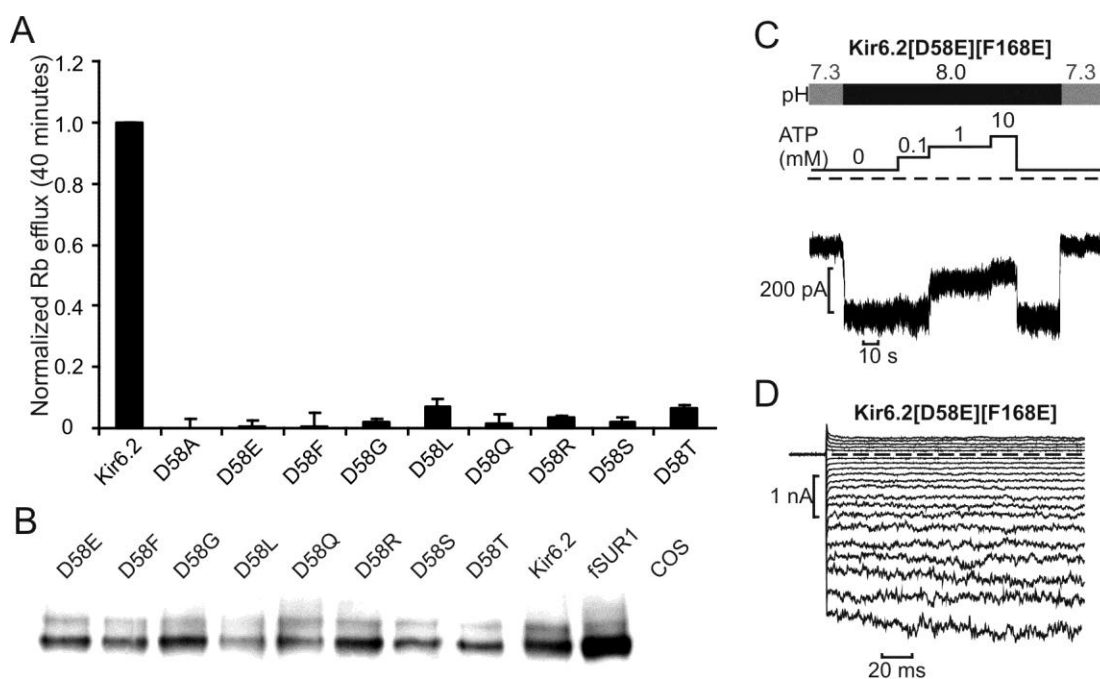


**FIGURE 18. Stringent aspartate requirement at position D58.** Numerous amino acid substations at position D58 were tested for *A.* functionality by Rb efflux assays, and *B.* cell surface expression by western blot (see Fig. 2). *C.* Continuous inside-out patch clamp recording at  $-50\text{mV}$  for CosM6 cells expressing an exemplar D58 mutant (co-expressed with SUR1), as described in Fig. 16. *D.* Patch was pulsed between  $-150\text{ mV}$  and  $+50\text{ mV}$  in  $10\text{ mV}$  steps, as described in Fig. 17. The conservative D58E mutation renders channels ATP-insensitive, and abolishes voltage-dependent gating kinetics.

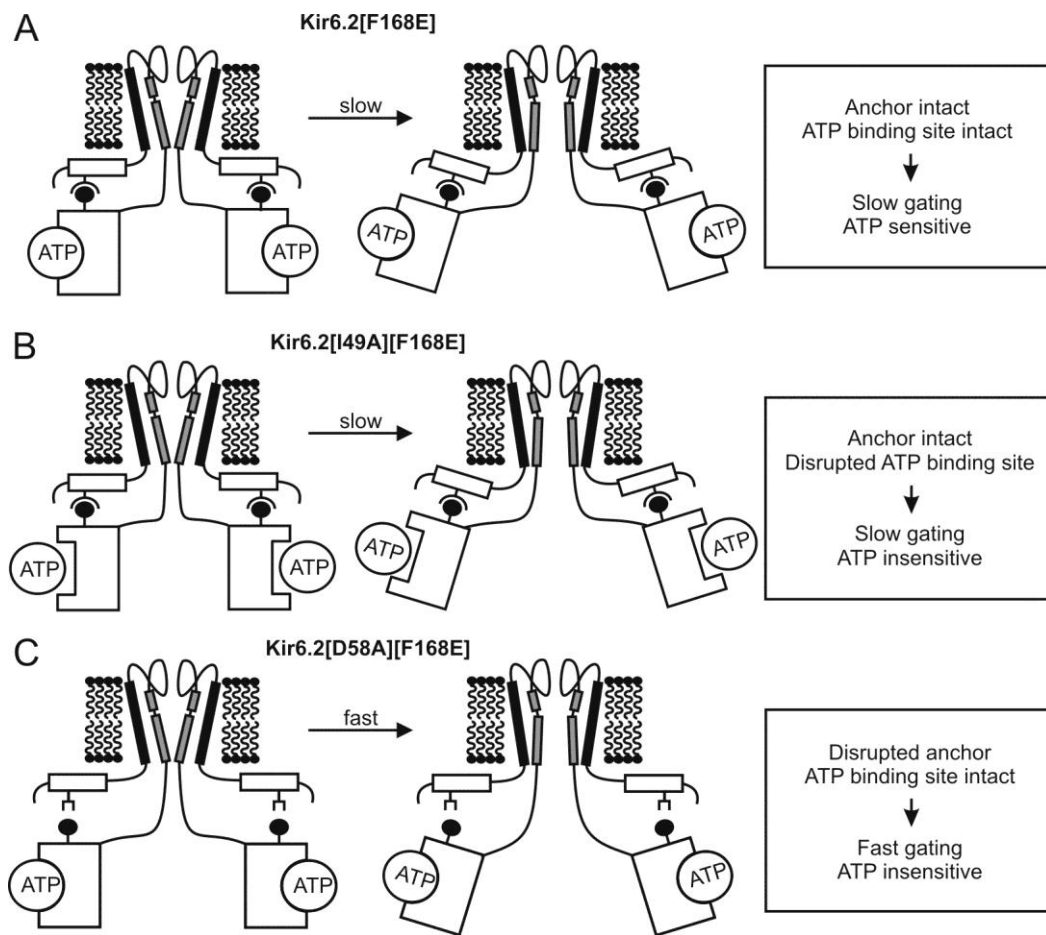


**FIGURE 19. Schematic model illustrating ATP-binding and gating kinetics of Kir6.2[F168E] channels with slide helix mutations.** *A.* Kir6.2[F168E] channels have an intact ATP binding site and coupling mechanism between cytoplasmic (CTD) and transmembrane (TMD) domains, enabling ATP-dependent inhibition and slow voltage-dependent kinetics. *B.* The I49A mutation disrupts the ATP binding site without affecting the coupling mechanism between CTD and TMD, resulting in loss of ATP-sensitivity, but persistence of slow voltage-dependent gating kinetics. *C.* The D58A mutation disrupts the aspartate anchor coupling between CTD and TMD. This prevents transduction of ATP-binding to the channel gate (resulting in ATP-insensitivity), together with fast voltage-dependent gating kinetics.

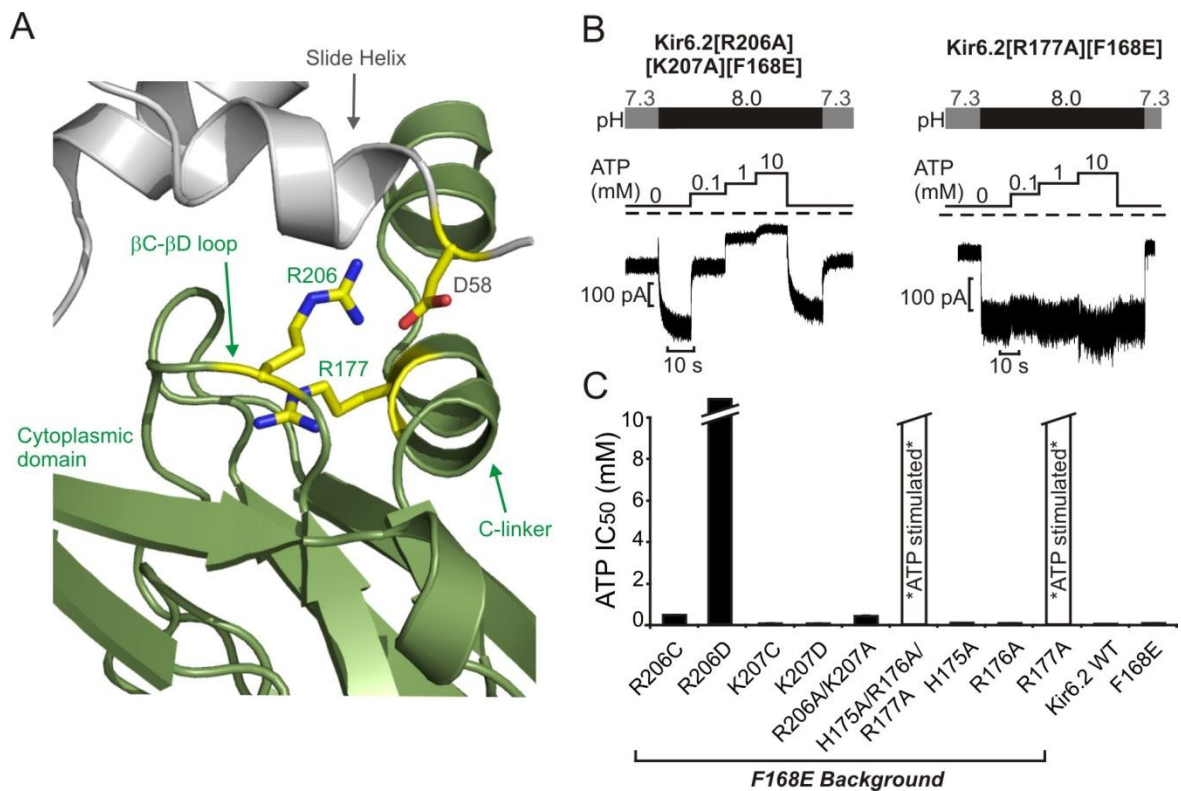


**FIGURE 20. Functional assessment of potential D58 interacting partners.** *A.* Continuous inside-out patch clamp recordings at -50mV for CosM6 cells expressing Kir6.2[F168E] with mutations of candidate residues for slide helix interactions (all co-expressed with SUR1), as described in Fig. 3. *B.* IC<sub>50</sub> for ATP-inhibition of mutant channels was determined, again using the F168E mutation to rescue loss-of-function mutations. Remarkably, mutations of R177 completely abolish ATP-inhibition, and instead appear to impart mild stimulation in the presence of very high ATP concentrations. Unfilled bars indicate that IC<sub>50</sub> values were not measured due to stimulation of inward currents by ATP.

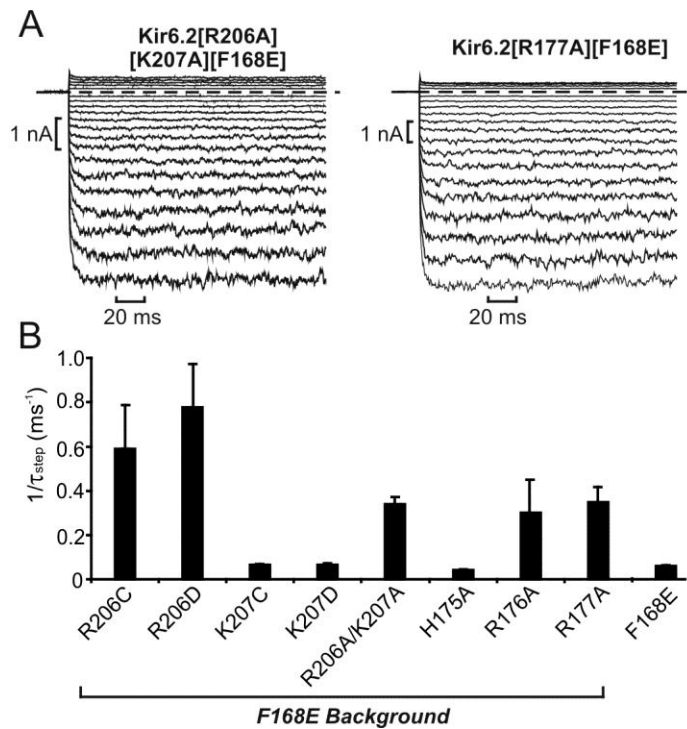


FIGURE 21. **Kinetic effects of mutations of candidate D58 interacting partners.** *A.* Patches were pulsed between -150 mV and +50 mV in 10 mV steps, as described in Fig. 17. *B.* Activating components of current after voltage steps to -150 mV were fit with a single exponential equation to extract the time constant  $\tau_{\text{step}}$  at pH 8 (see Fig. 17).

## CONCLUSION

Inwardly-rectifying K<sup>+</sup> channels are essential to many physiological processes such as control of membrane excitability, repolarization of the cardiac action potential, and control of hormone secretion. Their roles depend highly on how specific Kir families are regulated and gated. Two major gating mechanisms are inward rectification (voltage-dependent channel block by Mg<sup>2+</sup> and polyamines) and ligand-dependent regulation. Inward rectification is most prominent in strong inward rectifiers such as the Kir2 family, while ATP-inhibition of Kir6 channels is a prototypical example of ligand-dependent gating. This thesis aimed to provide mechanistic details about Kir channel gating and function via these two regulatory mechanisms. A better understanding of molecular aspects of channel function will grant us a better understanding of Kir channel physiology and associated diseases, creating novel therapeutic potentials.

### **Polyamine block underlying inward rectification of Kir channels**

In the first part of the thesis (Chapter I), we took a biophysical perspective on polyamine block in Kir channels. First, by using sterically expanded polyamine blockers in the prototypical strong rectifier Kir2.1, we were able to refine our understanding of high-affinity polyamine binding in a deep inner cavity site. It has been long accepted that coupled ion movement underlies the excess valence associated with voltage-dependent spermine block (Hille and Schwarz, 1978; Oliver et al., 1998; Spassova and Lu, 1998) but it has been unclear whether polyamines interact with or even enter the selectivity filter contributing to this steep voltage-dependence. On one hand, studies have shown that spermine binds beyond the rectification controller (John et al., 2004; Kurata et al., 2004; Kurata et al., 2010b; Chang et al., 2003) and based on the assumption that the most favoured conformation of spermine is linear, this suggests that spermine and other polyamines directly interact with the intracellular entrance of the selectivity filter, with a high possibility of intrusion into the filter. On the other hand, the sterically expanded bis-TMA-C10 has been previously shown to produce an effective valence comparable to spermine (Shin and Lu, 2005); this suggests that steep voltage-dependence does not involve blocker-filter interactions based on the assumption that bis-TMA-C10 is physically excluded from the selectivity filter. However, the notion of a flexible and compliant filter (Noskov et al., 2004) renders the latter result ambiguous.

By using blockers with further expanded termini (especially bis-QUIN-C10 which has immobile carbon atoms surrounding the terminal nitrogens), our results suggest the improbability of direct polyamine interactions with the selectivity filter contributing to steep voltage-dependence of block. Moreover, steric expansion of blocker termini did not remove  $[K^+]_o$ -dependence of block, strengthening the notion of a coupled flow of  $K^+$  ions and polyamines along the Kir pore. Together, these data suggest that steep voltage-dependence does not require direct interactions between polyamines and the selectivity filter and is possibly attributable entirely to coupled ion movement.

Our findings do not by any means disregard a deep binding site beyond the rectification controller suggested for spermine. In fact, from Chapter II of the thesis, a model for high-affinity spermine binding may be envisioned that accommodates both a deep binding site as well as the absence of blocker-filter interactions. From energy-minimized models of MTS modification at I176C in the inner cavity of Kir2.1, we see that MTS reagents used reach as far as the D172 side-chains. The fact that spermine unbinding is dramatically slowed from MTSET modification suggests a lock-in phenomenon where spermine is bound beyond the plane of D172 side-chains and the MTS amine moiety. Furthermore, the divergent differences between spermine and diamine analogs in effects of MTS modification on blocker affinity and unbinding kinetics suggest that the molecular mechanisms of high-affinity polyamine block are dependent on structural elements of the blocker. Comparing spermine with diamine decane (primary terminal amines, closest diamine analog to spermine), the biggest difference is the number of amine groups in the blocker. Blockers with four amine groups (spermine and Me<sub>10</sub>-spermine) exhibited the lock-in effect by MTSET while those with two amine groups did not. This suggests that having four evenly spaced positive charges enables spermine to bind stably in a deep site beyond the rectification controller. It is thus hard to ignore the possibility that spermine, instead of adopting a linear conformation, bends to form a ring shape to maximize interactions between its four amine groups and the ring of four D172 side-chains. The implication of this speculation is that a deep binding site near the selectivity filter does not contradict the absence of blocker-filter interactions; we should not fixate on the classic image of a linear polyamine molecule sitting parallel to the Kir pore axis, and consider dynamic molecular conformations that may underlie differential blocking profiles of various polyamines.

Modeling of polyamine block based on kinetics of sterically expanded blockers reinforced a 3-state 2-step blocking process (Chapter I). A biphasic nature of the blocking rate-voltage relationship is indicative of 2 successive equilibria where increasing the energetic barrier of either equilibrium will decrease the rate of transition for its corresponding “phase”. The higher energetic barrier was achieved in our study using steric expansion of polyamine blockers, and also achieved via introduction of MTS moieties into the channel pore (Kurata et al., 2010b). Large blockers introduce heightened energetic barriers to both low-affinity (shallow) and high-affinity (steep) block, which was reflected by the reduction in both shallow and steep “phases” of the blocking rate-voltage relationship. The modeling done in our study provides direct robust evidence for the validity of the previously introduced 3-state 2-step model of polyamine block.

One of the goals of the thesis was to determine inner cavity interactions responsible for high-affinity polyamine binding in Kir channels. The presence of an acidic pore-lining residue is essential and it is generally thought that deprotonated aspartate or glutamate side-chains carrying negative charges confer electrostatic interactions with positively charged polyamines. However, having four negatively charged side-chains in close proximity raises doubts about whether they behave the same as in an open aqueous solution (i.e. an environment with a high dielectric constant). Due to thermodynamic instability, close proximity of acidic side-chains can alter their pKa (Lindman et al., 2007; Cymes and Grosman, 2011; Khurana et al., 2011) which suggests that an acidic rectification controller may not even be negatively charged in the inner cavity. This possibility led us to suspect that non-electrostatic interactions underlie, at least partially, high-affinity polyamine binding in the Kir inner cavity. In Chapter II, we introduced “competitive” MTS amines with varying hydrogen bonding propensities into the Kir2.1 inner cavity, and found that “stronger” competitors (i.e. MTSEA and MTSEM) disrupted spermine block more than “weak” competitors (i.e. MTSET and MTSED). Moreover, we utilized a hydrogen bond-deficient blocker, Me<sub>10</sub>-spermine, and the hydrogen bond-diminished disease mutant channel D172N, to find that D172N affected block by Me<sub>10</sub>-spermine minimally; block by Me<sub>10</sub>-spermine was also similar in MTSEA and MTSET modified channels. These results together strongly suggest the importance of hydrogen bonding between the rectification controller and polyamines in high-affinity block. It is therefore

insufficient to consider only electrostatic interactions when studying high-affinity block in Kir channels, and future studies in this area must incorporate other chemical interactions to fully and accurately describe inward rectification.

### **Regulation of Kir channels by nucleotides**

$K_{ATP}$  channels are stimulated by NDP-binding at the SUR subunits (D'hahan et al., 1999; Gribble et al., 1997; Matsuoka et al., 2000) and inhibited by nucleotide-binding (both ATP and ADP in the absence of  $Mg^{2+}$ ) at the CTD of Kir6 channels (Antcliff et al., 2005; Haider et al., 2005; Craig et al., 2008). The molecular mechanisms behind both regulations remain elusive; however, the interface between the TMD and CTD of Kir channels (especially the slide helix) seems essential to ligand transduction (Decher et al., 2007; Tani et al., 2007; Proks et al., 2004; Proks et al., 2005). In Chapter III, we aimed to identify potential molecular mechanisms underlying the transduction of ATP-binding to the closing of the bundle-crossing gate in Kir6.2, by scanning the functional properties of numerous slide helix mutants. Among all slide helix mutants tested, mutations at just one residue, D58, severely impaired channel function – D58 mutations abolished ATP-sensitivity as well as voltage-dependent gating kinetics which originated from a novel “forced gating” background mutation, F168E. By exploiting unique kinetic characteristics of F168E channels, we developed a hypothesis for the role of the slide helix in ligand transduction: the D58 “aspartate anchor” interacts with CTD residues, coupling conformational changes in the CTD to those in the TM gate. Along with absolute conservation of this slide helix aspartate in Kir channels, its necessity and intolerance to mutations (even to a glutamate) perhaps explain why D58 mutations are not associated with disease phenotypes – developing embryos with such mutations probably do not survive.

We also attempted to identify binding partners for D58 in the Kir6.2 CTD. Two residues seem to be crucial for ligand transduction, R206 and R177, although it is unclear whether they directly interact with D58 as mutations in these two residues did not disrupt channel function to the same extent as D58 mutations. Specifically, ATP-sensitivity was significantly impaired with R206D but not R206A, suggesting that R206 likely does not directly interact with the slide helix – charge reversal introduces repulsion that uncouples the CTD from the slide helix. With these findings, we speculate that there are multiple interactions between the slide helix and CTD that mediate ligand transduction in Kir channels by

converging at the aspartate anchor. This notion is consistent with the fact that multiple ligands can simultaneously affect channel gating (e.g. PIP<sub>2</sub> and ATP) where changes in the CTD are “summed” at the aspartate anchor, generating an overall signal to the aspartate anchor which then transmits the signal to the bundle-crossing gate.

### **Strengths, limitations, and future directions**

To determine the molecular basis behind steep voltage-dependence of high-affinity polyamine block, we arrived at our conclusions based on one assumption – the largest blockers, bis-QUIN-C10 and bis-TEA-C10, are unable to closely interact with the selectivity filter due to physical constraints. Albeit this is a rational assumption, there is unfortunately little we can do to prove that is the case. Having a crystal structure of the Kir channel pore containing a polyamine blocker would provide definitive evidence regarding high-affinity binding, but that is a challenge that has yet to be successful. On another note, the effects of MTS modification on the affinity and unbinding kinetics of diamine analogs (Chapter II) suggest that diamine blockers bind very differently in the Kir inner cavity when compared to spermine. Specifically, they likely flicker between a deep binding site beyond the rectification controller and a shallower site that physically clashes with MTS moieties. This hypothesis supports the notion that these diamine analogs do not interact closely with the selectivity filter, but reveals caveats of drawing conclusions about spermine binding using results from diamine analogs. Hence, we cannot completely eliminate the possibility that spermine interacts with the selectivity filter, and can only confidently say that steep voltage-dependence of high-affinity polyamine block does not require such interactions.

The experiments for determining the importance of hydrogen bonding between the rectification controller and polyamines were reliable to indicate that non-electrostatic interactions are involved in high-affinity binding. Considering the nature of the approaches (using MTS reagents that differ only by their hydrogen bonding propensity, and using a hydrogen bond-deficient analog of spermine) as well as the chemistry involved (carboxylic acid functional group interacting with amines), our results confidently suggest that hydrogen bonding indeed plays a major role in high-affinity spermine block. Again, it is noteworthy to remember that our data do not deny the electrostatic interactions, but rather refine our understanding of the chemistry involved.

The next step in determining the necessity of a negatively charged side-chain in the inner cavity for high-affinity spermine block is to incorporate a non-natural amino acid in place of the rectification controller. To do this, nonsense suppression should be used where channel mRNA will be synthesized with a stop codon at the rectification controller position; a synthetic non-natural amino acid will then be coupled to the stop-tRNA *in vitro*. Both channel mRNA and the tRNA-non-natural amino acid complex will then be injected into oocytes followed by two-electrode voltage clamp and/or patch clamp electrophysiology. The tRNA should recognize mRNA stop codons including those at the rectification controller position of injected channel mRNA. The incorporation of the non-natural amino acid will then “suppress” the translation of an otherwise truncated protein. This method allows us to study the effects of any chemical moiety incorporated anywhere in the channel on channel function, limited only by synthesis of the chemical moiety and channel expression. With that said, substituting the rectification controller with a moiety that structurally mimics a carboxylate but is neutral, would truly reveal whether a negative charge in the inner cavity is required for high-affinity polyamine binding. For example, we can substitute the amide functional group of N160 in Kir6.2 with a nitro functional group (which has 2 oxygen atoms acting as hydrogen bond acceptors, as in the case with a carboxylate, but is an overall neutral moiety) to see whether this reconstitutes inward rectification in a weakly-rectifying channel. Having this powerful procedure at hand will surely provide otherwise inaccessible insights on chemical determinants of not only high-affinity block in Kir channels, but also any protein interactions.

Functional screening of point mutations in the slide helix, at least the test for ATP-sensitivity, is a fast and accurate way to determine which residues are important for ligand transduction. The novel “forced gating” mutation F168E in Kir6.2 rescues seemingly “dead” channel mutants that are trafficked to the cell membrane but are functionally impaired. This rescue mechanism would be a powerful tool to study the function of otherwise elusive LOF mutants (e.g. D58 mutants). On the other hand, the voltage-dependent characteristic of F168E mutant channels is a less reliable functional indicator since the underlying mechanism is unknown. The introduction of an acidic pore-lining side-chain at the bundle-crossing gate confers an energetic barrier to reach voltage-dependent steady state conduction – specifically only at hyperpolarizing voltages did the slow gating kinetics manifest. Furthermore, this

intrinsic gating property (in the absence of blocking ions or polyamines) was more apparent or slower at pH 8 than at pH 7.3 (data not shown). The rationale behind using F168E is that at higher pH, the glutamate side-chains become more deprotonated or negatively charged, which causes mutual repulsion forcing the bundle-crossing gate to open further (Khurana et al., 2011). Therefore, deprotonation of F168E (at pH 8) somehow increases the energetic barrier for the open channel to reach maximal conductance at a given hyperpolarizing voltage. Nonetheless, this extra gating feature allowed us another criterion in categorizing channel mutants. Overall, results unquestionably indicate that a single slide helix aspartate in Kir channels (D58 in Kir6.2) is necessary for ligand transduction (e.g. ATP-binding to channel closure).

We identified two CTD residues in Kir6.2 (R206 and R177) that seem important to ligand transduction and may potentially interact with the aspartate anchor D58. A promising candidate is R177 and crystal structures suggest a nearby CTD aspartate (D204) that may interact with R177. This prompts speculation that R177 transmits CTD movement to the slide helix by switching interaction with D204 to D58. Future functional assessment of this hypothesis (currently being studied in the lab) will include testing of mutations in these pairs of residues – D204/R177, R177/D58. For example, D204/R177 can be substituted with cysteines to allow disulfide bond formation upon application of an oxidizing agent; whether this forced interaction retains ligand transduction will reveal the importance of coupling between these two residues and whether R177-D58 interaction is required. Similarly, D204R/R177D and D204E/R177K preserve an electrostatic pairing, and these pairs of mutations will tell us whether attraction between the two residues is sufficient for ligand transduction or if structural specificity is necessary. The same approach can be applied to the pair R177/D58 (i.e. R177D/D58R, R177K/D58E). These experiments may pave the path for determining molecular mechanisms behind Kir channel ligand transduction, as well as pathophysiology of associated diseases.

As far as therapeutic applications of the research presented in this thesis go, molecular understanding of various gating mechanisms behind Kir channel function is the first step to developing channel-specific treatments that target the cause of associated diseases rather than tackling disease symptoms. For example, Andersen's syndrome (associated with LOF mutations in Kir2.1) is often

accompanied by periodic muscle paralysis and cardiac arrhythmias (Plaster et al., 2001;Tristani-Firouzi et al., 2002). Its treatments are currently limited to management of these clinical manifestations (carbonic anhydrase inhibitors for periodic paralysis,  $\beta$ -blockers and  $\text{Ca}^{2+}$  channel blockers for LQT)(Tawil et al., 1994;Sansone et al., 1997;Sansone and Tawil, 2007). On the other hand, neonatal diabetes associated with GOF mutations in Kir6.2 have been treated with sulfonylureas which specifically target and inhibit pancreatic  $\text{K}_{\text{ATP}}$  channels. Discovery of sulfonylureas perfectly reflects the importance of understanding the molecular basis for channelopathies. In severe cases however (e.g. slide helix mutations), insulin injections are necessary; an ambitious goal might be to incorporate gene therapy that aims to deliver functional channels to replace “dead” mutant channels. Nonetheless, it will be an endeavour to utilize what we know about a channel’s molecular physiology to design novel channel-specific treatments. An especially challenging obstacle is to prevent systemic side-effects as Kir channels are abundantly expressed throughout major body organs.

## BIBLIOGRAPHY

- (1997) Mutations in the Gene Encoding the Inwardly-Rectifying Renal Potassium Channel, ROMK, Cause the Antenatal Variant of Bartter Syndrome: Evidence for Genetic Heterogeneity. International Collaborative Study Group for Bartter-Like Syndromes. *Hum Mol Genet* **6**:17-26.
- Adams DJ and Hill M A (2004) Potassium Channels and Membrane Potential in the Modulation of Intracellular Calcium in Vascular Endothelial Cells. *J Cardiovasc Electrophysiol* **15**:598-610.
- Aguilar-Bryan L, Nichols C G, Wechsler S W, Clement J P, Boyd A E, III, Gonzalez G, Herrera-Sosa H, Nguy K, Bryan J and Nelson D A (1995) Cloning of the Beta Cell High-Affinity Sulfonylurea Receptor: a Regulator of Insulin Secretion. *Science* **268**:423-426.
- Alekseev AE, Brady P A and Terzic A (1998) Ligand-Insensitive State of Cardiac ATP-Sensitive K<sup>+</sup> Channels. Basis for Channel Opening. *J Gen Physiol* **111**:381-394.
- Antcliff JF, Haider S, Proks P, Sansom M S and Ashcroft F M (2005) Functional Analysis of a Structural Model of the ATP-Binding Site of the KATP Channel Kir6.2 Subunit. *EMBO J* **24**:229-239.
- Ashcroft FM (1988) Adenosine 5'-Triphosphate-Sensitive Potassium Channels. *Annu Rev Neurosci* **11**:97-118.
- Ashcroft FM (2005) ATP-Sensitive Potassium Channelopathies: Focus on Insulin Secretion. *J Clin Invest* **115**:2047-2058.
- Ashcroft FM and Kakei M (1989) ATP-Sensitive K<sup>+</sup> Channels in Rat Pancreatic Beta-Cells: Modulation by ATP and Mg<sup>2+</sup> Ions. *J Physiol* **416**:349-367.
- Ashcroft FM and Rorsman P (1989) Electrophysiology of the Pancreatic Beta-Cell. *Prog Biophys Mol Biol* **54**:87-143.
- Ashford ML, Boden P R and Treherne J M (1990) Glucose-Induced Excitation of Hypothalamic Neurons Is Mediated by ATP-Sensitive K<sup>+</sup> Channels. *Pflugers Arch* **415**:479-483.
- Babenko AP and Bryan J (2002) SUR-Dependent Modulation of KATP Channels by an N-Terminal KIR6.2 Peptide. Defining Intersubunit Gating Interactions. *J Biol Chem* **277**:43997-44004.
- Babenko AP and Bryan J (2003) Sur Domains That Associate With and Gate KATP Pores Define a Novel Gatekeeper. *J Biol Chem* **278**:41577-41580.
- Bao L, Hadjiolova K, Coetzee W A and Rindler M J (2011) Endosomal KATP Channels As a Reservoir After Myocardial Ischemia: a Role for SUR2 Subunits. *Am J Physiol Heart Circ Physiol* **300**:H262-H270.
- Batulan Z, Haddad G A and Blunck R (2010) An Intersubunit Interaction Between S4-S5 Linker and S6 Is Responsible for the Slow Off-Gating Component in Shaker K<sup>+</sup> Channels. *J Biol Chem* **285**:14005-14019.
- Baukowitz T, Schulte U, Oliver D, Herlitz S, Krauter T, Tucker S J, Ruppertsberg J P and Fakler B (1998) PIP<sub>2</sub> and PIP As Determinants for ATP Inhibition of KATP Channels. *Science* **282**:1141-1144.
- Bavro VN, De Z R, Schmidt M R, Muniz J R, Zubcevic L, Sansom M S, Venien-Bryan C and Tucker S J (2012) Structure of a KirBac Potassium Channel With an Open Bundle Crossing Indicates a Mechanism of Channel Gating. *Nat Struct Mol Biol*.

- Beeler GW, Jr. and Reuter H (1970) Voltage Clamp Experiments on Ventricular Myocardial Fibres. *J Physiol* **207**:165-190.
- Bendahhou S, Donaldson M R, Plaster N M, Tristani-Firouzi M, Fu Y H and Ptacek L J (2003) Defective Potassium Channel Kir2.1 Trafficking Underlies Andersen-Tawil Syndrome. *J Biol Chem* **278**:51779-51785.
- Bienengraeber M, Alekseev A E, Abraham M R, Carrasco A J, Moreau C, Vivaudou M, Dzeja P P and Terzic A (2000) ATPase Activity of the Sulfonylurea Receptor: a Catalytic Function for the KATP Channel Complex. *FASEB J* **14**:1943-1952.
- Bond CT, Pessia M, Xia X M, Lagrutta A, Kavanaugh M P and Adelman J P (1994) Cloning and Expression of a Family of Inward Rectifier Potassium Channels. *Receptors Channels* **2**:183-191.
- Burgen AS and Terroux K G (1953) On the Negative Inotropic Effect in the Cat's Auricle. *J Physiol* **120**:449-464.
- Cannell MB and Nichols C G (1991) Effects of Pipette Geometry on the Time Course of Solution Change in Patch Clamp Experiments. *Biophys J* **60**:1156-1163.
- Chan KW, Sui J L, Vivaudou M and Logothetis D E (1997) Specific Regions of Heteromeric Subunits Involved in Enhancement of G Protein-Gated K<sup>+</sup> Channel Activity. *J Biol Chem* **272**:6548-6555.
- Chang HK, Yeh S H and Shieh R C (2003) The Effects of Spermine on the Accessibility of Residues in the M2 Segment of Kir2.1 Channels Expressed in Xenopus Oocytes. *J Physiol* **553**:101-112.
- Chang HK, Yeh S H and Shieh R C (2005) A Ring of Negative Charges in the Intracellular Vestibule of Kir2.1 Channel Modulates K<sup>+</sup> Permeation. *Biophys J* **88**:243-254.
- Choe H, Sackin H and Palmer L G (2001) Gating Properties of Inward-Rectifier Potassium Channels: Effects of Permeant Ions. *J Membr Biol* **184**:81-89.
- Ciani S, Krasne S, Miyazaki S and Hagiwara S (1978) A Model for Anomalous Rectification: Electrochemical-Potential-Dependent Gating of Membrane Channels. *J Membr Biol* **44**:103-134.
- Clapham DE and Neer E J (1993) New Roles for G-Protein Beta Gamma-Dimers in Transmembrane Signalling. *Nature* **365**:403-406.
- Claydon TW, Makary S Y, Dibb K M and Boyett M R (2003) The Selectivity Filter May Act As the Agonist-Activated Gate in the G Protein-Activated Kir3.1/Kir3.4 K<sup>+</sup> Channel. *J Biol Chem* **278**:50654-50663.
- Craig TJ, Ashcroft F M and Proks P (2008) How ATP Inhibits the Open K(ATP) Channel. *J Gen Physiol* **132**:131-144.
- Cymes GD and Grosman C (2011) Estimating the PKa Values of Basic and Acidic Side Chains in Ion Channels Using Electrophysiological Recordings: a Robust Approach to an Elusive Problem. *Proteins* **79**:3485-3493.
- D'Alonzo AJ, Darbenzio R B, Parham C S and Grover G J (1992) Effects of Intracoronary Cromakalim on Postischaemic Contractile Function and Action Potential Duration. *Cardiovasc Res* **26**:1046-1053.

- D'hahan N, Moreau C, Prost A L, Jacquet H, Alekseev A E, Terzic A and Vivaudou M (1999) Pharmacological Plasticity of Cardiac ATP-Sensitive Potassium Channels Toward Diazoxide Revealed by ADP. *Proc Natl Acad Sci U S A* **96**:12162-12167.
- Dart C and Leyland M L (2001) Targeting of an A Kinase-Anchoring Protein, AKAP79, to an Inwardly Rectifying Potassium Channel, Kir2.1. *J Biol Chem* **276**:20499-20505.
- Decher N, Renigunta V, Zuzarte M, Soom M, Heinemann S H, Timothy K W, Keating M T, Daut J, Sanguinetti M C and Splawski I (2007) Impaired Interaction Between the Slide Helix and the C-Terminus of Kir2.1: a Novel Mechanism of Andersen Syndrome. *Cardiovasc Res* **75**:748-757.
- Depaulis A, Vergnes M and Marescaux C (1994) Endogenous Control of Epilepsy: the Nigral Inhibitory System. *Prog Neurobiol* **42**:33-52.
- Donaldson MR, Jensen J L, Tristani-Firouzi M, Tawil R, Bendahhou S, Suarez W A, Cobo A M, Poza J J, Behr E, Wagstaff J, Szepietowski P, Pereira S, Mozaffar T, Escolar D M, Fu Y H and Ptacek L J (2003) PIP2 Binding Residues of Kir2.1 Are Common Targets of Mutations Causing Andersen Syndrome. *Neurology* **60**:1811-1816.
- Doyle DA, Morais C J, Pfuetzner R A, Kuo A, Gulbis J M, Cohen S L, Chait B T and MacKinnon R (1998) The Structure of the Potassium Channel: Molecular Basis of K<sup>+</sup> Conduction and Selectivity. *Science* **280**:69-77.
- Du X, Zhang H, Lopes C, Mirshahi T, Rohacs T and Logothetis D E (2004) Characteristic Interactions With Phosphatidylinositol 4,5-Bisphosphate Determine Regulation of Kir Channels by Diverse Modulators. *J Biol Chem* **279**:37271-37281.
- Dunne MJ, Cosgrove K E, Shepherd R M, Aynsley-Green A and Lindley K J (2004) Hyperinsulinism in Infancy: From Basic Science to Clinical Disease. *Physiol Rev* **84**:239-275.
- Dunne MJ and Petersen O H (1986) Intracellular ADP Activates K<sup>+</sup> Channels That Are Inhibited by ATP in an Insulin-Secreting Cell Line. *FEBS Lett* **208**:59-62.
- Edghill EL, Gloyn A L, Gillespie K M, Lambert A P, Raymond N T, Swift P G, Ellard S, Gale E A and Hattersley A T (2004) Activating Mutations in the KCNJ11 Gene Encoding the ATP-Sensitive K<sup>+</sup> Channel Subunit Kir6.2 Are Rare in Clinically Defined Type 1 Diabetes Diagnosed Before 2 Years. *Diabetes* **53**:2998-3001.
- El HA, McPate M J, Zhang Y, Zhang H and Hancox J C (2009) Action Potential Clamp and Chloroquine Sensitivity of Mutant Kir2.1 Channels Responsible for Variant 3 Short QT Syndrome. *J Mol Cell Cardiol* **47**:743-747.
- Fakler B, Brandle U, Glowatzki E, Weidemann S, Zenner H P and Ruppersberg J P (1995) Strong Voltage-Dependent Inward Rectification of Inward Rectifier K<sup>+</sup> Channels Is Caused by Intracellular Spermine. *Cell* **80**:149-154.
- Fang K, Csanady L and Chan K W (2006a) The N-Terminal Transmembrane Domain (TMD0) and a Cytosolic Linker (L0) of Sulphonylurea Receptor Define the Unique Intrinsic Gating of KATP Channels. *J Physiol* **576**:379-389.
- Fang Y, Mohler E R, III, Hsieh E, Osman H, Hashemi S M, Davies P F, Rothblat G H, Wilensky R L and Levitan I (2006b) Hypercholesterolemia Suppresses Inwardly Rectifying K<sup>+</sup> Channels in Aortic Endothelium in Vitro and in Vivo. *Circ Res* **98**:1064-1071.

- Ficker E, Tagliatela M, Wible B A, Henley C M and Brown A M (1994) Spermine and Spermidine As Gating Molecules for Inward Rectifier K<sup>+</sup> Channels. *Science* **266**:1068-1072.
- Filosa JA, Bonev A D, Straub S V, Meredith A L, Wilkerson M K, Aldrich R W and Nelson M T (2006) Local Potassium Signaling Couples Neuronal Activity to Vasodilation in the Brain. *Nat Neurosci* **9**:1397-1403.
- Findlay I (1987) The Effects of Magnesium Upon Adenosine Triphosphate-Sensitive Potassium Channels in a Rat Insulin-Secreting Cell Line. *J Physiol* **391**:611-629.
- Findlay I (1988) *Pflugers Arch* **412**:37-41.
- Fischer-Lougheed J, Liu J H, Espinos E, Mordasini D, Bader C R, Belin D and Bernheim L (2001) Human Myoblast Fusion Requires Expression of Functional Inward Rectifier Kir2.1 Channels. *J Cell Biol* **153**:677-686.
- Franchini L, Levi G and Visentin S (2004) Inwardly Rectifying K<sup>+</sup> Channels Influence Ca<sup>2+</sup> Entry Due to Nucleotide Receptor Activation in Microglia. *Cell Calcium* **35**:449-459.
- French RJ and Shoukimas J J (1985) An Ion's View of the Potassium Channel. The Structure of the Permeation Pathway As Sensed by a Variety of Blocking Ions. *J Gen Physiol* **85**:669-698.
- Fujiwara Y and Kubo Y (2006) Functional Roles of Charged Amino Acid Residues on the Wall of the Cytoplasmic Pore of Kir2.1. *J Gen Physiol* **127**:401-419.
- Gilman AG (1987) G Proteins: Transducers of Receptor-Generated Signals. *Annu Rev Biochem* **56**:615-649.
- Glowatzki E, Fakler G, Brandle U, Rexhausen U, Zenner H P, Ruppersberg J P and Fakler B (1995) Subunit-Dependent Assembly of Inward-Rectifier K<sup>+</sup> Channels. *Proc Biol Sci* **261**:251-261.
- Gloyn AL, Pearson E R, Antcliff J F, Proks P, Bruining G J, Slingerland A S, Howard N, Srinivasan S, Silva J M, Molnes J, Edghill E L, Frayling T M, Temple I K, Mackay D, Shield J P, Sumnik Z, van Rhijn A, Wales J K, Clark P, Gorman S, Aisenberg J, Ellard S, Njolstad P R, Ashcroft F M and Hattersley A T (2004) Activating Mutations in the Gene Encoding the ATP-Sensitive Potassium-Channel Subunit Kir6.2 and Permanent Neonatal Diabetes. *N Engl J Med* **350**:1838-1849.
- Gloyn AL, Reimann F, Girard C, Edghill E L, Proks P, Pearson E R, Temple I K, Mackay D J, Shield J P, Freedenberg D, Noyes K, Ellard S, Ashcroft F M, Gribble F M and Hattersley A T (2005) Relapsing Diabetes Can Result From Moderately Activating Mutations in KCNJ11. *Hum Mol Genet* **14**:925-934.
- Goldman DE (1943) POTENTIAL, IMPEDANCE, AND RECTIFICATION IN MEMBRANES. *J Gen Physiol* **27**:37-60.
- Gribble FM, Tucker S J and Ashcroft F M (1997) The Essential Role of the Walker A Motifs of SUR1 in K-ATP Channel Activation by Mg-ADP and Diazoxide. *EMBO J* **16**:1145-1152.
- Gross GJ and Auchampach J A (1992) Blockade of ATP-Sensitive Potassium Channels Prevents Myocardial Preconditioning in Dogs. *Circ Res* **70**:223-233.
- Gumina RJ, Pucar D, Bast P, Hodgson D M, Kurtz C E, Dzeja P P, Miki T, Seino S and Terzic A (2003) Knockout of Kir6.2 Negates Ischemic Preconditioning-Induced Protection of Myocardial Energetics. *Am J Physiol Heart Circ Physiol* **284**:H2106-H2113.

- Guo D and Lu Z (2003) Interaction Mechanisms Between Polyamines and IRK1 Inward Rectifier K<sup>+</sup> Channels. *J Gen Physiol* **122**:485-500.
- Hagiwara S, Miyazaki S, Moody W and Patlak J (1978) Blocking Effects of Barium and Hydrogen Ions on the Potassium Current During Anomalous Rectification in the Starfish Egg. *J Physiol* **279**:167-185.
- Hagiwara S, Miyazaki S and Rosenthal N P (1976) Potassium Current and the Effect of Cesium on This Current During Anomalous Rectification of the Egg Cell Membrane of a Starfish. *J Gen Physiol* **67**:621-638.
- Hagiwara S and Takahashi K (1974) The Anomalous Rectification and Cation Selectivity of the Membrane of a Starfish Egg Cell. *J Membr Biol* **18**:61-80.
- Haider S, Antcliff J F, Proks P, Sansom M S and Ashcroft F M (2005) Focus on Kir6.2: a Key Component of the ATP-Sensitive Potassium Channel. *J Mol Cell Cardiol* **38**:927-936.
- Hansen SB, Tao X and MacKinnon R (2011) Structural Basis of PIP<sub>2</sub> Activation of the Classical Inward Rectifier K<sup>+</sup> Channel Kir2.2. *Nature* **477**:495-498.
- Hassinen M, Paajanen V and Vornanen M (2008) A Novel Inwardly Rectifying K<sup>+</sup> Channel, Kir2.5, Is Upregulated Under Chronic Cold Stress in Fish Cardiac Myocytes. *J Exp Biol* **211**:2162-2171.
- He C, Zhang H, Mirshahi T and Logothetis D E (1999) Identification of a Potassium Channel Site That Interacts With G Protein Betagamma Subunits to Mediate Agonist-Induced Signaling. *J Biol Chem* **274**:12517-12524.
- Heginbotham L, Lu Z, Abramson T and MacKinnon R (1994) Mutations in the K<sup>+</sup> Channel Signature Sequence. *Biophys J* **66**:1061-1067.
- Henry P, Pearson W L and Nichols C G (1996) Protein Kinase C Inhibition of Cloned Inward Rectifier (HRK1/KIR2.3) K<sup>+</sup> Channels Expressed in *Xenopus* Oocytes. *J Physiol* **495** ( Pt 3):681-688.
- Hibino H, Inanobe A, Furutani K, Murakami S, Findlay I and Kurachi Y (2010) Inwardly Rectifying Potassium Channels: Their Structure, Function, and Physiological Roles. *Physiol Rev* **90**:291-366.
- Hilgemann DW and Ball R (1996) Regulation of Cardiac Na<sup>+</sup>,Ca<sup>2+</sup> Exchange and KATP Potassium Channels by PIP<sub>2</sub>. *Science* **273**:956-959.
- Hille B and Schwarz W (1978) Potassium Channels As Multi-Ion Single-File Pores. *J Gen Physiol* **72**:409-442.
- Ho IH and Murrell-Lagnado R D (1999) Molecular Determinants for Sodium-Dependent Activation of G Protein-Gated K<sup>+</sup> Channels. *J Biol Chem* **274**:8639-8648.
- Hodgkin AL and Huxley A F (1952) A Quantitative Description of Membrane Current and Its Application to Conduction and Excitation in Nerve. *J Physiol* **117**:500-544.
- Hofherr A, Fakler B and Klocker N (2005) Selective Golgi Export of Kir2.1 Controls the Stoichiometry of Functional Kir2.x Channel Heteromers. *J Cell Sci* **118**:1935-1943.
- Hollenstein K, Dawson R J and Locher K P (2007) Structure and Mechanism of ABC Transporter Proteins. *Curr Opin Struct Biol* **17**:412-418.

Horio Y, Morishige K, Takahashi N and Kurachi Y (1996) Differential Distribution of Classical Inwardly Rectifying Potassium Channel MRNAs in the Brain: Comparison of IRK2 With IRK1 and IRK3. *FEBS Lett* **379**:239-243.

Huang CL, Feng S and Hilgemann D W (1998) Direct Activation of Inward Rectifier Potassium Channels by PIP2 and Its Stabilization by Gbetagamma. *Nature* **391**:803-806.

Huang CL, Jan Y N and Jan L Y (1997) Binding of the G Protein Betagamma Subunit to Multiple Regions of G Protein-Gated Inward-Rectifying K<sup>+</sup> Channels. *FEBS Lett* **405**:291-298.

Huang CL, Slesinger P A, Casey P J, Jan Y N and Jan L Y (1995) Evidence That Direct Binding of G Beta Gamma to the GIRK1 G Protein-Gated Inwardly Rectifying K<sup>+</sup> Channel Is Important for Channel Activation. *Neuron* **15**:1133-1143.

Huopio H, Reimann F, Ashfield R, Komulainen J, Lenko H L, Rahier J, Vauhkonen I, Kere J, Laakso M, Ashcroft F and Otonkoski T (2000) Dominantly Inherited Hyperinsulinism Caused by a Mutation in the Sulfonylurea Receptor Type 1. *J Clin Invest* **106**:897-906.

Hutter OF and Trautwein W (1956) Vagal and Sympathetic Effects on the Pacemaker Fibers in the Sinus Venosus of the Heart. *J Gen Physiol* **39**:715-733.

Iadarola MJ and Gale K (1982) Substantia Nigra: Site of Anticonvulsant Activity Mediated by Gamma-Aminobutyric Acid. *Science* **218**:1237-1240.

Inagaki N, Gono T, Clement J P, Namba N, Inazawa J, Gonzalez G, Aguilar-Bryan L, Seino S and Bryan J (1995a) Reconstitution of IKATP: an Inward Rectifier Subunit Plus the Sulfonylurea Receptor. *Science* **270**:1166-1170.

Inagaki N, Gono T, Clement J P, Wang C Z, Aguilar-Bryan L, Bryan J and Seino S (1996) A Family of Sulfonylurea Receptors Determines the Pharmacological Properties of ATP-Sensitive K<sup>+</sup> Channels. *Neuron* **16**:1011-1017.

Inagaki N, Tsuura Y, Namba N, Masuda K, Gono T, Horie M, Seino Y, Mizuta M and Seino S (1995b) Cloning and Functional Characterization of a Novel ATP-Sensitive Potassium Channel Ubiquitously Expressed in Rat Tissues, Including Pancreatic Islets, Pituitary, Skeletal Muscle, and Heart. *J Biol Chem* **270**:5691-5694.

Inanobe A, Ito H, Ito M, Hosoya Y and Kurachi Y (1995) Immunological and Physical Characterization of the Brain G Protein-Gated Muscarinic Potassium Channel. *Biochem Biophys Res Commun* **217**:1238-1244.

Inanobe A, Matsuura T, Nakagawa A and Kurachi Y (2007) Structural Diversity in the Cytoplasmic Region of G Protein-Gated Inward Rectifier K<sup>+</sup> Channels. *Channels* **1**.

Ishihara K, Mitsuiye T, Noma A and Takano M (1989) The Mg<sup>2+</sup> Block and Intrinsic Gating Underlying Inward Rectification of the K<sup>+</sup> Current in Guinea-Pig Cardiac Myocytes. *J Physiol* **419**:297-320.

Isomoto S, Kondo C, Yamada M, Matsumoto S, Higashiguchi O, Horio Y, Matsuzawa Y and Kurachi Y (1996) A Novel Sulfonylurea Receptor Forms With BIR (Kir6.2) a Smooth Muscle Type ATP-Sensitive K<sup>+</sup> Channel. *J Biol Chem* **271**:24321-24324.

Ito H, Tung R T, Sugimoto T, Kobayashi I, Takahashi K, Katada T, Ui M and Kurachi Y (1992) On the Mechanism of G Protein Beta Gamma Subunit Activation of the Muscarinic K<sup>+</sup> Channel in Guinea Pig Atrial Cell Membrane. Comparison With the ATP-Sensitive K<sup>+</sup> Channel. *J Gen Physiol* **99**:961-983.

- Ivanina T, Varon D, Peleg S, Rishal I, Porozov Y, Dessauer C W, Keren-Raifman T and Dascal N (2004) Galphai1 and Galphai3 Differentially Interact With, and Regulate, the G Protein-Activated K<sup>+</sup> Channel. *J Biol Chem* **279**:17260-17268.
- Jiang C, Sigworth F J and Haddad G G (1994) Oxygen Deprivation Activates an ATP-Inhibitable K<sup>+</sup> Channel in Substantia Nigra Neurons. *J Neurosci* **14**:5590-5602.
- Jiang Y, Lee A, Chen J, Cadene M, Chait B T and MacKinnon R (2002) Crystal Structure and Mechanism of a Calcium-Gated Potassium Channel. *Nature* **417**:515-522.
- Jiang Y, Lee A, Chen J, Ruta V, Cadene M, Chait B T and MacKinnon R (2003) X-Ray Structure of a Voltage-Dependent K<sup>+</sup> Channel. *Nature* **423**:33-41.
- Jin T, Peng L, Mirshahi T, Rohacs T, Chan K W, Sanchez R and Logothetis D E (2002) The (Beta)Gamma Subunits of G Proteins Gate a K<sup>(+)</sup> Channel by Pivoted Bending of a Transmembrane Segment. *Mol Cell* **10**:469-481.
- John SA, Weiss J N and Ribalet B (2005) ATP Sensitivity of ATP-Sensitive K<sup>+</sup> Channels: Role of the Gamma Phosphate Group of ATP and the R50 Residue of Mouse Kir6.2. *J Physiol* **568**:931-940.
- John SA, Weiss J N, Xie L H and Ribalet B (2003) Molecular Mechanism for ATP-Dependent Closure of the K<sup>+</sup> Channel Kir6.2. *J Physiol* **552**:23-34.
- John SA, Xie L H and Weiss J N (2004) Mechanism of Inward Rectification in Kir Channels. *J Gen Physiol* **123**:623-625.
- Kajioka S, Kitamura K and Kuriyama H (1991) Guanosine Diphosphate Activates an Adenosine 5'-Triphosphate-Sensitive K<sup>+</sup> Channel in the Rabbit Portal Vein. *J Physiol* **444**:397-418.
- Kane GC, Behfar A, Dyer R B, O'Coilain D F, Liu X K, Hodgson D M, Reyes S, Miki T, Seino S and Terzic A (2006) KCNJ11 Gene Knockout of the Kir6.2 KATP Channel Causes Maladaptive Remodeling and Heart Failure in Hypertension. *Hum Mol Genet* **15**:2285-2297.
- Karle CA, Zitron E, Zhang W, Wendt-Nordahl G, Kathofer S, Thomas D, Gut B, Scholz E, Vahl C F, Katus H A and Kiehn J (2002) Human Cardiac Inwardly-Rectifying K<sup>+</sup> Channel Kir(2.1b) Is Inhibited by Direct Protein Kinase C-Dependent Regulation in Human Isolated Cardiomyocytes and in an Expression System. *Circulation* **106**:1493-1499.
- Karschin C, Dissmann E, Stuhmer W and Karschin A (1996) IRK(1-3) and GIRK(1-4) Inwardly Rectifying K<sup>+</sup> Channel MRNAs Are Differentially Expressed in the Adult Rat Brain. *J Neurosci* **16**:3559-3570.
- Katz B (1949) Les Constantes Electriques De La Membrane Du Muscle. *Arch Sci Physiol* **3**:285-299.
- Khurana A, Shao E S, Kim R Y, Vilin Y Y, Huang X, Yang R and Kurata H T (2011) Forced Gating Motions by a Substituted Titratable Side Chain at the Bundle Crossing of a Potassium Channel. *J Biol Chem* **286**:36686-36693.
- Knot HJ, Zimmermann P A and Nelson M T (1996) Extracellular K<sup>(+)</sup>-Induced Hyperpolarizations and Dilatations of Rat Coronary and Cerebral Arteries Involve Inward Rectifier K<sup>(+)</sup> Channels. *J Physiol* **492** ( Pt 2):419-430.

Konig S, Hinard V, Arnaudeau S, Holzer N, Potter G, Bader C R and Bernheim L (2004) Membrane Hyperpolarization Triggers Myogenin and Myocyte Enhancer Factor-2 Expression During Human Myoblast Differentiation. *J Biol Chem* **279**:28187-28196.

Koster JC, Kurata H T, Enkvetchakul D and Nichols C G (2008) DEND Mutation in Kir6.2 (KCNJ11) Reveals a Flexible N-Terminal Region Critical for ATP-Sensing of the K-ATP Channel. *Biophysical Journal* **95**:4689-4697.

Koster JC, Remedi M S, Dao C and Nichols C G (2005) ATP and Sulfonylurea Sensitivity of Mutant ATP-Sensitive K<sup>+</sup> Channels in Neonatal Diabetes: Implications for Pharmacogenomic Therapy. *Diabetes* **54**:2645-2654.

Krapivinsky G, Gordon E A, Wickman K, Velimirovic B, Krapivinsky L and Clapham D E (1995) The G-Protein-Gated Atrial K<sup>+</sup> Channel IKACH Is a Heteromultimer of Two Inwardly Rectifying K(+)-Channel Proteins. *Nature* **374**:135-141.

Kubo Y, Baldwin T J, Jan Y N and Jan L Y (1993) Primary Structure and Functional Expression of a Mouse Inward Rectifier Potassium Channel. *Nature* **362**:127-133.

Kubo Y and Murata Y (2001) Control of Rectification and Permeation by Two Distinct Sites After the Second Transmembrane Region in Kir2.1 K<sup>+</sup> Channel. *J Physiol* **531**:645-660.

Kuo A, Gulbis J M, Antcliff J F, Rahman T, Lowe E D, Zimmer J, Cuthbertson J, Ashcroft F M, Ezaki T and Doyle D A (2003) Crystal Structure of the Potassium Channel KirBac1.1 in the Closed State. *Science* **300**:1922-1926.

Kurachi Y (1985) Voltage-Dependent Activation of the Inward-Rectifier Potassium Channel in the Ventricular Cell Membrane of Guinea-Pig Heart. *J Physiol* **366**:365-385.

Kurachi Y (1995) G Protein Regulation of Cardiac Muscarinic Potassium Channel. *Am J Physiol* **269**:C821-C830.

Kurachi Y, Nakajima T and Sugimoto T (1986) On the Mechanism of Activation of Muscarinic K<sup>+</sup> Channels by Adenosine in Isolated Atrial Cells: Involvement of GTP-Binding Proteins. *Pflugers Arch* **407**:264-274.

Kurata HT, Cheng W W, Arrabit C, Slesinger P A and Nichols C G (2007) The Role of the Cytoplasmic Pore in Inward Rectification of Kir2.1 Channels. *J Gen Physiol* **130**:145-155.

Kurata HT, Cheng W W and Nichols C G (2011) Polyamine Block of Inwardly Rectifying Potassium Channels. *Methods Mol Biol* **720**:113-126.

Kurata HT, Diraviyam K, Marton L J and Nichols C G (2008) Blocker Protection by Short Spermine Analogs: Refined Mapping of the Spermine Binding Site in a Kir Channel. *Biophysical Journal* **95**:3827-3839.

Kurata HT, Marton L J and Nichols C G (2006) The Polyamine Binding Site in Inward Rectifier K<sup>+</sup> Channels. *J Gen Physiol* **127**:467-480.

Kurata HT, Phillips L R, Rose T, Loussouarn G, Herlitz S, Fritzenschaft H, Enkvetchakul D, Nichols C G and Baukowitz T (2004) Molecular Basis of Inward Rectification: Polyamine Interaction Sites Located by Combined Channel and Ligand Mutagenesis. *J Gen Physiol* **124**:541-554.

- Kurata HT, Rapedius M, Kleinman M J, Baukowitz T and Nichols C G (2010a) Voltage-Dependent Gating in a "Voltage Sensor-Less" Ion Channel. *PLoS Biol* **8**:e1000315.
- Kurata HT, Zhu E A and Nichols C G (2010b) Locale and Chemistry of Spermine Binding in the Archetypal Inward Rectifier Kir2.1. *J Gen Physiol* **135**:495-508.
- Kwan HY, Leung P C, Huang Y and Yao X (2003) Depletion of Intracellular Ca<sup>2+</sup> Stores Sensitizes the Flow-Induced Ca<sup>2+</sup> Influx in Rat Endothelial Cells. *Circ Res* **92**:286-292.
- Lederer WJ and Nichols C G (1989) Nucleotide Modulation of the Activity of Rat Heart ATP-Sensitive K<sup>+</sup> Channels in Isolated Membrane Patches. *J Physiol* **419**:193-211.
- Lee SY, Banerjee A and MacKinnon R (2009) Two Separate Interfaces Between the Voltage Sensor and Pore Are Required for the Function of Voltage-Dependent K<sup>(+)</sup> Channels. *PLoS Biol* **7**:e47.
- Li L, Wang J and Drain P (2000) The I182 Region of K(Ir)6.2 Is Closely Associated With Ligand Binding in K(ATP) Channel Inhibition by ATP. *Biophys J* **79**:841-852.
- Lindman S, Linse S, Mulder F A and Andre I (2007) PK(a) Values for Side-Chain Carboxyl Groups of a PGB1 Variant Explain Salt and PH-Dependent Stability. *Biophys J* **92**:257-266.
- Liu XK, Yamada S, Kane G C, Alekseev A E, Hodgson D M, O'Coilain F, Jahangir A, Miki T, Seino S and Terzic A (2004) Genetic Disruption of Kir6.2, the Pore-Forming Subunit of ATP-Sensitive K<sup>+</sup> Channel, Predisposes to Catecholamine-Induced Ventricular Dysrhythmia. *Diabetes* **53 Suppl 3**:S165-S168.
- Logothetis DE, Kurachi Y, Galper J, Neer E J and Clapham D E (1987) The Beta Gamma Subunits of GTP-Binding Proteins Activate the Muscarinic K<sup>+</sup> Channel in Heart. *Nature* **325**:321-326.
- Long SB, Campbell E B and MacKinnon R (2005a) Crystal Structure of a Mammalian Voltage-Dependent Shaker Family K<sup>+</sup> Channel. *Science* **309**:897-903.
- Long SB, Campbell E B and MacKinnon R (2005b) Voltage Sensor of Kv1.2: Structural Basis of Electromechanical Coupling. *Science* **309**:903-908.
- Long SB, Tao X, Campbell E B and MacKinnon R (2007) Atomic Structure of a Voltage-Dependent K<sup>+</sup> Channel in a Lipid Membrane-Like Environment. *Nature* **450**:376-382.
- Lopatin AN, Makhina E N and Nichols C G (1994) Potassium Channel Block by Cytoplasmic Polyamines As the Mechanism of Intrinsic Rectification. *Nature* **372**:366-369.
- Lopatin AN, Makhina E N and Nichols C G (1995) The Mechanism of Inward Rectification of Potassium Channels: "Long-Pore Plugging" by Cytoplasmic Polyamines. *J Gen Physiol* **106**:923-955.
- Lopatin AN and Nichols C G (1996a) [K<sup>+</sup>] Dependence of Open-Channel Conductance in Cloned Inward Rectifier Potassium Channels (IRK1, Kir2.1). *Biophys J* **71**:682-694.
- Lopatin AN and Nichols C G (1996b) [K<sup>+</sup>] Dependence of Polyamine-Induced Rectification in Inward Rectifier Potassium Channels (IRK1, Kir2.1). *J Gen Physiol* **108**:105-113.
- Lopes CM, Zhang H, Rohacs T, Jin T, Yang J and Logothetis D E (2002) Alterations in Conserved Kir Channel-PIP2 Interactions Underlie Channelopathies. *Neuron* **34**:933-944.

- Lu T, Nguyen B, Zhang X and Yang J (1999) Architecture of a K<sup>+</sup> Channel Inner Pore Revealed by Stoichiometric Covalent Modification. *Neuron* **22**:571-580.
- Lu Z (2004) Mechanism of Rectification in Inward-Rectifier K<sup>+</sup> Channels. *Annu Rev Physiol* **66**:103-129.
- Lu Z, Klem A M and Ramu Y (2002) Coupling Between Voltage Sensors and Activation Gate in Voltage-Gated K<sup>+</sup> Channels. *J Gen Physiol* **120**:663-676.
- Lu Z and MacKinnon R (1994) Electrostatic Tuning of Mg<sup>2+</sup> Affinity in an Inward-Rectifier K<sup>+</sup> Channel. *Nature* **371**:243-246.
- Ma D, Zerangue N, Lin Y F, Collins A, Yu M, Jan Y N and Jan L Y (2001) Role of ER Export Signals in Controlling Surface Potassium Channel Numbers. *Science* **291**:316-319.
- Mannikko R, Jefferies C, Flanagan S E, Hattersley A, Ellard S and Ashcroft F M (2010) Interaction Between Mutations in the Slide Helix of Kir6.2 Associated With Neonatal Diabetes and Neurological Symptoms. *Hum Mol Genet* **19**:963-972.
- Mannikko R, Stansfeld P J, Ashcroft A S, Hattersley A T, Sansom M S, Ellard S and Ashcroft F M (2011) A Conserved Tryptophan at the Membrane-Water Interface Acts As a Gatekeeper for Kir6.2/SUR1 Channels and Causes Neonatal Diabetes When Mutated. *J Physiol* **589**:3071-3083.
- Matsuda H (1988) Open-State Substructure of Inwardly Rectifying Potassium Channels Revealed by Magnesium Block in Guinea-Pig Heart Cells. *J Physiol* **397**:237-258.
- Matsuda H, Hayashi M and Okada M (2010) Voltage-Dependent Block by Internal Spermine of the Murine Inwardly Rectifying K<sup>+</sup> Channel, Kir2.1, With Asymmetrical K<sup>+</sup> Concentrations. *J Physiol* **588**:4673-4681.
- Matsuda H, Oishi K and Omori K (2003) Voltage-Dependent Gating and Block by Internal Spermine of the Murine Inwardly Rectifying K<sup>+</sup> Channel, Kir2.1. *J Physiol* **548**:361-371.
- Matsuda H, Saigusa A and Irisawa H (1987) Ohmic Conductance Through the Inwardly Rectifying K Channel and Blocking by Internal Mg<sup>2+</sup>. *Nature* **325**:156-159.
- Matsuo M, Tanabe K, Kioka N, Amachi T and Ueda K (2000) Different Binding Properties and Affinities for ATP and ADP Among Sulfonylurea Receptor Subtypes, SUR1, SUR2A, and SUR2B. *J Biol Chem* **275**:28757-28763.
- Matsuoka T, Matsushita K, Katayama Y, Fujita A, Inageda K, Tanemoto M, Inanobe A, Yamashita S, Matsuzawa Y and Kurachi Y (2000) C-Terminal Tails of Sulfonylurea Receptors Control ADP-Induced Activation and Diazoxide Modulation of ATP-Sensitive K(+) Channels. *Circ Res* **87**:873-880.
- Mavri J and Vogel H J (1994) Ion Pair Formation Involving Methylated Lysine Side Chains: a Theoretical Study. *Proteins* **18**:381-389.
- McAllister RE and Noble D (1966) The Time and Voltage Dependence of the Slow Outward Current in Cardiac Purkinje Fibres. *J Physiol* **186**:632-662.
- McCarron JG and Halpern W (1990) Potassium Dilates Rat Cerebral Arteries by Two Independent Mechanisms. *Am J Physiol* **259**:H902-H908.
- McNeill TH, Brown S A, Rafols J A and Shoulson I (1988) Atrophy of Medium Spiny I Striatal Dendrites in Advanced Parkinson's Disease. *Brain Res* **455**:148-152.

- Minor DL, Jr., Masseling S J, Jan Y N and Jan L Y (1999) Transmembrane Structure of an Inwardly Rectifying Potassium Channel. *Cell* **96**:879-891.
- Misgeld U, Muller W and Brunner H (1989) Effects of (-)Baclofen on Inhibitory Neurons in the Guinea Pig Hippocampal Slice. *Pflugers Arch* **414**:139-144.
- Miyazaki SI, Takahashi K, Tsuda K and Yoshii M (1974) Analysis of Non-Linearity Observed in the Current-Voltage Relation of the Tunicate Embryo. *J Physiol* **238**:55-77.
- Morais-Cabral JH, Zhou Y and MacKinnon R (2001) Energetic Optimization of Ion Conduction Rate by the K<sup>+</sup> Selectivity Filter. *Nature* **414**:37-42.
- Murry CE, Jennings R B and Reimer K A (1986) Preconditioning With Ischemia: a Delay of Lethal Cell Injury in Ischemic Myocardium. *Circulation* **74**:1124-1136.
- Nelson MT, Cheng H, Rubart M, Santana L F, Bonev A D, Knot H J and Lederer W J (1995) Relaxation of Arterial Smooth Muscle by Calcium Sparks. *Science* **270**:633-637.
- Nichols CG (2006) KATP Channels As Molecular Sensors of Cellular Metabolism. *Nature* **440**:470-476.
- Nichols CG and Lopatin A N (1997) Inward Rectifier Potassium Channels. *Annu Rev Physiol* **59**:171-191.
- Nilius B and Droogmans G (2001) Ion Channels and Their Functional Role in Vascular Endothelium. *Physiol Rev* **81**:1415-1459.
- Nishida M, Cadene M, Chait B T and MacKinnon R (2007) Crystal Structure of a Kir3.1-Prokaryotic Kir Channel Chimera. *EMBO J* **26**:4005-4015.
- Nishida M and MacKinnon R (2002) Structural Basis of Inward Rectification: Cytoplasmic Pore of the G Protein-Gated Inward Rectifier GIRK1 at 1.8 Å Resolution. *Cell* **111**:957-965.
- Noma A, Nakayama T, Kurachi Y and Irisawa H (1984) Resting K Conductances in Pacemaker and Non-Pacemaker Heart Cells of the Rabbit. *Jpn J Physiol* **34**:245-254.
- Noskov SY, Berneche S and Roux B (2004) Control of Ion Selectivity in Potassium Channels by Electrostatic and Dynamic Properties of Carbonyl Ligands. *Nature* **431**:830-834.
- Ohno-Shosaku T, Zunkler B J and Trube G (1987) Dual Effects of ATP on K<sup>+</sup> Currents of Mouse Pancreatic Beta-Cells. *Pflugers Arch* **408**:133-138.
- Olesen SP, Clapham D E and Davies P F (1988) Haemodynamic Shear Stress Activates a K<sup>+</sup> Current in Vascular Endothelial Cells. *Nature* **331**:168-170.
- Oliver D, Hahn H, Antz C, Ruppertsberg J P and Fakler B (1998) Interaction of Permeant and Blocking Ions in Cloned Inward-Rectifier K<sup>+</sup> Channels. *Biophys J* **74**:2318-2326.
- Paynter JJ, Andres-Enguix I, Fowler P W, Tottey S, Cheng W, Enkvetchakul D, Bavro V N, Kusakabe Y, Sansom M S, Robinson N J, Nichols C G and Tucker S J (2010) Functional Complementation and Genetic Deletion Studies of KirBac Channels: Activatory Mutations Highlight Gating-Sensitive Domains. *J Biol Chem* **285**:40754-40761.
- Pearson WL and Nichols C G (1998) Block of the Kir2.1 Channel Pore by Alkylamine Analogues of Endogenous Polyamines. *J Gen Physiol* **112**:351-363.

- Pegan S, Arrabit C, Slesinger P A and Choe S (2006) Andersen's Syndrome Mutation Effects on the Structure and Assembly of the Cytoplasmic Domains of Kir2.1. *Biochemistry* **45**:8599-8606.
- Pegan S, Arrabit C, Zhou W, Kwiatkowski W, Collins A, Slesinger P A and Choe S (2005) Cytoplasmic Domain Structures of Kir2.1 and Kir3.1 Show Sites for Modulating Gating and Rectification. *Nat Neurosci* **8**:279-287.
- Peleg S, Varon D, Ivanina T, Dessauer C W and Dascal N (2002) G(Alpha)(i) Controls the Gating of the G Protein-Activated K(+) Channel, GIRK. *Neuron* **33**:87-99.
- Perier F, Radeke C M and Vandenberg C A (1994) Primary Structure and Characterization of a Small-Conductance Inwardly Rectifying Potassium Channel From Human Hippocampus. *Proc Natl Acad Sci U S A* **91**:6240-6244.
- Petit-Jacques J, Sui J L and Logothetis D E (1999) Synergistic Activation of G Protein-Gated Inwardly Rectifying Potassium Channels by the Betagamma Subunits of G Proteins and Na(+) and Mg(2+) Ions. *J Gen Physiol* **114**:673-684.
- Plaster NM, Tawil R, Tristani-Firouzi M, Canun S, Bendahhou S, Tsunoda A, Donaldson M R, Iannaccone S T, Brunt E, Barohn R, Clark J, Deymeer F, George A L, Jr., Fish F A, Hahn A, Nitu A, Ozdemir C, Serdaroglu P, Subramony S H, Wolfe G, Fu Y H and Ptacek L J (2001) Mutations in Kir2.1 Cause the Developmental and Episodic Electrical Phenotypes of Andersen's Syndrome. *Cell* **105**:511-519.
- Preisig-Muller R, Schlichthorl G, Goerge T, Heinen S, Bruggemann A, Rajan S, Derst C, Veh R W and Daut J (2002) Heteromerization of Kir2.x Potassium Channels Contributes to the Phenotype of Andersen's Syndrome. *Proc Natl Acad Sci U S A* **99**:7774-7779.
- Priori SG, Pandit S V, Rivolta I, Berenfeld O, Ronchetti E, Dhamoon A, Napolitano C, Anumonwo J, di Barletta M R, Gudapakkam S, Bosi G, Stramba-Badiale M and Jalife J (2005) A Novel Form of Short QT Syndrome (SQT3) Is Caused by a Mutation in the KCNJ2 Gene. *Circ Res* **96**:800-807.
- Proks P, Antcliff J F, Lippiat J, Gloyn A L, Hattersley A T and Ashcroft F M (2004) Molecular Basis of Kir6.2 Mutations Associated With Neonatal Diabetes or Neonatal Diabetes Plus Neurological Features. *Proc Natl Acad Sci U S A* **101**:17539-17544.
- Proks P, Girard C, Haider S, Gloyn A L, Hattersley A T, Sansom M S and Ashcroft F M (2005) A Gating Mutation at the Internal Mouth of the Kir6.2 Pore Is Associated With DEND Syndrome. *EMBO Rep* **6**:470-475.
- Proks P, Gribble F M, Adhikari R, Tucker S J and Ashcroft F M (1999) Involvement of the N-Terminus of Kir6.2 in the Inhibition of the KATP Channel by ATP. *J Physiol* **514** ( Pt 1):19-25.
- Pruss H, Derst C, Lommel R and Veh R W (2005) Differential Distribution of Individual Subunits of Strongly Inwardly Rectifying Potassium Channels (Kir2 Family) in Rat Brain. *Brain Res Mol Brain Res* **139**:63-79.
- Qu Z, Yang Z, Cui N, Zhu G, Liu C, Xu H, Chanchevalap S, Shen W, Wu J, Li Y and Jiang C (2000) Gating of Inward Rectifier K+ Channels by Proton-Mediated Interactions of N- and C-Terminal Domains. *J Biol Chem* **275**:31573-31580.
- Quayle JM, McCarron J G, Brayden J E and Nelson M T (1993) Inward Rectifier K+ Currents in Smooth Muscle Cells From Rat Resistance-Sized Cerebral Arteries. *Am J Physiol* **265**:C1363-C1370.

- Quayle JM, Nelson M T and Standen N B (1997) ATP-Sensitive and Inwardly Rectifying Potassium Channels in Smooth Muscle. *Physiol Rev* **77**:1165-1232.
- Raab-Graham KF, Radeke C M and Vandenberg C A (1994) Molecular Cloning and Expression of a Human Heart Inward Rectifier Potassium Channel. *Neuroreport* **5**:2501-2505.
- Raab-Graham KF and Vandenberg C A (1998) Tetrameric Subunit Structure of the Native Brain Inwardly Rectifying Potassium Channel Kir 2.2. *J Biol Chem* **273**:19699-19707.
- Rapedius M, Fowler P W, Shang L, Sansom M S, Tucker S J and Baukrowitz T (2007) H Bonding at the Helix-Bundle Crossing Controls Gating in Kir Potassium Channels. *Neuron* **55**:602-614.
- Reimann F, Huopio H, Dabrowski M, Proks P, Gribble F M, Laakso M, Otonkoski T and Ashcroft F M (2003) Characterisation of New KATP-Channel Mutations Associated With Congenital Hyperinsulinism in the Finnish Population. *Diabetologia* **46**:241-249.
- Reimann F, Ryder T J, Tucker S J and Ashcroft F M (1999) The Role of Lysine 185 in the Kir6.2 Subunit of the ATP-Sensitive Channel in Channel Inhibition by ATP. *J Physiol* **520 Pt 3**:661-669.
- Riven I, Iwanir S and Reuveny E (2006) GIRK Channel Activation Involves a Local Rearrangement of a Preformed G Protein Channel Complex. *Neuron* **51**:561-573.
- Riven I, Kalmanzon E, Segev L and Reuveny E (2003) Conformational Rearrangements Associated With the Gating of the G Protein-Coupled Potassium Channel Revealed by FRET Microscopy. *Neuron* **38**:225-235.
- Robertson JL, Palmer L G and Roux B (2008) Long-Pore Electrostatics in Inward-Rectifier Potassium Channels. *J Gen Physiol* **132**:613-632.
- Romanenko VG, Fang Y, Byfield F, Travis A J, Vandenberg C A, Rothblat G H and Levitan I (2004) Cholesterol Sensitivity and Lipid Raft Targeting of Kir2.1 Channels. *Biophys J* **87**:3850-3861.
- Romanenko VG, Rothblat G H and Levitan I (2002) Modulation of Endothelial Inward-Rectifier K<sup>+</sup> Current by Optical Isomers of Cholesterol. *Biophys J* **83**:3211-3222.
- Routh VH (2002) Glucose-Sensing Neurons: Are They Physiologically Relevant? *Physiol Behav* **76**:403-413.
- Ryan DP, da Silva M R, Soong T W, Fontaine B, Donaldson M R, Kung A W, Jongjaroenprasert W, Liang M C, Khoo D H, Cheah J S, Ho S C, Bernstein H S, Maciel R M, Brown R H, Jr. and Ptacek L J (2010) Mutations in Potassium Channel Kir2.6 Cause Susceptibility to Thyrotoxic Hypokalemic Periodic Paralysis. *Cell* **140**:88-98.
- Sadja R, Smadja K, Alagem N and Reuveny E (2001) Coupling Gbetagamma-Dependent Activation to Channel Opening Via Pore Elements in Inwardly Rectifying Potassium Channels. *Neuron* **29**:669-680.
- Sagen JV, Raeder H, Hathout E, Shehadeh N, Gudmundsson K, Baevre H, Abuelo D, Phornphutkul C, Molnes J, Bell G I, Gloyn A L, Hattersley A T, Molven A, Sovik O and Njolstad P R (2004) Permanent Neonatal Diabetes Due to Mutations in KCNJ11 Encoding Kir6.2: Patient Characteristics and Initial Response to Sulfonylurea Therapy. *Diabetes* **53**:2713-2718.
- Sakmann B and Trube G (1984) Conductance Properties of Single Inwardly Rectifying Potassium Channels in Ventricular Cells From Guinea-Pig Heart. *J Physiol* **347**:641-657.

- Sansone V, Griggs R C, Meola G, Ptacek L J, Barohn R, Iannaccone S, Bryan W, Baker N, Janas S J, Scott W, Ririe D and Tawil R (1997) Andersen's Syndrome: a Distinct Periodic Paralysis. *Ann Neurol* **42**:305-312.
- Sansone V and Tawil R (2007) Management and Treatment of Andersen-Tawil Syndrome (ATS). *Neurotherapeutics* **4**:233-237.
- Schimpf R, Wolpert C, Gaita F, Giustetto C and Borggrefe M (2005) Short QT Syndrome. *Cardiovasc Res* **67**:357-366.
- Schram G, Melnyk P, Pourrier M, Wang Z and Nattel S (2002) Kir2.4 and Kir2.1 K(+) Channel Subunits Co-Assemble: a Potential New Contributor to Inward Rectifier Current Heterogeneity. *J Physiol* **544**:337-349.
- Schulz R, Rose J and Heusch G (1994) Involvement of Activation of ATP-Dependent Potassium Channels in Ischemic Preconditioning in Swine. *Am J Physiol* **267**:H1341-H1352.
- Schwappach B, Zerangue N, Jan Y N and Jan L Y (2000) Molecular Basis for K(ATP) Assembly: Transmembrane Interactions Mediate Association of a K<sup>+</sup> Channel With an ABC Transporter. *Neuron* **26**:155-167.
- Shang L and Tucker S J (2008) Non-Equivalent Role of TM2 Gating Hinges in Heteromeric Kir4.1/Kir5.1 Potassium Channels. *Eur Biophys J* **37**:165-171.
- Shen W, Tian X, Day M, Ulrich S, Tkatch T, Nathanson N M and Surmeier D J (2007) Cholinergic Modulation of Kir2 Channels Selectively Elevates Dendritic Excitability in Striatopallidal Neurons. *Nat Neurosci* **10**:1458-1466.
- Shimomura K, Girard C A, Proks P, Nazim J, Lippiat J D, Cerutti F, Lorini R, Ellard S, Hattersley A T, Barbetti F and Ashcroft F M (2006) Mutations at the Same Residue (R50) of Kir6.2 (KCNJ11) That Cause Neonatal Diabetes Produce Different Functional Effects. *Diabetes* **55**:1705-1712.
- Shin HG and Lu Z (2005) Mechanism of the Voltage Sensitivity of IRK1 Inward-Rectifier K<sup>+</sup> Channel Block by the Polyamine Spermine. *J Gen Physiol* **125**:413-426.
- Shin HG, Xu Y and Lu Z (2005) Evidence for Sequential Ion-Binding Loci Along the Inner Pore of the IRK1 Inward-Rectifier K<sup>+</sup> Channel. *J Gen Physiol* **126**:123-135.
- Shyng S, Ferrigni T and Nichols C G (1997a) Control of Rectification and Gating of Cloned KATP Channels by the Kir6.2 Subunit. *J Gen Physiol* **110**:141-153.
- Shyng S, Ferrigni T and Nichols C G (1997b) Regulation of KATP Channel Activity by Diazoxide and MgADP. Distinct Functions of the Two Nucleotide Binding Folds of the Sulfonylurea Receptor. *J Gen Physiol* **110**:643-654.
- Shyng SL, Cukras C A, Harwood J and Nichols C G (2000) Structural Determinants of PIP(2) Regulation of Inward Rectifier K(ATP) Channels. *J Gen Physiol* **116**:599-608.
- Shyng SL and Nichols C G (1998) Membrane Phospholipid Control of Nucleotide Sensitivity of KATP Channels. *Science* **282**:1138-1141.
- Signorini S, Liao Y J, Duncan S A, Jan L Y and Stoffel M (1997) Normal Cerebellar Development but Susceptibility to Seizures in Mice Lacking G Protein-Coupled, Inwardly Rectifying K<sup>+</sup> Channel GIRK2. *Proc Natl Acad Sci U S A* **94**:923-927.

- Slesinger PA, Patil N, Liao Y J, Jan Y N, Jan L Y and Cox D R (1996) Functional Effects of the Mouse Weaver Mutation on G Protein-Gated Inwardly Rectifying K<sup>+</sup> Channels. *Neuron* **16**:321-331.
- Slesinger PA, Reuveny E, Jan Y N and Jan L Y (1995) Identification of Structural Elements Involved in G Protein Gating of the GIRK1 Potassium Channel. *Neuron* **15**:1145-1156.
- Spasova M and Lu Z (1998) Coupled Ion Movement Underlies Rectification in an Inward-Rectifier K<sup>+</sup> Channel. *J Gen Physiol* **112**:211-221.
- Stockklausner C and Klocker N (2003) Surface Expression of Inward Rectifier Potassium Channels Is Controlled by Selective Golgi Export. *J Biol Chem* **278**:17000-17005.
- Stockklausner C, Ludwig J, Ruppertsberg J P and Klocker N (2001) A Sequence Motif Responsible for ER Export and Surface Expression of Kir2.0 Inward Rectifier K(+) Channels. *FEBS Lett* **493**:129-133.
- Suzuki M, Sasaki N, Miki T, Sakamoto N, Ohmoto-Sekine Y, Tamagawa M, Seino S, Marban E and Nakaya H (2002) Role of Sarcolemmal K(ATP) Channels in Cardioprotection Against Ischemia/Reperfusion Injury in Mice. *J Clin Invest* **109**:509-516.
- Takahashi N, Morishige K, Jahangir A, Yamada M, Findlay I, Koyama H and Kurachi Y (1994) Molecular Cloning and Functional Expression of cDNA Encoding a Second Class of Inward Rectifier Potassium Channels in the Mouse Brain. *J Biol Chem* **269**:23274-23279.
- Takano M, Qin D Y and Noma A (1990) ATP-Dependent Decay and Recovery of K<sup>+</sup> Channels in Guinea Pig Cardiac Myocytes. *Am J Physiol* **258**:H45-H50.
- Tani Y, Miura D, Kurokawa J, Nakamura K, Ouchida M, Shimizu K, Ohe T and Furukawa T (2007) T75M-KCNJ2 Mutation Causing Andersen-Tawil Syndrome Enhances Inward Rectification by Changing Mg<sup>2+</sup> Sensitivity. *J Mol Cell Cardiol* **43**:187-196.
- Tao X, Avalos J L, Chen J and MacKinnon R (2009) Crystal Structure of the Eukaryotic Strong Inward-Rectifier K<sup>+</sup> Channel Kir2.2 at 3.1 Å Resolution. *Science* **326**:1668-1674.
- Tawil R, Ptacek L J, Pavlakis S G, DeVivo D C, Penn A S, Ozdemir C and Griggs R C (1994) Andersen's Syndrome: Potassium-Sensitive Periodic Paralysis, Ventricular Ectopy, and Dysmorphic Features. *Ann Neurol* **35**:326-330.
- Terzic A, Jahangir A and Kurachi Y (1995) Cardiac ATP-Sensitive K<sup>+</sup> Channels: Regulation by Intracellular Nucleotides and K<sup>+</sup> Channel-Opening Drugs. *Am J Physiol* **269**:C525-C545.
- Terzic A, Tung R T, Inanobe A, Katada T and Kurachi Y (1994) G Proteins Activate ATP-Sensitive K<sup>+</sup> Channels by Antagonizing ATP-Dependent Gating. *Neuron* **12**:885-893.
- Thomas P, Ye Y and Lightner E (1996) Mutation of the Pancreatic Islet Inward Rectifier Kir6.2 Also Leads to Familial Persistent Hyperinsulinemic Hypoglycemia of Infancy. *Hum Mol Genet* **5**:1809-1812.
- Thomas PM, Cote G J, Wohllk N, Haddad B, Mathew P M, Rabl W, Aguilar-Bryan L, Gagel R F and Bryan J (1995) Mutations in the Sulfonylurea Receptor Gene in Familial Persistent Hyperinsulinemic Hypoglycemia of Infancy. *Science* **268**:426-429.
- Thompson SM and Gahwiler B H (1992) Comparison of the Actions of Baclofen at Pre- and Postsynaptic Receptors in the Rat Hippocampus in Vitro. *J Physiol* **451**:329-345.

- Thompson SM, Haas H L and Gahwiler B H (1992) Comparison of the Actions of Adenosine at Pre- and Postsynaptic Receptors in the Rat Hippocampus in Vitro. *J Physiol* **451**:347-363.
- Tinker A, Jan Y N and Jan L Y (1996) Regions Responsible for the Assembly of Inwardly Rectifying Potassium Channels. *Cell* **87**:857-868.
- Tong X, Porter L M, Liu G, Dhar-Chowdhury P, Srivastava S, Pountney D J, Yoshida H, Artman M, Fishman G I, Yu C, Iyer R, Morley G E, Gutstein D E and Coetzee W A (2006) Consequences of Cardiac Myocyte-Specific Ablation of KATP Channels in Transgenic Mice Expressing Dominant Negative Kir6 Subunits. *Am J Physiol Heart Circ Physiol* **291**:H543-H551.
- Topert C, Doring F, Wischmeyer E, Karschin C, Brockhaus J, Ballanyi K, Derst C and Karschin A (1998) Kir2.4: a Novel K<sup>+</sup> Inward Rectifier Channel Associated With Motoneurons of Cranial Nerve Nuclei. *J Neurosci* **18**:4096-4105.
- Trapp S, Haider S, Jones P, Sansom M S and Ashcroft F M (2003) Identification of Residues Contributing to the ATP Binding Site of Kir6.2. *EMBO J* **22**:2903-2912.
- Trapp S, Proks P, Tucker S J and Ashcroft F M (1998) Molecular Analysis of ATP-Sensitive K Channel Gating and Implications for Channel Inhibition by ATP. *J Gen Physiol* **112**:333-349.
- Tristani-Firouzi M, Jensen J L, Donaldson M R, Sansone V, Meola G, Hahn A, Bendahhou S, Kwiecinski H, Fidzianska A, Plaster N, Fu Y H, Ptacek L J and Tawil R (2002) Functional and Clinical Characterization of KCNJ2 Mutations Associated With LQT7 (Andersen Syndrome). *J Clin Invest* **110**:381-388.
- Tucker SJ, Gribble F M, Proks P, Trapp S, Ryder T J, Haug T, Reimann F and Ashcroft F M (1998) Molecular Determinants of KATP Channel Inhibition by ATP. *EMBO J* **17**:3290-3296.
- Tucker SJ, Gribble F M, Zhao C, Trapp S and Ashcroft F M (1997) Truncation of Kir6.2 Produces ATP-Sensitive K<sup>+</sup> Channels in the Absence of the Sulphonylurea Receptor. *Nature* **387**:179-183.
- Tung RT and Kurachi Y (1991) On the Mechanism of Nucleotide Diphosphate Activation of the ATP-Sensitive K<sup>+</sup> Channel in Ventricular Cell of Guinea-Pig. *J Physiol* **437**:239-256.
- Wang Z, Yue L, White M, Pelletier G and Nattel S (1998) Differential Distribution of Inward Rectifier Potassium Channel Transcripts in Human Atrium Versus Ventricle. *Circulation* **98**:2422-2428.
- Wellman GC and Bevan J A (1995) Barium Inhibits the Endothelium-Dependent Component of Flow but Not Acetylcholine-Induced Relaxation in Isolated Rabbit Cerebral Arteries. *J Pharmacol Exp Ther* **274**:47-53.
- Whorton MR and MacKinnon R (2011) Crystal Structure of the Mammalian GIRK2 K<sup>+</sup> Channel and Gating Regulation by G Proteins, PIP<sub>2</sub>, and Sodium. *Cell* **147**:199-208.
- Wible BA, De B M, Majumder K, Taglialatela M and Brown A M (1995) Cloning and Functional Expression of an Inwardly Rectifying K<sup>+</sup> Channel From Human Atrium. *Circ Res* **76**:343-350.
- Wible BA, Taglialatela M, Ficker E and Brown A M (1994) Gating of Inwardly Rectifying K<sup>+</sup> Channels Localized to a Single Negatively Charged Residue. *Nature* **371**:246-249.
- Wickman K, Nemej J, Gendler S J and Clapham D E (1998) Abnormal Heart Rate Regulation in GIRK4 Knockout Mice. *Neuron* **20**:103-114.

- Woodhull AM (1973) Ionic Blockage of Sodium Channels in Nerve. *J Gen Physiol* **61**:687-708.
- Xie LH, John S A and Weiss J N (2002) Spermine Block of the Strong Inward Rectifier Potassium Channel Kir2.1: Dual Roles of Surface Charge Screening and Pore Block. *J Gen Physiol* **120**:53-66.
- Xu Y and Lu Z (2004) Characterization of Inward-Rectifier K<sup>+</sup> Channel Inhibition by Antiarrhythmic Piperazine. *Biochemistry* **43**:15577-15583.
- Xu Y, Shin H G, Szep S and Lu Z (2009) Physical Determinants of Strong Voltage Sensitivity of K<sup>(+)</sup> Channel Block. *Nat Struct Mol Biol*.
- Yamada K, Ji J J, Yuan H, Miki T, Sato S, Horimoto N, Shimizu T, Seino S and Inagaki N (2001) Protective Role of ATP-Sensitive Potassium Channels in Hypoxia-Induced Generalized Seizure. *Science* **292**:1543-1546.
- Yamada M, Ishii M, Hibino H and Kurachi Y (2004) Mutation in Nucleotide-Binding Domains of Sulfonylurea Receptor 2 Evokes Na-ATP-Dependent Activation of ATP-Sensitive K<sup>+</sup> Channels: Implication for Dimerization of Nucleotide-Binding Domains to Induce Channel Opening. *Mol Pharmacol* **66**:807-816.
- Yamada M, Isomoto S, Matsumoto S, Kondo C, Shindo T, Horio Y and Kurachi Y (1997) Sulphonylurea Receptor 2B and Kir6.1 Form a Sulphonylurea-Sensitive but ATP-Insensitive K<sup>+</sup> Channel. *J Physiol* **499** ( Pt 3):715-720.
- Yamada M and Kurachi Y (1995) Spermine Gates Inward-Rectifying Muscarinic but Not ATP-Sensitive K<sup>+</sup> Channels in Rabbit Atrial Myocytes. Intracellular Substance-Mediated Mechanism of Inward Rectification. *J Biol Chem* **270**:9289-9294.
- Yan F, Lin C W, Weisiger E, Cartier E A, Taschenberger G and Shyng S L (2004) Sulfonylureas Correct Trafficking Defects of ATP-Sensitive Potassium Channels Caused by Mutations in the Sulfonylurea Receptor. *J Biol Chem* **279**:11096-11105.
- Yan FF, Lin Y W, Macmullen C, Ganguly A, Stanley C A and Shyng S L (2007) Congenital Hyperinsulinism-Associated ABCC8 Mutations That Cause Defective Trafficking of ATP-Sensitive Potassium Channels: Identification and Rescue. *Diabetes*.
- Yang J, Jan Y N and Jan L Y (1995) Determination of the Subunit Stoichiometry of an Inwardly Rectifying Potassium Channel. *Neuron* **15**:1441-1447.
- Yellon DM and Downey J M (2003) Preconditioning the Myocardium: From Cellular Physiology to Clinical Cardiology. *Physiol Rev* **83**:1113-1151.
- Yi BA, Lin Y F, Jan Y N and Jan L Y (2001) Yeast Screen for Constitutively Active Mutant G Protein-Activated Potassium Channels. *Neuron* **29**:657-667.
- Zaritsky JJ, Redell J B, Tempel B L and Schwarz T L (2001) The Consequences of Disrupting Cardiac Inwardly Rectifying K<sup>(+)</sup> Current (I<sub>K1</sub>) As Revealed by the Targeted Deletion of the Murine Kir2.1 and Kir2.2 Genes. *J Physiol* **533**:697-710.
- Zerangue N, Schwappach B, Jan Y N and Jan L Y (1999) A New ER Trafficking Signal Regulates the Subunit Stoichiometry of Plasma Membrane K(ATP) Channels. *Neuron* **22**:537-548.
- Zhou Y, Morais-Cabral J H, Kaufman A and MacKinnon R (2001) Chemistry of Ion Coordination and Hydration Revealed by a K<sup>+</sup> Channel-Fab Complex at 2.0 Å Resolution. *Nature* **414**:43-48.

- Zhu G, Qu Z, Cui N and Jiang C (1999) Suppression of Kir2.3 Activity by Protein Kinase C Phosphorylation of the Channel Protein at Threonine 53. *J Biol Chem* **274**:11643-11646.
- Zingman LV, Alekseev A E, Bienengraeber M, Hodgson D, Karger A B, Dzeja P P and Terzic A (2001) Signaling in Channel/Enzyme Multimers: ATPase Transitions in SUR Module Gate ATP-Sensitive K<sup>+</sup> Conductance. *Neuron* **31**:233-245.
- Zingman LV, Hodgson D M, Bast P H, Kane G C, Perez-Terzic C, Gumina R J, Pucar D, Bienengraeber M, Dzeja P P, Miki T, Seino S, Alekseev A E and Terzic A (2002) Kir6.2 Is Required for Adaptation to Stress. *Proc Natl Acad Sci U S A* **99**:13278-13283.
- Zitron E, Gunth M, Scherer D, Kiesecker C, Kulzer M, Bloehs R, Scholz E P, Thomas D, Weidenhammer C, Kathofer S, Bauer A, Katus H A and Karle C A (2008) Kir2.x Inward Rectifier Potassium Channels Are Differentially Regulated by Adrenergic Alpha1A Receptors. *J Mol Cell Cardiol* **44**:84-94.
- Zitron E, Kiesecker C, Luck S, Kathofer S, Thomas D, Kreye V A, Kiehn J, Katus H A, Schoels W and Karle C A (2004) Human Cardiac Inwardly Rectifying Current IKir2.2 Is Upregulated by Activation of Protein Kinase A. *Cardiovasc Res* **63**:520-527.
- Zobel C, Cho H C, Nguyen T T, Pekhletski R, Diaz R J, Wilson G J and Backx P H (2003) Molecular Dissection of the Inward Rectifier Potassium Current (IK1) in Rabbit Cardiomyocytes: Evidence for Heteromeric Co-Assembly of Kir2.1 and Kir2.2. *J Physiol* **550**:365-372.